Using Road Weather Information Systems (RWIS) to optimize the Scheduling of Load Restrictions on Northern Ontario's Low-volume Highways

by

Sarah Baïz

A thesis
presented to the University of Waterloo
in fulfillment of the
thesis requirement for the degree of
Master of Applied Science
in
Civil Engineering

Waterloo, Ontario, Canada, 2007

AUTHOR'S DECLARATION

I hereby declare that I am the sole author of this thesis. This is a true copy of the thesis, including any required final revisions, as accepted by my examiners. I understand that my thesis may be made electronically available to the public.

Sarah Baïz

ABSTRACT

Covering the Northern part of the Province, Ontario's low-volume roads provide a link from remote resource areas to markets. Thus, preserving this transportation asset from the two main sources of pavement deterioration, namely traffic loading and the environment is extremely critical to the movement of goods and to the economy. In particular, Northern Ontario's secondary highways are challenged by a combination of heavy, low frequency traffic loading and a high number of freeze-thaw cycles for which most of these highways have not been structurally designed. Therefore they experience environmental damage and premature traffic-induced deterioration.

To cope with this issue, the Ontario Ministry of Transportation places Spring Load Restrictions (SLR) every year during spring-thaw. For economic reasons, the duration of SLRs is usually fixed in advance and is not applied proactively or according to conditions in a particular year. This rigidity in the schedule needs to be addressed, as it can translate into economic losses either when the payload is unnecessarily restricted or when pavement deterioration occurs. While the traditional approaches are usually qualitative and rely on visual observations, engineering judgment and historical records to make SLR decisions, the latest approaches resort to climatic and deflection data to better assess the bearing capacity of the roadway.

The main intent of this research was to examine how the use of a predictor for frost formation and thawing could improve the scheduling of load restrictions by tracking the frost-strengthening and thaw-weakening of the pavement structure. Based on field data captured in Northern Ontario, and on a preliminary analysis that found good correlation between frost thickness in the roadway and Road Weather Information Systems (RWIS) variables, more advanced frost and thaw predictors were developed as part of this research and are presented herein. The report outlines how the model was developed, details the calculation algorithms, and proposes an empirical methodology for a systematic site-specific calibration.

This research also involved several experimental and numerical tools, including the use of a Portable Falling Weight Deflectometer (PFWD) to estimate pavement strength during spring thaw, and the use of the Mechanistic-Empirical Pavement Design Guide (MEPDG) software to simulate the impact of SLR on the performance of typical Northern Ontario low volume roads.

ACKNOWLEDGMENTS

Firstly, I would express my gratefulness to my supervisors, Professor Carl Haas and Professor Susan Tighe for their support and guidance throughout this research project, and for welcoming me in such an inspiring team. I would also like to thank Brian Mills for his valuable input in this research and Ken Huen for his help.

In addition, I would like to acknowledge the contributions of the Ministry of Transportation of Ontario (MTO) through the Highway Infrastructure Innovation Funding Program (HIIFP). In particular, I would like to thank Max Perchanok for his feedback, and members of the MTO Regional staff, including Ken Mossop, Mickey Major, Doug Flegel, Brian Scott, Vic Lawrence and Alain Presseault for their assistance in the field.

Finally, I would like to extend my appreciation to the University of Waterloo's Faculty and Staff, to all the Transportation graduate students for the great memories, and of course, to my family in France for their warm thoughts.

TABLE OF CONTENTS

LIST OF FIGURES

LIST OF TABLES

LIST OF APPENDICES

GLOSSARY

BBR	Benkelman Beam Rebound
CPATT	Center for Pavement and Transportation Technologies
CTI	Central Tire Inflation
FHWA	Federal Highway Administration
FWD	Falling Weight Deflectometer
GIS	Geographical Information Systems
GPS	Ground Point Coordinates
HMA	Hot-Mix Asphalt
IRI	International Roughness Index
LCCA	Life-Cycle Cost Analysis
MEPDG	Mechanistic-Empirical Pavement Design Guide
MTO	Ministry of Transportation of Ontario
NE	Northeast
NW	Northwest
PFWD	Portable Falling Weight Deflectometer
RWIS	Road Weather Information Systems
SLR	Spring Load Restrictions
UW	University of Waterloo
WWP	Winter Weight Premiums

Chapter 1
INTRODUCTION

1.1 Research Rationale

Low volume roads in Northern Ontario carry heavily loaded commercial trucks and face very low temperatures in the winter, multiple freeze-thaw cycles and high temperatures in the summer. In order to minimize the weakening effects that seasonal shifts in moisture and temperature cause within the pavement structure, frost-resistant structural layers with high bearing capacity can be used. However, low-volume road design, maintenance and rehabilitation are generally constrained by tight budgets, as opposed to the higher volume highways [Coghlan 2000]. Therefore, in an attempt to protect the road infrastructure from premature deterioration, the Ministry of Transportation (MTO) uses alternative pavement preservation strategies such as the imposition of variable load periods: Spring Load Restrictions (SLR) and Winter Weight Premiums (WWP).

Ideally, restrictions should be imposed when the pavement structure is weak and only then. However, the imposition of SLR and WWP (which are traditionally based on historical records, expert observation and point testing) can be inaccurate or too rigid and lead to economic losses. The transportation and resources industries are penalized when the payload is unnecessarily restricted and maintenance expenses increase when fully loaded trucks are allowed on a weakened pavement. This problem can be further compounded by enforcement-related issues such as the five-day notice traditionally given to the trucking industry to disseminate the information and abide by the weight restrictions. There is therefore a need to assist policy makers on when to enforce and lift SLR and WWP.

1.2 Research Approach

The prime objective of this research was to develop the basis of a decision support tool that can help the MTO decide when to impose SLR and WWP. A solution was to investigate practical and systematic ways to track the bearing capacity of low-volume pavements throughout the seasons. This can be done using deflection testing, however a potentially less expensive but adequate solution may exist. In particular, as the capabilities and geographic coverage of Road Weather Information Systems (RWIS) in Ontario are expanding, the use of the readily available climatic and road data provided by RWIS suggests a starting point.

1.3 Thesis objectives and organization

This research started in June 2006 as the second phase of a two-year project (Sept.2005-Sept.2007) entitled "Using RWIS to Control Load Restrictions on Gravel and Surface Treated Highways" and was carried out at the University of Waterloo in association with the MTO. The first phase of the project (Sept.2005-June 2006) was based on data collected in Northern Ontario and showed good correlation between frost depth in the soil and a few RWIS variables. Excerpts from the technical progress report that was prepared for the MTO in May 2006 are provided in Appendix B.

The focus of this thesis was firstly to follow up on this preliminary analysis. Alongside the instrumentation, polling and troubleshooting of the test sites, measurable indicators of the critical shifts of the roadway's strength were introduced, in the form of predictors for the depth of frost and the depth of thaw in the pavement. Also, emphasis was put on the development of a simple and systematic calibration methodology so that any of the models developed could be easily transferable from one site to the other, and would be flexible enough to evolve alongside the improvements in the sensing, collection and prediction of climatic data. Moreover, the more urgent data collection needs were outlined.

Another focus of this research was to evaluate the impact of SLR in terms of pavement preservation and the Mechanistic Empirical Pavement Design Guide (MEPDG) software was used for this purpose. A preliminary assessment of the impact of timing and duration of SLR on the pavement life for typical Northern Ontario low-volume roads was derived from the MEPDG results. Finally, the findings were summarized into practical recommendations with the intent to provide the MTO with guidance on the application of SLR and WWP. FIGURE 1-1 below summarizes the research components.

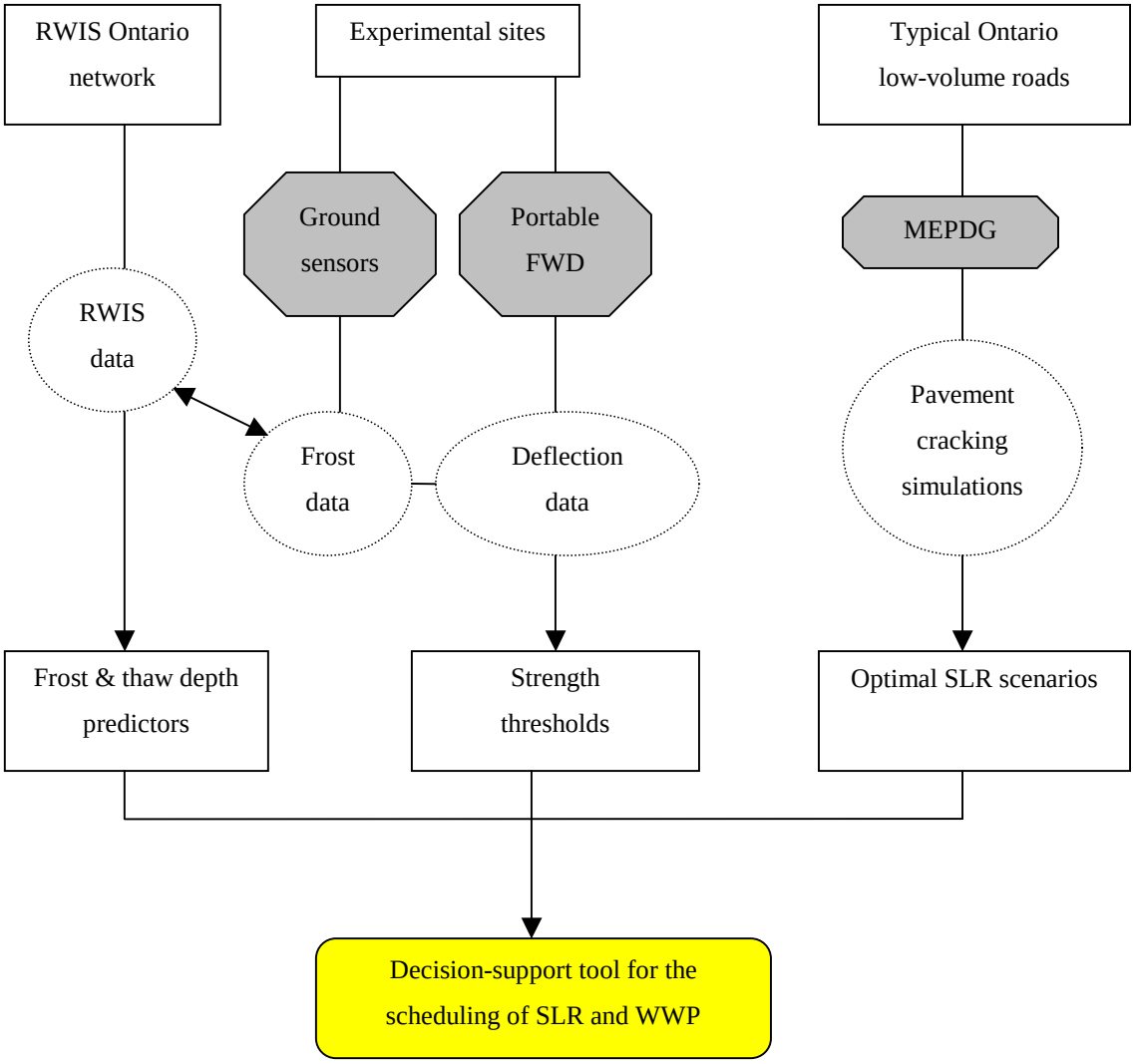

FIGURE 1-1 Summary of the Research Components

Chapter 2

LITERATURE REVIEW

2.1 Low Volume Roads in Northern Ontario

In Ontario, there are about 3,715 center-line kilometers in length of low-volume roads, which by definition carry less than 1,000 vehicles a day [Ninguyan 2006], but are typically remote access industrial and resource roads, thus subject to low frequency but high magnitude traffic loading. Apart from a few roads which are still gravel-surfaced since their construction in the 1950s, most of Ontario's secondary highways have been rehabilitated or re-constructed several times since 1985 into hard-surfaced (asphalt paved) or surface-treated roads with a thin bituminous layer, and thus belong to the flexible pavement category [Ninguyan 2006]. FIGURE 2-1 below illustrates the general layering of flexible pavement. Each layer is designed to provide adequate structural capacity and drainage to the pavement structure.

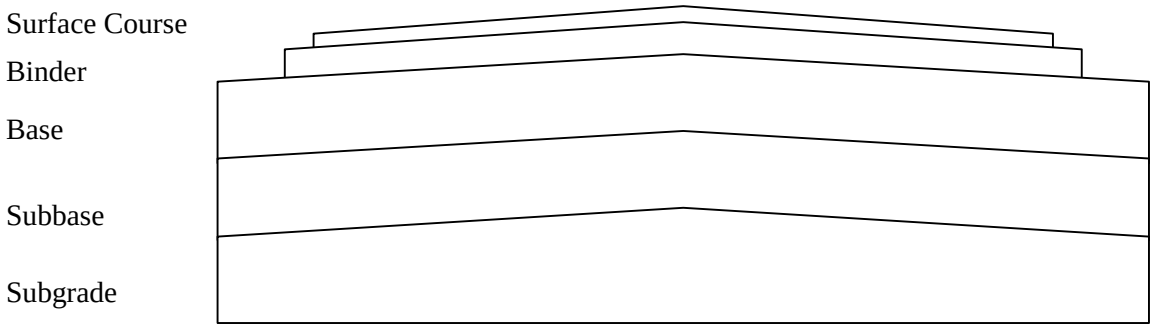

FIGURE 2-1 General Structure of a Flexible Pavement

While the subgrade consists of the native soil in the area, which can range from organic matter to bedrock, the base and subbase are typically of granular aggregate material. Temperature variations are normally incorporated in asphalt pavement design and construction through selection of asphalt cements (and asphalt emulsions for surface treated roads) associated with minimal thermal cracking under cold temperatures and minimal traffic-associated rutting under summer temperatures [Haas 2004]. However, while most low-volume roads are built to handle year-round unrestricted traffic volumes, they are not structurally designed for frost effects for economic reasons and are therefore likely to experience premature deterioration unless preventive action is taken.

2.2 Frost Action in Flexible Pavements

2.2.1 Frost Heave

A flexible road normally transfers traffic loading vertically from one structural layer down to the other in such a way that the whole pavement structure bends without rutting or breaking [TAC 1997]. During Northern Ontario's winters, the moisture that has accumulated within the pavement structure and in the subgrade soil freezes. Consequently, the pavement structure contracts like any other material at low temperatures, and the structure is uplifted as a result of ice segregation (see Appendix A). The subgrade's volumetric expansion is all the more important when the soil contains a high percentage of fine particles. For example, clays will retain moisture more aggressively compared to sandy soils [TAC 1997]. Flexible pavements can usually accommodate small amounts of expansion and contraction without excessive damage and even exhibit increased strength, but extreme temperature variations or subgrades with high frost-susceptibility can lead to longitudinal cracking and pavement failure.

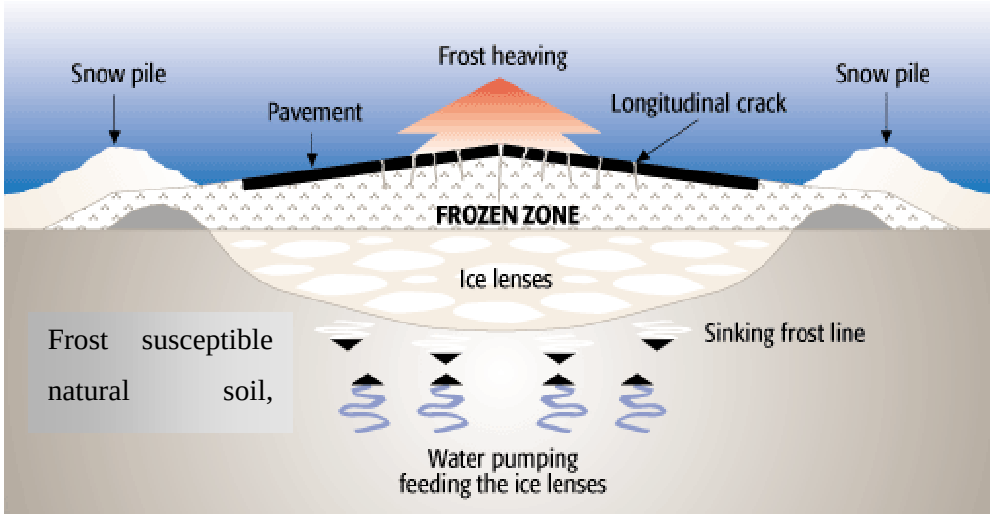

FIGURE 2-2 Frost Heave in the Pavement Structure (Courtesy of www.mtq.gouv.qc.ca)

2.2.2 Spring Thaw

In addition to pavement distresses that are caused by frost heave in cold regions, the roadway can lose up to 50% of its normal bearing capacity during spring thaw [Mokwa 2004]. During warmer winters or upon the arrival of spring, the pavement can reach a critical state where the upper and lower layers are thawed while the ones in-between are frozen. Subsurface water from melting of frost, additional moisture from rain and melting snow, as well as groundwater in the subgrade are trapped. Such a saturated structure is unable to transfer traffic loading properly and premature deformation occurs [Tighe 2006]. Depending on the degree of thawing and saturation, damage can affect some or all of the layers in the form of potholes, alligator cracking, or rutting [Bullock 2006]. Studies have found that up to 90% of pavement damage occurs during the spring-thaw period [Janoo 2002].

2.2.3 Mitigating Frost Action on Low-volume Roads

Most of Canada and much of the US is subject to frost action [Haas 1985]. The weakening effects of freeze and thaw action can be reduced by performing either preventive action at the design and construction stage, or by taking corrective action during rehabilitation and reconstruction. Typical practices include the removal of frost-susceptible soils at least down to the typical frost depth to protect the subgrade from frost action, the provision of a capillary break to reduce frost heave, or pavement design based on a poor subgrade support constraint [Isotalo 1995]. However, low volume roads are generally built to lower standards than more heavily traveled, higher speed highways, and do not include such pavement preservation solutions [Bullock 2006].

2.3 Variable Load Restrictions

2.3.1 Spring Load Restrictions (SLR) and Winter Weight Premiums (WWP)

The United States, Canada, France, Finland, Norway, and Sweden are among the countries that have load restrictions policies [Ninguyan 2006]. As an alternative to constructing roads that are capable of carrying the normal loads at any time of the year, many transportation agencies choose to mitigate road deterioration by imposing upper load limits on vehicles using the low-volume roads when these are suspected to perform poorer as a result of frost action and thaw weakening. Conversely, overweight permits are allowed during winter on secondary highways to reflect the additional bearing capacity of a pavement in frozen condition, and thus increase the payload [Bullock 2006].

The main concern today with most methods of setting SLR is how to increase the accuracy of restriction dates so that scenarios including overly conservative duration or delayed restriction enforcement are avoided. Moreover, trucking agencies need sufficient advance notice (typically 5 days) to reorganize their trips and loads and meet the restrictions [Bullock 2006]. It is therefore critical to develop predictive capacities of pavement weakening and be able to disseminate advance SLR warning accordingly.

2.3.2 Methods of Imposition of SLR and WWP

The primary goal in implementing SLR and WWP is to find an optimal balance between limiting road damage and maintenance costs and adversely impacting economic activity by restricting weights for trucks. A market scan performed in 2005 by IBI Group in association with other experts for Transport Canada summarized the various methods used across Canada for determining start and stop dates for load restrictions [Bullock 2006]. Firstly, pavement structures that should receive an SLR schedule are typically identified using design criteria and strength, such as whether or not the frost penetrates down to a frost susceptible subgrade soil. Then, each jurisdiction has their own method to estimate the threshold dates to impose and lift load restrictions, among them: field testing, prescheduled restrictions

or empirical models [Goodings 2000]. The imposition of WWP is most typically done on fixed dates across Canada, except in Alberta where frost depth and the number of days at temperatures less than 0^0C are used [Bullock 2006].

2.3.2.1 Calendar-based Restrictions

Many jurisdictions such as Ontario utilize experience with historic data to select fixed start and end dates for the SLR or WWP. These schedules are locally determined by District Engineers using weather conditions and visual inspections of the highway [Bullock 2006].

2.3.2.2 Field Testing

The provinces of Manitoba, British Columbia, Quebec and Alberta use historical information and visual observations in conjunction with regular and systematic field measurements to assess the state of the pavement structure. Sensors are installed in the centerline of a road to determine the frost depth and deflection testing used to determine the modulus of the supporting structure and whether it has reached a value that will result in permanent deformation if the current loads remain [Leong 2005]. Limitations of field testing include the required presence of personnel on site to perform the tests. Moreover, when the testing reveals that a critical thaw depth has been reached, the dissemination of rerouting procedures by the road agency to truckers usually takes at least a few days, during which severe damage can occur.

2.3.2.3 Empirical Models

In the recent years, the state of Minnesota and the provinces of Manitoba and Quebec have developed analytical approaches (see Appendix C). Empirical models utilize field data to develop a relationship between readily available data such as air temperature and a response variable such as frost depth to predict the probable critical timeframe whereby the soil strength is compromised. Once instrumentation is installed and data acquired, calibration and validation of the proposed model are performed to account for the unique soil, climatic and traffic loading parameters of the jurisdiction in which the model is used.

2.3.2.4 Reduced Tire Pressure

More recently, British Columbia's truckers can have shorter SLR periods when they use the Central Tire Inflation (CTI) system to abide by "reduced tire-pressure" periods. Provided that tire pressure is dynamically adjusted to accommodate for the bearing capacity loss of the pavement structure, the road can carry more load without any further damage [Bullock 2006].

2.3.3 Load Restrictions in Ontario

SLR are currently imposed and lifted on certain date thresholds in Ontario, through "Schedule 2' (King's Highways) and 'Schedule 3' (Local Roads Board) listings and usually from March to May and

March to June respectively [MTO 2007]. Even though weight restriction periods are commonly called "half load periods", section 122 of the Highway Traffic Act specifies the load restriction limit to be 5,000 kg per single axle [Highway Traffic Act 1990]. Vehicles exceeding this limit have to take alternative routes or be subject to the penalties described in the Act. Also, oversized load permits are restricted during an SLR period.

2.4 Pavement Deflection Testing

2.4.1 Role of Deflection Data in SLR and WWP Decision-making

Many transportation agencies collect pavement deflection data throughout spring, link it to Ground Positioning System (GPS) coordinates, and integrate it into a Geographical Information Systems (GIS) map before storing it in a database and using it to identify weak links in the road network [Bullock 2006]. Overall, deflection values are used to determine the limit magnitudes [Haas 1985]. Depending on the jurisdiction, the implementation and removal of SLR or WWP rely on thaw and/deflection-based thresholds, related to the inflection points in pavement strength trends. Relationships between deflection measurements, pavement strength and the approximate pavement remaining life have been the focus of many studies and are still under investigation. An initial study involved about 5,500 pavement sections across Canada [CGRA 1962] and resulted in the development of load restrictions through monitoring deflection on a set of representative test sections, a procedure now commonly called the Canadian Good Roads Association method and still used by several agencies as a basis of setting SLR.

2.4.2 Theoretical Background

The amount of deflection that results from the application of a load on a flexible pavement surface given a specific set of environmental conditions is an important indicator of its structural capacity, material properties, and subsequent pavement performance [FHWA-LTPP 2000]. While moisture affects the unbound layers, especially in areas with fine-grained unbound soils and important frost penetration, hourly and seasonal temperature changes impact the behavior of asphalt concrete layers. Since deflections are usually larger on a hot summer day than during a cooler period, deflection measurements have to be normalized to a reference temperature before they are converted into resilient moduli and used to calculate pavement deterioration indicators [TAC 1997].

2.4.3 Non-destructive in-situ Deflection Testing

Non-destructive in-situ deflection testing typically includes static measurements of road strength using the Benkelman Bean Rebound (BBR), dynamic measurements, or characterization of pavement response to an impact load using the Falling Weight Deflectometer (FWD) whose magnitude and duration represent the passage of a truck wheel [TAC 1997]. Each method has strengths and

drawbacks, and even if agencies moving from one technique to the other try to correlate the measurements, the results are still open to criticism [Bullock 2006]. Because of its accuracy and speed, FWD testing is used extensively by many jurisdictions and has enabled correlation of pavement weakness with the beginning of thaw [Popik 2005].

2.4.4 Light or Portable Falling Weight Deflectometer (PFWD)

In addition to low purchase and operating costs, portable FWD devices have the advantage of being small enough to be easily operated by one person and moved from site to site, and have thus become the focus of increased interest [Hoffmann 2003]. Recent studies have evaluated the use of PFWD testing as a practical and reliable alternative to conventional BBR or FWD to measure the in-situ elastic modulus of highway materials [Nazzal 2007]. It has been shown that the PFWD is able to follow seasonal stiffness variations on both asphalt and gravel surfaces and could therefore be used to determine when to place and remove spring load restrictions, especially on low-volume paved roads which usually have thin surface layers (less than 127mm) [Kestler 2005].

2.5 The Mechanistic-Empirical Pavement Design Guide

2.5.1 Introduction to Pavement Design

Highway agencies need to evaluate the pavement performance of different sets of pavement materials and geometries under certain loading and climatic conditions in order to design pavements. In general, one or more of the following techniques are used [Bullock 2006]: Design based on experience of how different pavements historically performed under certain traffic loading and environmental conditions; design based on jurisdiction-specific pavement performance mathematical models developed from field data; design based on the estimation of pavement behavior (stresses, strains and deflections) using mechanistic principles; and finally, design based on the use of mechanistic-empirical models which combine mechanistic equations with empirical failure criteria that use field data.

2.5.2 Mechanistic-Empirical Approach

Compared to a purely mechanistic design, the advantage of combining a mechanistic analysis with empirical relationships is that it can be used in the jurisdiction for which it has been calibrated with more reliability and fewer inputs. Such an approach has become very popular among highway agencies [Bullock 2006].

In pavement design, the mathematical equations are usually derived from the layered elastic theory, which assumes that each pavement structural layer is homogeneous, isotropic and linearly elastic, and will therefore rebound to its original form once the load is removed [ARA 2004]. The modulus of elasticity, Poisson’s ratio and thickness of each layer on the one hand, and the magnitude, geometry

and repetition of the applied load on the other hand are inputted in the model and to compute stresses, strains and deflections at any point in the pavement structure.

Field deflection measurements obtained from FWD testing can be inputted into empirical failure definitions and equations to determine the existing pavement structural support and estimate the remaining pavement life or number of loading cycles to failure. Currently, two types of failure criteria are widely recognized, one relating to fatigue cracking (using the horizontal tensile strain at the bottom of the asphalt layers and the elastic modulus of the asphalt mix) and the other to rutting initiating in the subgrade (using the vertical compressive strain at the top of the subgrade) [University of Washington 2005]. SLR applications can use relationships based on the deflection measured at the pavement surface during springtime, such as the AASHO Road Test and Roads and Transportation Association of Canada (RTAC) criteria. These failure criteria are empirically established and must therefore be calibrated to specific local conditions, and are generally not applicable on a national scale.

2.5.3 The Mechanistic-Empirical Pavement Design Guide (MEPDG Software)

Using the Mechanistic-Empirical Pavement Design Guide (MEPDG), the designer can estimate new or existing pavement design alternatives [ARA 2004]. The effects of climate, age and vehicle loading configurations can be incorporated. Pavement performance is computed in terms of cracking, rutting and surface roughness. Since its first development in 1997 by the AASHTO Joint Task Force on Pavement (JTFP) under National Cooperative Highway Research Program Projects 1-37 and 1-37A [ARA 2004], the MEPDG software has considerably improved along with progress in model accuracy and computer science, as well as increased amount of available pavement data. The latest version of the software (MEPDG v.0.9) became available online in July 2006 [NCHRP 2007] and reflected changes recommended by “the NCHRP 1-40A independent review team, the NCHRP 1-40 panel, the general design community, various other re-searchers, and the Project 1-40D team itself” [NCHRP 2006]. In particular, the Enhanced Integrated Climatic Model (EICM) was greatly improved to incorporate about 40% of its analysis dealing with climatic influence, versus 5% in the previous generations [Wagner 2005].

2.5.4 The Enhanced Integrated Climatic Model (EICM)

As explained in section 2.2, strengthening and weakening of the pavement structure occurs in a cyclic manner. With the “Enhanced Integrated Climatic Model” (EICM) feature, the MEPDG software is able to calculate hourly temperatures and moisture within each pavement layer and within the subgrade over the entire design period. Its outputs are used in various ways to estimate material properties throughout the design life, using a combination of the Climatic-Materials-Structural (CMS) model, the Rainfall-Infiltration-Drainage (ID) model and the CRREL Frost Heave and Thaw Settlement model [ARA 2004].

2.6 Economic Viability of SLR

In the conventional process of pavement selection, design options that meet the structural and performance requirements are compared using a Life Cycle Cost Analysis (LCCA), and the most cost-effective alternative over the specified analysis period is typically selected [Ahmed 2006]. In addition to considering initial construction costs, user costs and expected maintenance and rehabilitation costs, the selection process can also take into account other criteria such as aesthetics, safety, performance, environmental impacts, functionality, constructability or local availability of the technology and sustainability/extent of recycling. Overall, the objective of LCCA is to compare competing alternative investment strategies based on how best they achieve a desired level of service with the available funds, for the lowest cost over time.

To abide by the restrictions without reducing their payload, industries that rely on utilizing highway networks to transport goods may need to increase the number of trips along the restricted routes or to follow alternate, potentially longer routes. Both solutions generate additional costs to the haulers [Goodings 2000]. On the other hand, the implementation of SLR can result in cost savings by limiting pavement damage during spring thaw, provided the restrictions are applied at the right time. The benefits of implementing SLR on low-volume roads have been investigated by many agencies. According to the results of a mechanistic-empirical analysis that simulated Minnesota's local roads, up to a 14 % reduction in overall annual facility cost could be realized by implementing SLR [Levinson 2005]. Similarly, Quebec's flexible pavements indicated an increase of between 6 to 14 % in the average life expectancy of pavements due to SLR [Bullock 2006].

2.7 Road Weather Information Systems (RWIS)

Road Weather Information Systems (RWIS) stations monitor current road and weather conditions at point locations using environmental sensors deployed on and about the roadway [Buchanan 2005]. Real-time RWIS data is automatically collected every 20 minutes, 7-days per week and 24-hours per day, and uploaded within 2 minutes to a password protected web portal where is used to generate forecasts and archived [AMEC RWIS 2007]. RWIS installations include meteorological sensors that measure atmospheric temperature, relative humidity, wind speed and direction, precipitation and pavement sensors that measure pavement temperature, subgrade temperature, pavement condition (wet, dry, or frozen), and the freezing point of a wet surface [Boselly 1993]. Each station typically costs about $70,000 (CAD) for installation and $11,500 for annual operating cost [Buchanan 2005].

With about 115 stations across the National Highway System in Ontario and about 50 more stations in the process of being created on the provincial highway system, the MTO RWIS network is playing an increasingly important role in the deployment of winter maintenance operations [Buchanan 2005], for

example in “smart” salt applications and fixed automated spray technology (FAST) used to deice bridges at freeze conditions. Moreover, the MTO is a member of the AURORA program, which is an international partnership of public agencies that was launched in 1996 to support research in the field of weather and pavement data sensing and forecasting for efficient highway maintenance and provision of real-time information to travelers [AURORA 2007].

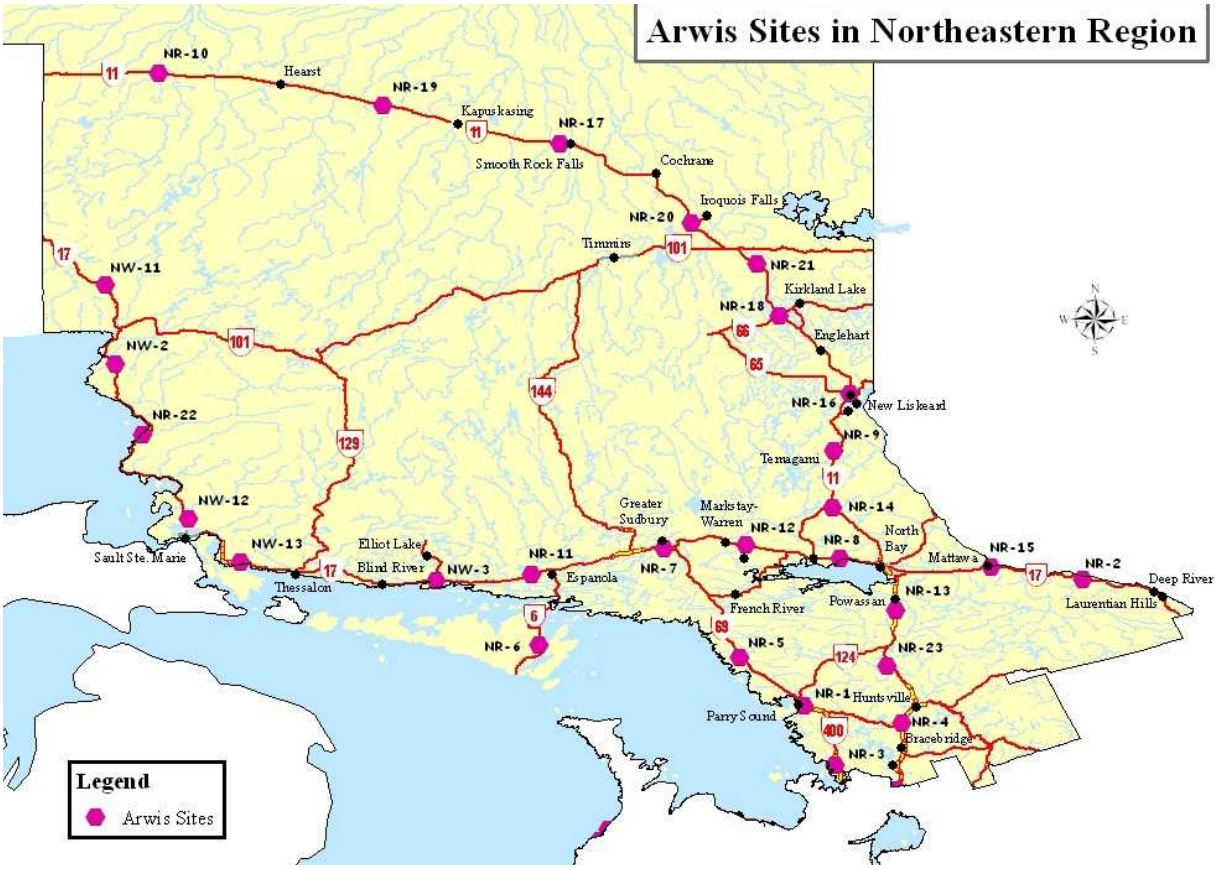

FIGURE 2-3 MTO RWIS Network in Northeastern Ontario (courtesy of http://www.ogra.org/)

Chapter 3
METHODOLOGY

3.1 Modeling Frost and Thaw Depth in the Pavement Structure

3.1.1 Starting Point

Frost formation or dissipation in the soil is related to the magnitude and duration of temperature gaps between the pavement's surface and the air [Bullock 2006]. Developing an indicator that can predict pavement strength could provide valuable input to transportation agencies. As the amount of frost in the pavement relates to seasonal fluctuations in the bearing capacity of the road, and more importantly, can be measured and intuitively understood, it could serve as such an indicator. WWP would be triggered once the frost depth and thickness rise above specified thresholds whereas SLR would be imposed once thaw depth and frost thickness fall under certain values.

As summarized in Appendix C, Minnesota, Manitoba and Quebec have developed jurisdiction-specific models able to relate air temperatures to freezing and thawing indices and to the depth of frost in the pavement. Inspired by this approach, a preliminary one-year analysis (as per section 1.3.1) adapted the empirical model to Ontario conditions and related the amount of frost in the pavement structure to some RWIS environmental data. As a follow-up to this preliminary analysis, the model was further developed during this thesis.

3.1.2 Sources of Data

3.1.2.1 Experimental Sites

In order to develop an empirical model that can be used on a specified set of roads, field data should be collected on sections that are representative of the design, environment and traffic conditions observed on these roads. Therefore, two sites located in Northwestern and Northeastern Ontario respectively (and both low-volume roads subject to SLR) were selected in the fall 2005. As represented on FIGURE 3-1, the Northeastern study site is located on Highway 569, 3km east of Highway 11, and the Northwestern study site is located on Highway 527, 0.5 km north of Highway 811.

FIGURE 3-1 Location of the Northeastern (NE) and Northwestern (NW) Experimental Sites

FIGURE 3-2 Northeastern Experimental Site

FIGURE 3-3 Northwestern Experimental Site

In the fall 2005, each study site was equipped with a thermistor assembly, a datalogger and a weather resistant cabinet housing for the recording equipment and power source (see FIGURE 3-4).

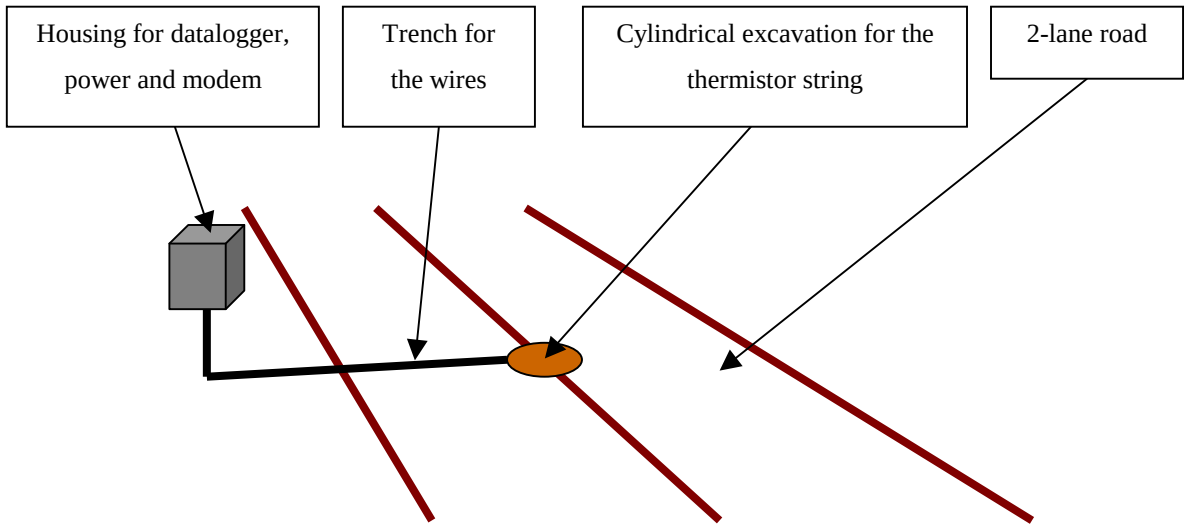

FIGURE 3-4 Overview of the Installation on the Experimental Sites

Thermistor probes are devices whose resistance changes with temperature. As illustrated on FIGURE 3-5, thirteen thermistors were inserted vertically in the centerline of the roadway, at 5cm, 15cm, 30cm, 45cm, 60cm, 75cm, 90cm, 105cm, 135cm, 165cm, 195cm, 225cm and 255cm deep on each site. The cylindrical excavation was refilled with the material that was taken out in layers and asphalt was used to patch the trench and the surface of the excavation.

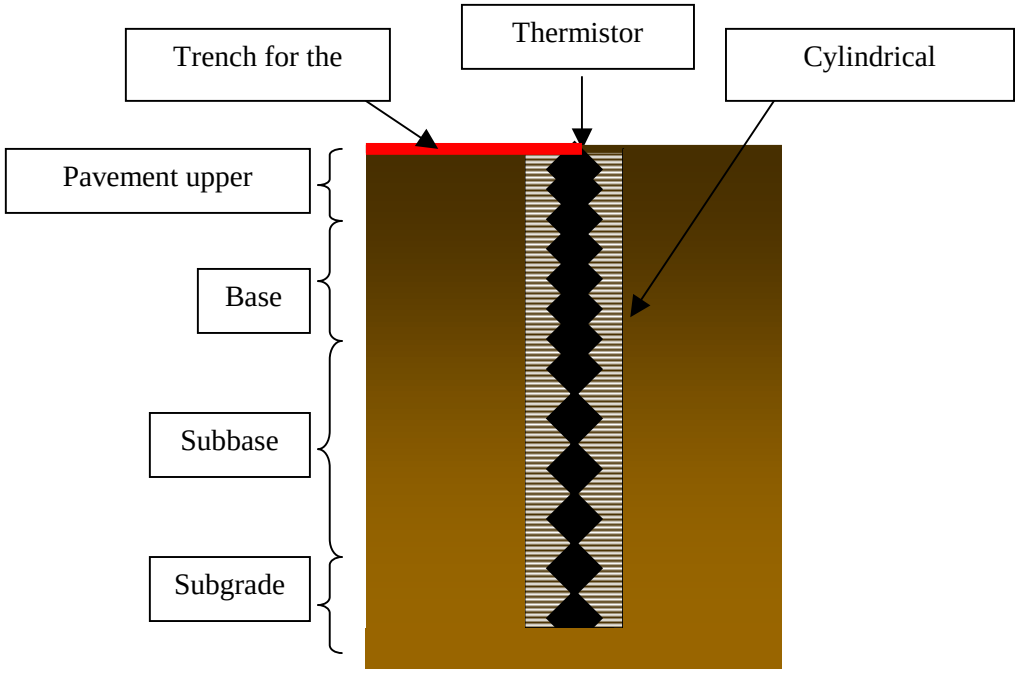

FIGURE 3-5 Thermistor String (Assembly of Temperature Probes) in the Ground

3.1.2.2 RWIS Stations

Through the RWIS website, climatic data was collected and used to estimate temperatures on the experimental sites using interpolation and data fusion algorithms. As each one-km deviation from the RWIS station can result in differences in the temperature readings, a minimum of three RWIS sites are required. As illustrated in FIGURES 3-6 and 3-7, the three closest RWIS stations were selected around each experimental site.

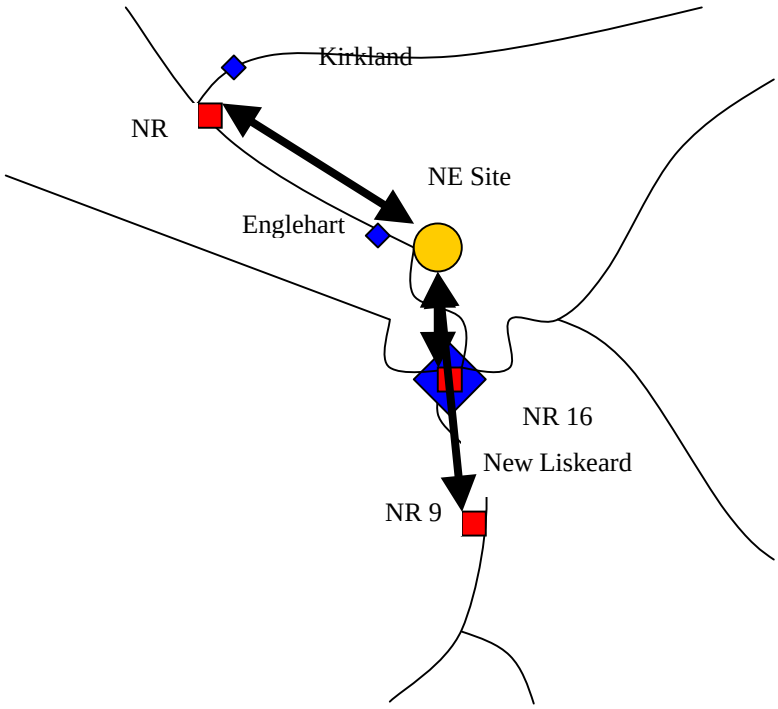

FIGURE 3-6 Selection of 3 RWIS stations for the Northeastern Experimental Site

NR14 and NR21 RWIS stations were identified by the MTO and used in the model developed during the preliminary analysis. In the model presented here, these stations have been replaced by closer ones: NR9 and NR18.

TABLE 3-1 Distances (linear, elevation-free) between the Northeastern Experimental Site and the surrounding RWIS stations

RWIS station identification	Approximate distance to Northeastern Experimental Site
NR16 : New Liskeard	D_{16} = 22 km
NR9 : Temagami	D_9 = 78 km
NR18 : South Y	D_{18} = 65 km

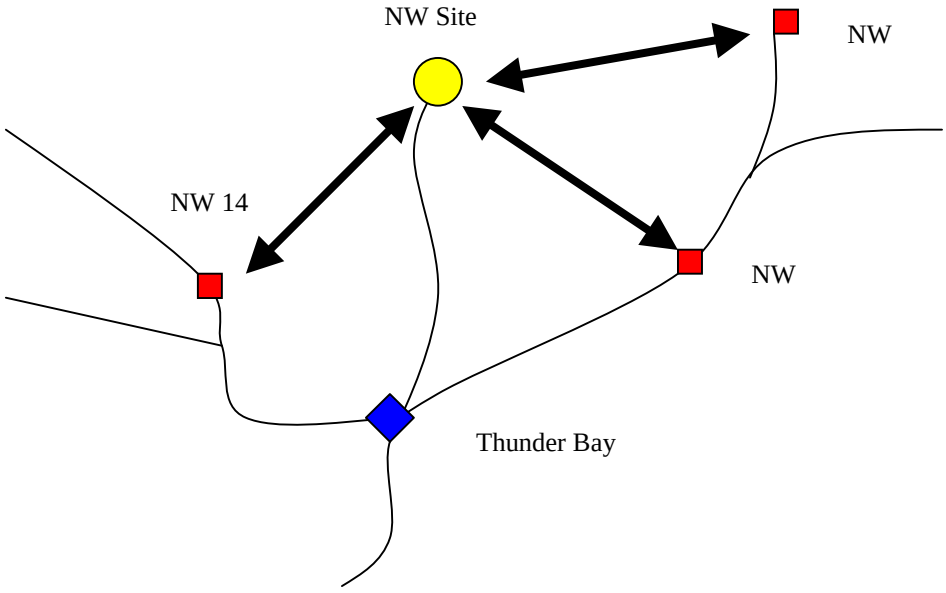

FIGURE 3-7 Selection of 3 RWIS stations for the Northwestern Experimental Site

TABLE 3-2 Distances (linear, elevation-free) between the Northwestern Experimental Site and the surrounding RWIS stations

RWIS station identification	Approximate distance to Northwestern Experimental Site
NW8 : Pearl	D_8 = 150 km
NW14 : Raith	D_{14} = 120 km
NW7: George Creek	D_7 = 150 km

3.1.3 Data Collection

3.1.3.1 Data Collection on the Experimental Sites

3.1.3.1.1 Data acquisition Program

The data acquisition program included core ground temperature measurements as well as internal and backup battery voltages, charging voltage and charging capacity available on the data card and internal memory.

3.1.3.1.2 Northeastern Experimental Site (3km east of Highway 11, on Highway 569)

The availability of a phone line on this site enabled the transfer of the thermistor data via a dial up modem starting from December 5, 2005. However, by the end of June 2006, the modem failed and was thus sent back to the manufacturer to be repaired. Some data was then intermittently collected throughout fall 2006 but only to reveal that seven of the thirteen thermistor probes were not working properly.

3.1.3.1.3 Northwestern Experimental Site (0.5 km north of Highway 811, on Highway 527)

As neither phone nor hydro were available on this site because of its location, data had to be collected manually on by swapping data cards at given time intervals, and an external power source (stand alone battery) was used. Data acquisition could not begin before February 15, 2006 because the datalogger unit encountered a power drain issue: Once the data card was being removed, the current drawn would return to a constant value of 350mA and would not enter into a lower power sleep mode again. This issue was fixed but the datalogger unit failed again during the winter 2006.

3.1.3.1.4 Summary Status of the Sites

Overall, a lot of technical issues were encountered on both pilot sites since their installation in fall 2005. In collaboration with the MTO Regional staff, many trips were made to diagnosis and troubleshoot the equipment. Data collection, which was scheduled to cover November 2005 through May 2006 and November 2006 through May 2007 on both sites, was successful only from December 6, 2005 to April 30, 2006. Frequent equipment failures due to manufacturing vices resulted in disruptions in data collection. In fall 2006, modem and sensors failed on the Northeastern site and the data acquisition system failed once more on the Northwestern site.

The thesis thus focused on proposing a model coherent with the data collected as well as developing on developing a calibration that could be used to calibrate the model to any site once field data is gathered. Also, along with troubleshooting work, further plans were made in close collaboration with the MTO to replace the failing devices and equip additional sites with similar installations. Efforts are currently under way by the MTO into the use of more reliable frost measurement sensing and data collection instruments as well as into equipping additional sites, including RWIS stations, with frost measurement sensors in an attempt to provide smoother and continuous field data in the near future.

3.1.3.1.5 Additional Instrumentation Plan

After many unsuccessful and time-consuming repair attempts, it was decided in conjunction with the MTO to put focus on the development of a comprehensive instrumentation plan, including replacement of the failing equipment on the existing sites, installation of additional stations in the area and provision for phone and electricity on all the sites. In particular, the creation of additional MTO RWIS stations that would be also equipped with ground temperature and soil moisture sensors was suggested (see TABLE 3-3 below). Upon the request of the MTO, a Memorandum was prepared in November 2006 and is provided in Appendix D.

TABLE 3-3 Status of the Equipment on the Existing and Projected Experimental Sites

Location	Status	Power	Phone	Modem	Datalogger	Thermistors	Moisture probes
Northeast							
Hwy 569	Existing	Yes	Yes	Broken	Yes	broken	No
Hwy 624	Recent	Yes	Yes	Yes	No	Yes	Yes
Hwy 66	Projected	Yes	Yes		Not yet	Not yet	Not yet
Northwest							
Hwy 527	Existing	No	No		Broken	Yes	
Hwy 643	Projected	No	No		Not yet	Not yet	Not yet
Hwy 599	Projected	No	No		Not yet	Not yet	Not yet
Hwy 671	Projected	No	No		Not yet	Not yet	Not yet

3.1.3.2 Data Collection from the RWIS stations

Air temperature as well as pavement surface temperature data for the six RWIS stations identified in section 3.1.2.2 were retrieved from the AMEC RWIS MTO password-protected website [AMEC RWIS 2007] from November 2005 to May 2006 and from November 2006 to May 2007, and copied into MS Excel files. Daily averages were calculated. Then, a spatial interpolation was done in order to (see FIGURE 3-8 below) according to the simple data fusion algorithms described below, allowing

estimation of climatic data for each experimental site based on values from three surrounding RWIS stations weighted by the distance from the site.

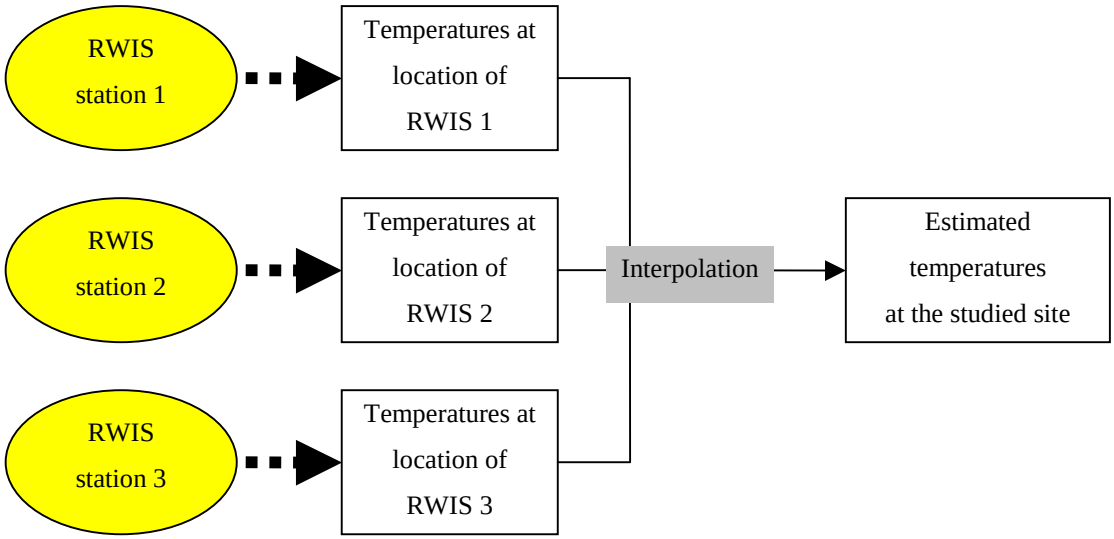

FIGURE 3-8 Estimation of Site-specific Climatic Data by Interpolation from RWIS Data

Interpolating in three dimensions requires several assumptions. The temperature between any given RWIS stations is typically unknown and may also vary with elevation. To simplify the process, inverse distance weighted averages were calculated according to the equations below.

$$T_i = \frac{\frac{T_{A_i}}{d_A} + \frac{T_{B_i}}{d_B} + \frac{T_{C_i}}{d_C}}{\frac{1}{d_A} + \frac{1}{d_B} + \frac{1}{d_C}} \qquad \textbf{3-1}$$

$$T_i = \frac{\frac{T_{B_i}}{d_B} + \frac{T_{C_i}}{d_C}}{\frac{1}{d_B} + \frac{1}{d_C}} \qquad \textbf{3-2}$$

$$T_i = T_{C_i} \qquad \textbf{3-3}$$

$$T_i = \frac{T_{i-2} + T_{i-1}}{2} \qquad \textbf{3-4}$$

Where d_A; d_B ; d_C Distance (in km) between the site and RWIS station A;B;C.

$T_{A_i}; T_{B_i}; T_{C_i}$ Daily averaged temperatures on day i for RWIS station $A; B; C$

T_i Triangulated air or surface temperature value on day i on the site

ϕ Blank (when no value was found in the database)

If ($T_{A_i} \neq \phi$), ($T_{B_i} \neq \phi$) and ($T_{C_i} \neq \phi$), then T_i is calculated according to Equation 3-1. If ($T_{A_i} = \phi$), ($T_{B_i} \neq \phi$) and ($T_{C_i} \neq \phi$), then T_i is calculated according to Equation 3-2. The two other cases can be derived by permuting A, B and C in both the condition and the equation. Similarly, if ($T_{A_i} = \phi$), ($T_{B_i} = \phi$) and ($T_{C_i} \neq \phi$), then T_i is calculated according to Equation 3-3. The two other cases can be derived by permuting A, B and C in both the condition and the equation. Finally, if ($T_{A_i} = \phi$), ($T_{B_i} = \phi$) and ($T_{C_i} = \phi$), then T_i is calculated according to Equation 3-4. In short, when for some reason, no value was available on a particular day for the three RWIS stations at once, then the final air or pavement temperature value was linearly interpolated from values of the two or more previous days.

3.1.3.3 Data Analysis

A milestone for this research is the enhancement of an empirical frost depth model that is based on a few RWIS variables. Development of this model goes through RWIS data (air temperature and pavement surface temperatures) and field data (temperatures at different depths in the ground). As proper calibration of the model to Ontario conditions requires gathering a lot more Ontario climatic and road data than what was collected as part of this research, only a temporary calibration is attempted in this research.

3.1.4 Findings of the Preliminary Data Analysis

The preliminary Ontario model presented in Appendix B used RWIS data as well as the ground temperature data acquired on the Northeastern experimental site from November 6, 2005 to April 30, 2006. Firstly, ground temperatures were converted into maximum frost depths in the pavement.

Secondly, RWIS data (air temperatures, pavement surface temperatures) was used to calculate a Freezing Index (FI) and a Thawing index (TI). Calculation of both the FI and the TI are triggered when the daily average of RWIS air temperature first falls below 0^0C, as the freezing season begins (November 10, 2005 here). The calculation of the TI relies on the determination of a site-specific constant called the reference temperature (see section 4.2.1.2). The steps are summarized in FIGURE 3-9 below.

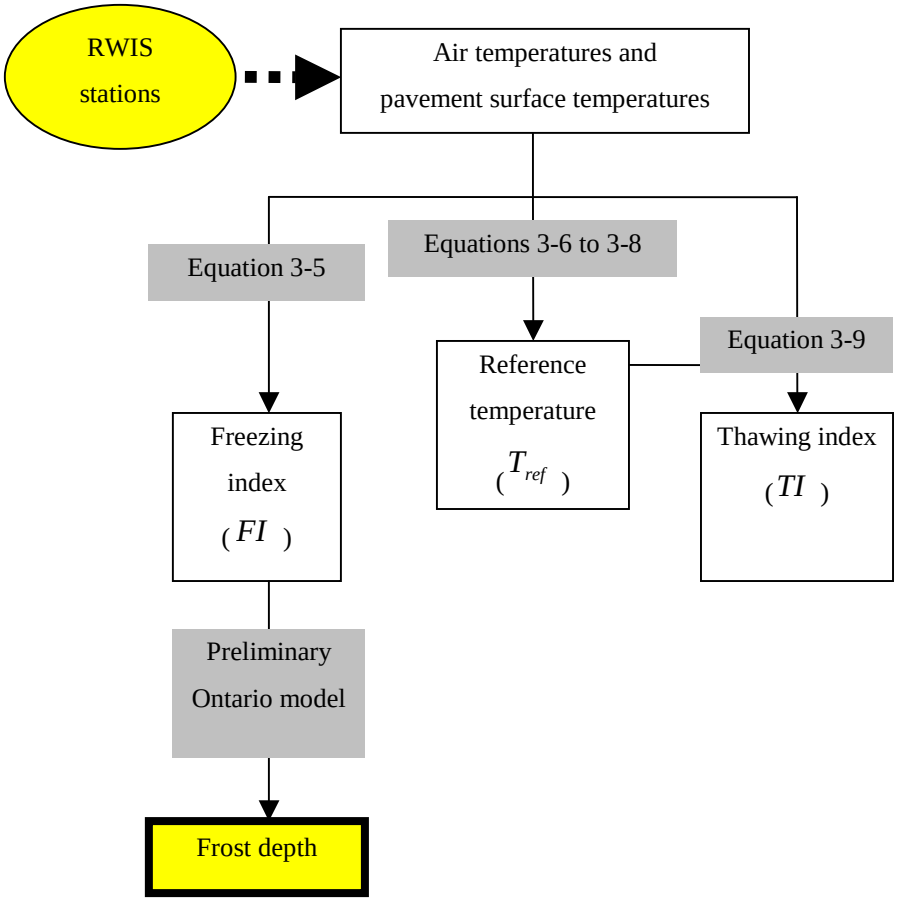

FIGURE 3-9 Steps for Frost Depth Calculation using the Preliminary Ontario Model

3.1.4.1 Calculation of the Freezing Index using RWIS Data

The Freezing Index (FI), as defined in Equation 3-5, captures the magnitude of air temperature gradients over given periods of time [Tighe 2006].

$$\begin{cases} FI_0 = -T_0 \\ FI_{i+1} = FI_i - T_{i+1} \\ FI_i < 0 \Rightarrow FI_i \equiv 0 \end{cases} \qquad \textbf{3-5}$$

Where i Number of days after the day indexed as day $i = 0$

$i = 0$ Day on which T_{Air_i} first falls below 0^0C

FI_0 Freezing Index value on day $i = 0$ (in ^0C -days)

FI_i Freezing Index value on day i (in ^0C -days)

3.1.4.2 Calculation of the reference temperature using RWIS Data

The reference temperature is a constant which represents the temperature lag between the air temperature and the pavement's surface temperature. This constant is site-specific, as it is generally

linked to parameters such as the amount of solar radiation or to some properties of the pavement materials [Tighe 2006].

As per the preliminary analysis (see Appendix B), this constant can be calculated by finding the y-axis intercept of the best fit line, after plotting the RWIS pavement temperatures on the x-axis and the RWIS air temperatures on the y-axis. The function "intercept" available on Excel is able to calculate such a constant. The calculation steps can also be mathematically expressed as followed:

$$\overline{T_{Air}} = \sum_{i=1}^{N} T_{Air_i} \qquad \textbf{3-6}$$

$$\overline{T_{Sfc}} = \sum_{i=1}^{N} T_{Sfc_i} \qquad \textbf{3-7}$$

$$T_{ref} = \overline{T_{Air}} - \overline{T_{Sfc}} * \frac{\sum (T_{Sfc_i} - \overline{T_{Sfc}}) * (T_{Air_i} - \overline{T_{Air}})}{\sum (T_{Sfc_i} - \overline{T_{Sfc}})^2} \qquad \textbf{3-8}$$

Where T_{ref} Reference temperature (in °C)

N Number of points used in the linear regression analysis

T_{Air_i} Air temperature value on the site on day i

T_{Sfc_i} Surface temperature value on the site on day i

The reference temperature was found to be equal to $-5.5^0 C$ on the Northeastern site.

3.1.4.3 Calculation of the Thawing Index using RWIS Data

The Thawing Index (TI) calculation is presented in Equation 3-9 and utilizes the reference temperature defined in section 3.1.4.2. The TI provides an indication of the duration of warmer weather and its effect on the pavement surface. TI and FI are currently being used by a number of jurisdictions (in Minnesota for e.g.) as part of analytical approaches to SLR scheduling (see Appendix C).

$$\begin{cases} TI_0 = -T_{ref} \\ TI_{i+1} = T_{i+1} - TI_i \\ TI_i < 0 \Rightarrow TI_i \equiv 0 \end{cases} \qquad \textbf{3-9}$$

Where i Number of days after the day indexed as day $i = 0$

$i = 0$ Day on which T_{Air_i} first falls below 0^0C

TI_0 Thawing Index value on day $i = 0$ (in $^0 C$ -days)

TI_i Thawing Index value on day i (in ^0C -days)

T_{ref} Reference temperature on the Northeastern site (-5.5^0C)

3.1.4.4 Main findings

A regression analysis based on the 8100 data points that were recorded from December 2005 through May 2006 (and averaged into 107 points) showed that the depth of frost on the site could be estimated using a linear function of the square root of the Freezing Index ($\sqrt{FI}$), with a coefficient of determination of 98% (see Appendix B). Moreover, it was suggested that the Thawing Index be used to track the duration of spring-thaw in the pavement.

3.1.5 Model Completion

3.1.5.1 Data Analysis Plan

Based on the conclusions of the preliminary analysis, further qualitative and quantitative analysis was performed as part of this thesis, using RWIS data and the available field data. First of all, a new procedure was used to calculate the reference temperature used in the Thawing index algorithms. Then, predictors for both the depth of frost and the depth of thaw in the pavement were developed and a sample calibration was performed.

3.1.5.2 Calculation of the Depth of Frost and Thaw using Ground Temperatures

As seen in section 3.1.2.1, field data comprised temperature readings at thirteen different depths in the pavement, down to 255 cm deep. Based on these temperatures, the depth of frost (maximum penetration depth) can be defined as the depth for which the associated temperature probe displays a negative value for the first time, provided the readings are collected from the deepest probe, up to the shallower ones. Similarly, the depth of thaw (extent of thaw from the top down) can be defined as the depth for which the associated temperature probe displays a positive value for the first time, provided the readings are collected from the shallowest probe, down to the deeper ones. FIGURE 3-10 below illustrates this approach.

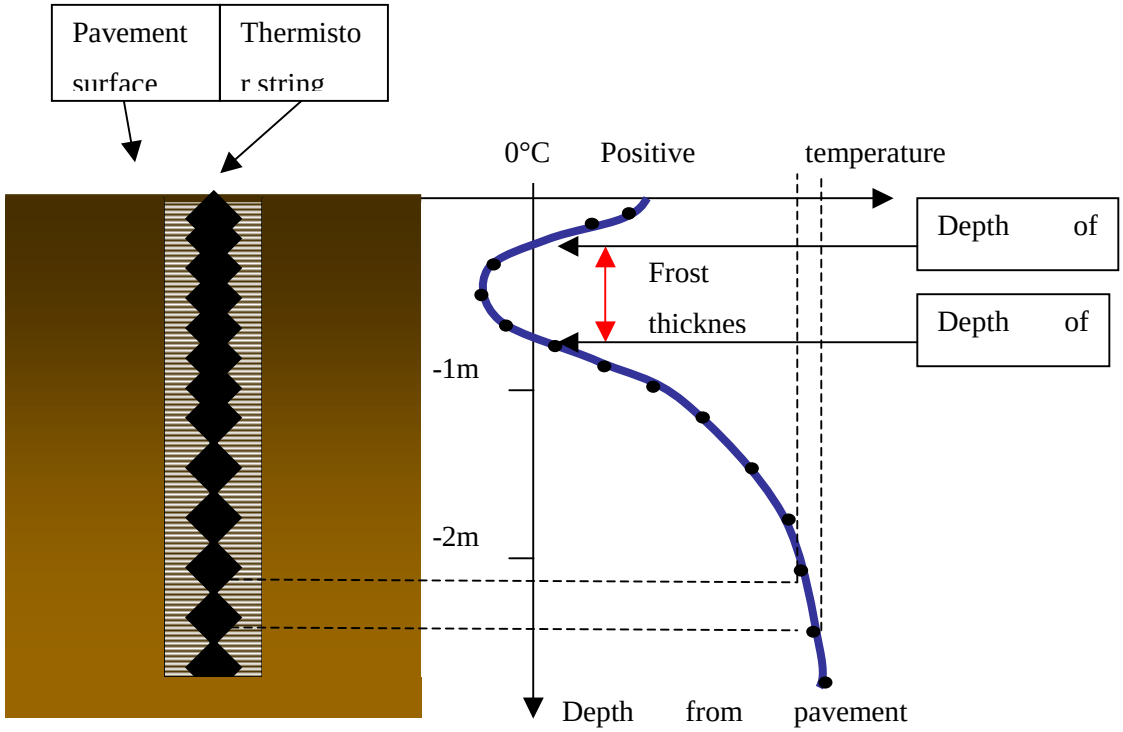

FIGURE 3-10 Determination of Frost and Thaw Depths using Thermistor Data

As there are only thirteen temperature sensors and temperature variations in the pavement can be assumed to be linear on local segments in the pavement section, linear interpolation algorithms were used to estimate the depths in between. An Excel macro able to automatically convert thermistor data into the depths of frost and thaw was developed and is provided in Appendix E.

3.2 Deflection Testing using the Portable Falling Weight Deflectometer (PFWD)

3.2.1 Description of the Equipment

Portable Falling Weight Deflectometer (FWD) testing was performed on the test sites to obtain on-site deflection data. The PFWD device used was the Prima 100 (Dynatest, Denmark, 2004) shown in FIGURE 3-9 below. In theory, the PFWD simulates traffic loading by dropping a mass (10kg, 15kg or 20kg) from a specific height (up to 85cm) on an anvil covered with 2 to 4 rubber buffers [Dynatest International 2004]. A schematic representation of the PFWD device is shown on FIGURE 3-11.

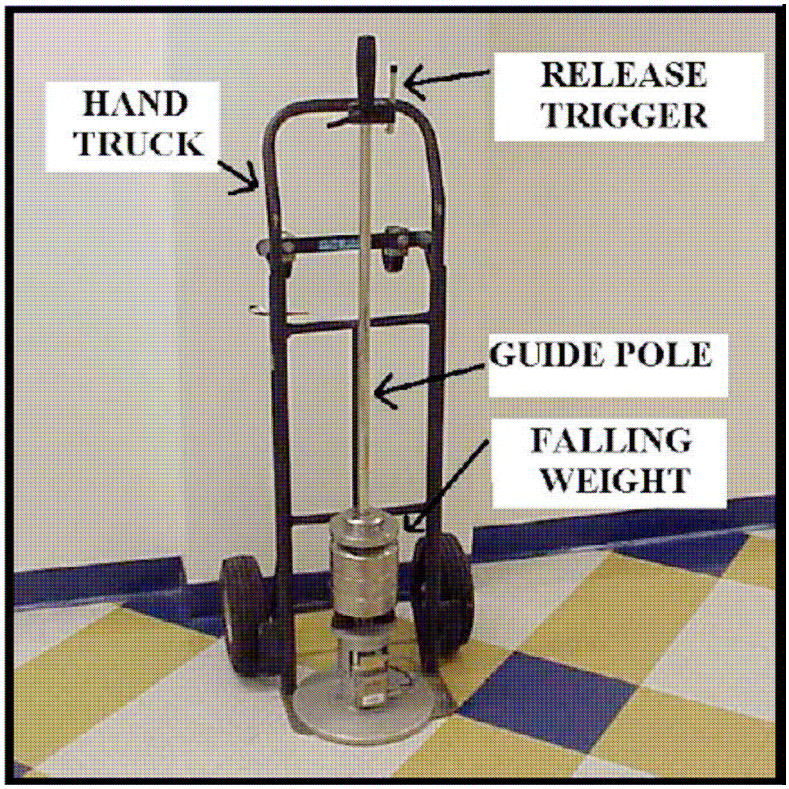

FIGURE 3-11 Dynatest Prima 100 PFWD

The impact load is transmitted to the pavement by a circular plate (200mm or 300mm diameter) in contact with the wearing surface during testing, allowing the stress waves to propagate in the pavement. A load cell measures the applied load time history and a central geophone (vertical transducer) captures the velocity in the center of the circular plate, which is then converted into a deflection value. Those measurements are automatically stored in a Personal Digital Assistant (PDA) through Bluetooth connection [Dynatest International 2004]. The PFWD device used to carry out the testing is the property of the University of Waterloo/ Centre for Pavement and Transportation Technologies (CPATT). The sensors (load cell and geophone) were calibrated by Dynatest Denmark on October 6, 2005.

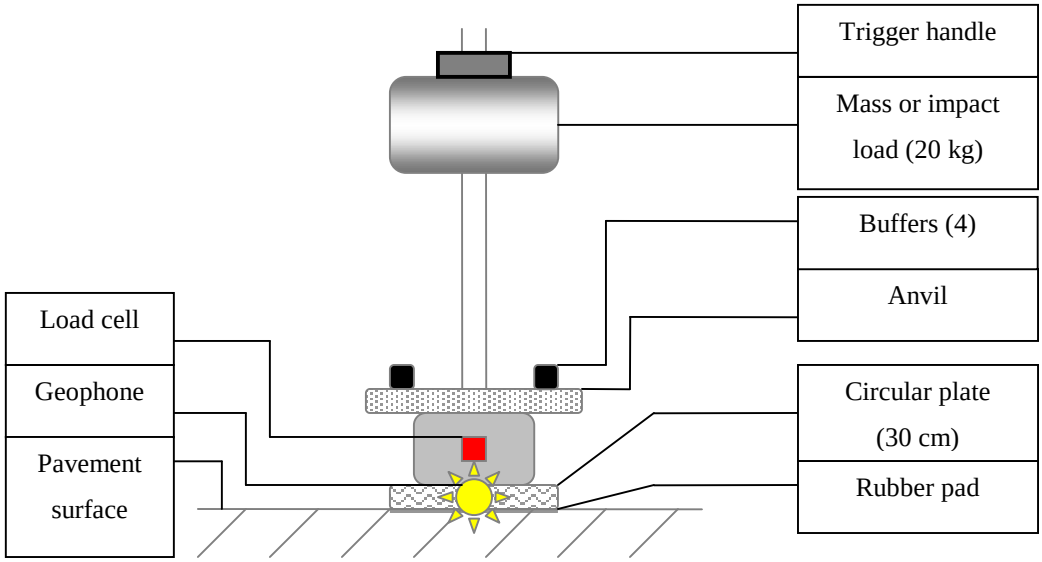

FIGURE 3-12 Schematic representation of the PFWD

3.2.2 Objectives of the PFWD Testing

As presented in section 2.4, many transportation agencies perform deflection testing on their roads as the weather starts to warm up in the spring to track loss of bearing capacity periods. The use of the PFWD is very limited compared to the use of BBR or FWD, but this testing method need to be evaluated. Therefore, the objective of collecting pavement deflection data throughout the 2007 spring thaw was to examine if PFWD measurements could be used to identify critical shifts in the pavement bearing capacity and ultimately correlate to the depth of frost in the soil.

3.2.3 Procedure and Schedule

Testing was scheduled to occur once a week throughout spring time on the Northeastern experimental site. No deflection testing was performed on the Northwestern site for practical reasons, including the fact that transporting the PFWD device back and forth between the two far-apart locations could cause damage to the load cell and deflection sensor. Ideally, PFWD testing should have been carried out on the Northeastern experimental site throughout spring time and further to capture pavement strength recovery. The testing started at the beginning of March 2007, but as the PFWD device was needed by other CPATT projects, data collection had to end on the last week of March 2007. Four weeks worth of data (testing once a week on six different point locations) were collected and analyzed to see how PFWD measurement changed from one week to the other and if this change was significant compared to spatial variations.

As pavement sections with surface discontinuities such as cracks or joints will generally exhibit higher deflections than a pavement section without those discontinuities [FHWA-LTPP 2000], testing locations were selected in such a way that deflection measurements were not biased by testing only crack-free areas or only cracked areas. On each of the 6 test points presented on FIGURE 3-13 below,

six identical measurements (replicates) were performed. Similarly to the thermistor probes, the points were located on the centre line.

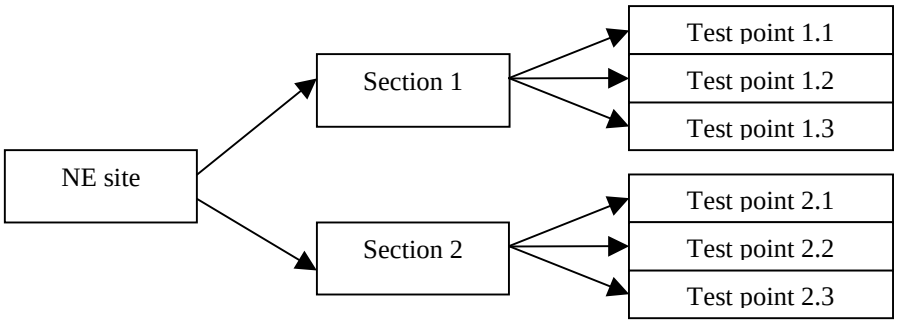

FIGURE 3-13 Location IDs for PFWD Testing

In order to guide the MTO operators in charge of the testing, technical information was retrieved from the user manual and updated with the findings of a recent study that involved the Prima 100 PFWD [Kestler 2005]. Guidelines were compiled into a testing procedure document (see Appendices F and G). In addition, a trip to the site was organized with the objectives of marking the test points and tutoring the first series of testing and data acquisition (see photos below).

FIGURE 3-14 PFWD Testing Tutorial on the NE Experimental Site (Hwy 569, March 8, 2007)

3.2.4 Data Analysis

As per the procedure provided in Appendix F, deflection data is transmitted via Bluetooth technology to a PDA and downloaded to a laptop where it is converted into Excel format. The Prima 100 PFWD internally converts deflection measurements into the elastic moduli through the PRIMADESIGN/ LWMOD backcalculation routine [Dynatest International 2004]. In accordance with the recommendations [Kestler 2005], the first step to carry out on each set of measurements taken on a particular spot is to neglect the results of the first drop and perform an average of the five other drops

to get a value that is representative of the spot. Also, as explained in section 2.4.2, the deflections should be corrected for temperature before any further analysis is performed.

3.3 Numerical Simulation of SLR using the MEPDG Software

3.3.1 Objective of the Analysis

In order to examine how the performance of low volume flexible pavements is affected by Northern Ontario's specific climatic and traffic constraints and to evaluate the benefits of implementing load restrictions on those roads, the Mechanistic-Empirical Pavement Design Guide (MEPDG) software v.0.9 was used to compute the key pavement distresses over a twenty-year design life. The physical condition of the pavement structure was evaluated in terms of fatigue cracking and rutting and the functional performance in terms of ride quality and comfort, using the International Roughness Index (IRI).

3.3.2 Determination of MEPDG Inputs

The MEPDG's three main categories of inputs are: traffic data, information on pavement structure and the climatic database required by the Enhanced Integrated Climatic Model (EICM) used within the MEPDG. The MEPDG can simulate the behavior of both new and rehabilitated structures at three input levels so that the designer can obtain these inputs with regard to the criticality of the project and the available data [Tighe 2005]. Level 1 enables the user to get the highest level of accuracy by requiring specific site and material information. Level 2 relies on values similar to the AASHTO Design Guides and provides the user with an intermediate level of accuracy. In this study, the MEPDG simulations were carried out on at Level 3 as it is suited to low volume pavements and allows nationally calibrated values (LTPP data) to be adopted when no other information is available [ARA 2004].

3.3.2.1 Pavement Structure Inputs

As part of an Ontario-based study about low-volume road performance, three typical low-volume pavement structures were identified using the Ministry of Transportation's Pavement Maintenance System (PMS/2) database and are represented on FIGURE 3-15 below [Ninguyan 2006].

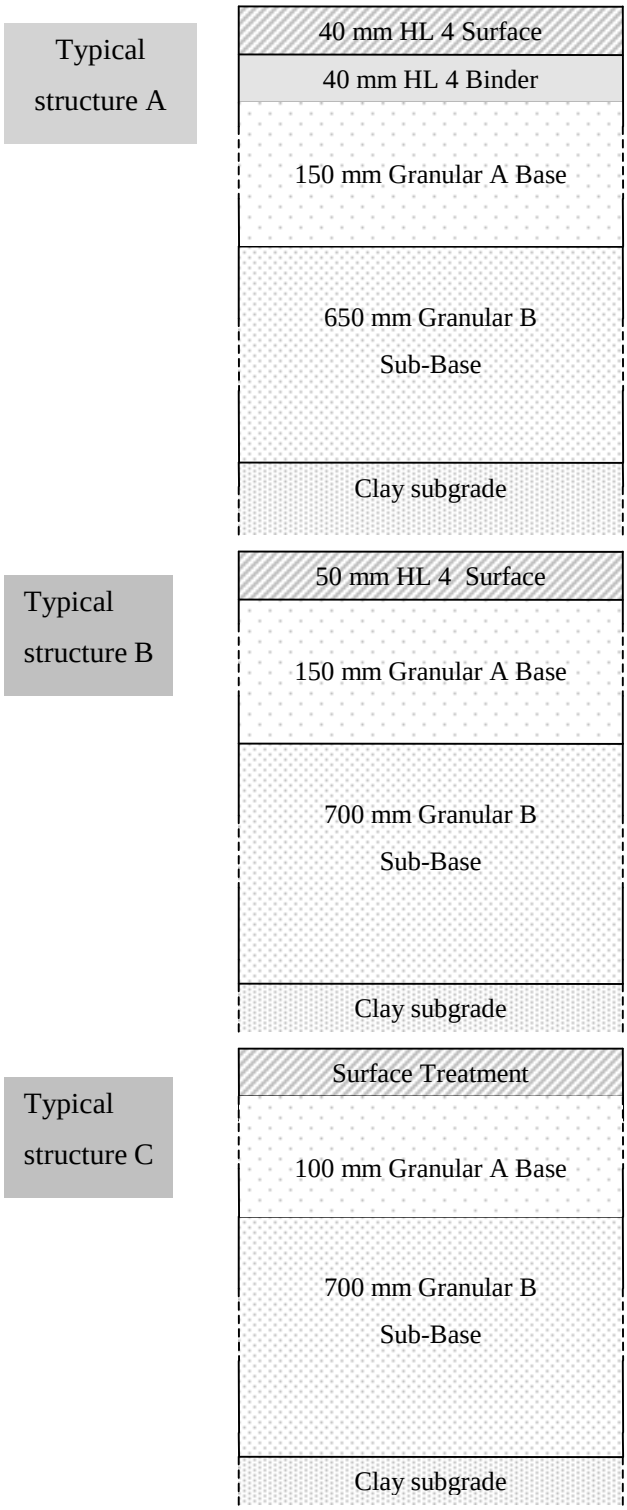

FIGURE 3-15 Typical Pavement Structures Used in Ontario for Low-Volume Roads

As the MEPDG software is not calibrated yet for surface-treated roads, only two cases were considered: Asphalt roads, and gravel roads that have been resurfaced with asphalt (see FIGURE 3-16 below). The MEPDG imposes that the user inputs the pavement structure by layers by specifying the nature and thickness of each layer. In the case of unbound materials, the site-specific sieve analysis

distribution and the compaction state can be entered. In the case of bound materials (asphalt-concrete), the binder and aggregates properties are specified. Both roads received a thin asphalt overlay in year number ten of their design life (starting arbitrarily from August 1980). In accordance with the Ontario Provincial Standards Specifications (OPSS), a Superpave PG 58-34 binder was selected to represent the HL 4 conventional asphalt mix.

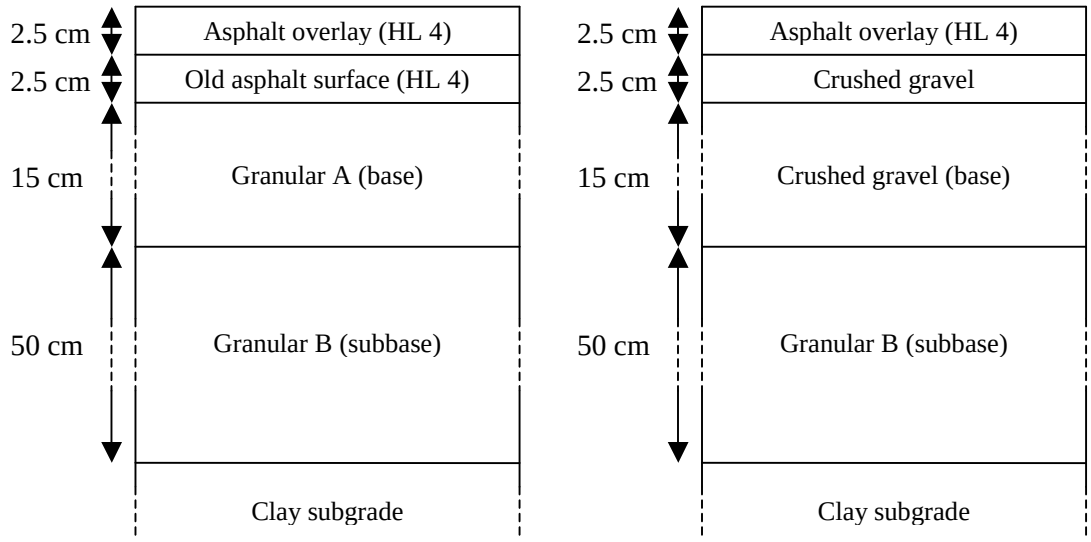

FIGURE 3-16 Typical Pavement Structures used in the MEPDG Analysis (left: “asphalt road”; right: “gravel road”)

3.3.2.2 Climatic Data

3.3.2.2.1 Requirements of the Enhanced Integrated Climatic Feature (EICM)

The EICM feature of the MEPDG (presented in section 2.5.4) requires years of hourly climatic data (temperature, precipitation, solar radiation, cloud cover and wind speed) for the location of the study site. When it is not available for this site, the MEPDG is able to generate a climatic file estimate by interpolating weather data from the stations surrounding the site. Therefore, fifteen years worth of data (1990-2005) were retrieved from fourteen Canadian stations (data provided by Environment Canada) and from eighty-three Northern USA stations (data provided by United States National Cooperative Highway Research Program [NCHRP 2007]), and then formatted according to the EICM requirements [EICM 2006]. Provided in Appendix H is the list of weather stations initially entered in the software.

3.3.2.2.2 Sources of Climatic Data

Climatic data was retrieved for the two experimental sites (Northeastern, Northwestern) from the Environment Canada database as it contains the regular twenty-minute interval data required by the EICM. Variables of interest including ‘Dry bulb temperature”, “Relative Humidity”, “Cloud Amount”

and “Wind Speed” were retrieved from 1990 to 2006 for the two nearest weather stations (Thunder Bay Airport for the Northwestern pilot site and Earlton Airport-Station for the Northeastern one). Environment Canada weather stations changed from Human observations to an Automated Weather Observing Site (AWOS) in 2005 and data in the new digital format was available from 2000 on. However, the files retrieved for the 1900-2000 period contained gaps (night hours) that required a time demanding tracking and several interpolations to fill the missing observations.

3.3.2.2.3 Interpolation of Climatic Data

The MEPDG is capable of creating a virtual weather station from up to six nearby existing stations by interpolating from the available ones. On the one hand, a climatic database for seventeen stations across Canada had been developed previously in the year as part of the Canadian Climatic Sensitivity Analysis Project. On the other hand, the NCRHP MEPDG website provides the user with all the climatic files that are necessary to run the analysis within the United States and its possessions. To generate a climatic file specific to each of the two studied site, the MEPDG selected four locations in Canada and eight locations in Northern U.S.A. The twelve stations are listed in TABLE 3-4 below.

TABLE 3-4 MEPDG Selection of Weather Stations for Spatial Interpolation

Study site	Coordinates	Stations selected for interpolation and distance from study site to weather station.
Northeastern region	Latitude: $48^0$10’ Longitude: -$80^0$00’ Elevation: 1040 ft	1. North Bay International Airport, ON - 109.1 miles 2. Ottawa International Airport, ON - 262.1 miles 3. Toronto Lester B. Pearson International Airport, ON - 287.7 miles 4. Toronto Buttonville International Airport, ON - 288.3 miles 5. Pellston Regional Airport, MI - 289 miles 6. Ostego County Airport, MI - 311.4 miles
Northwestern region	Latitude: $49^0$20’ Longitude: -$89^0$00’ Elevation: 459.3 ft	1. Houghton County Memorial Airport, MI - 151.5 miles 2. Falls International, MN - 206.4 miles 3. JFK Memorial Airport, WI -211.6 miles 4. Chisholm-Hibbing Airport, MN - 221.4 miles 5. Duluth International Airport, MN - 226.6 miles 6. Ford Airport, MI - 246.3 miles

3.3.2.3 Traffic Loading

3.3.2.3.1 Baseline Scenarios

Typical traffic volumes associated with the two experimental sites were retrieved from the Ministry of Ontario historical archives, in which the Annual Average Daily Truck Traffic (AADTT) is defined as "the twenty-four hour two-way traffic volume, averaged for the period of January 1st to December 31st"[MTO 2004]. The traffic volumes were then converted into equivalent single axle loads with default load distributions for each of the 4 to 13 traffic classes used in the MEPDG software. TABLE 3-5 below summarized the baseline scenarios inputs.

TABLE 3-5 Baseline scenarios used in the MEPDG Analysis

Typical Region	Northwestern		Northeastern	
Latitude	$48^0$10'		$49^0$20'	
Longitude	-$80^0$00'		-$89^0$00'	
Elevation	317 m		140 m	
Pavement type	AC road	Gravel road	AC road	Gravel road
Traffic inputs	Highway 527		Highway 569	
2-way AADTT	200		500	

3.3.2.3.2 SLR Scenarios

In accordance with the MTO load restrictions policy [Highway Traffic Act 1990], the simulation of SLR throughout the 20-year design life of the pavement was achieved by setting the axle load distributions factors equal to zero during a certain number of months for all the loads exceeding 5,000 kg (11,000 lbs to 41,000 lbs). Since the total volumes were kept constant, the axle load distribution factors had to be adjusted for loads 3,000 lbs to 10,000 lbs so that the sum of all the factors equals to 100%. It should be noted that the MEPDG software does not allow the user to change the distribution factors for periods less than one month. TABLE 3-6 below summarizes the various SLR scenarios (from February to June, one to five-month periods of SLR) that were simulated for each of the four typical sections presented in TABLE 3-5.

TABLE 3-6 Spring Load Restriction (SLR) Scenarios

Scenario	SLR in Feb.	SLR in March	SLR in April	SLR in May	SLR in June
1	NO	NO	NO	NO	NO
2	YES	NO	NO	NO	NO
3	NO	YES	NO	NO	NO
4	NO	NO	YES	NO	NO
5	NO	NO	NO	YES	NO
6	NO	NO	NO	NO	YES
7	YES	YES	NO	NO	NO
8	YES	YES	YES	NO	NO
9	YES	YES	YES	YES	NO
10	YES	YES	YES	YES	YES
11	NO	YES	YES	NO	NO
12	NO	YES	YES	YES	NO
13	NO	YES	YES	YES	YES
14	NO	NO	YES	YES	NO
15	NO	NO	YES	YES	YES
16	NO	NO	NO	YES	YES

3.3.2.4 Summary of inputs

As schematized on FIGURE 3-17 below, a total of $2 * 2 * (1 + 15) = 64$ different sets of MEPDG inputs were generated.

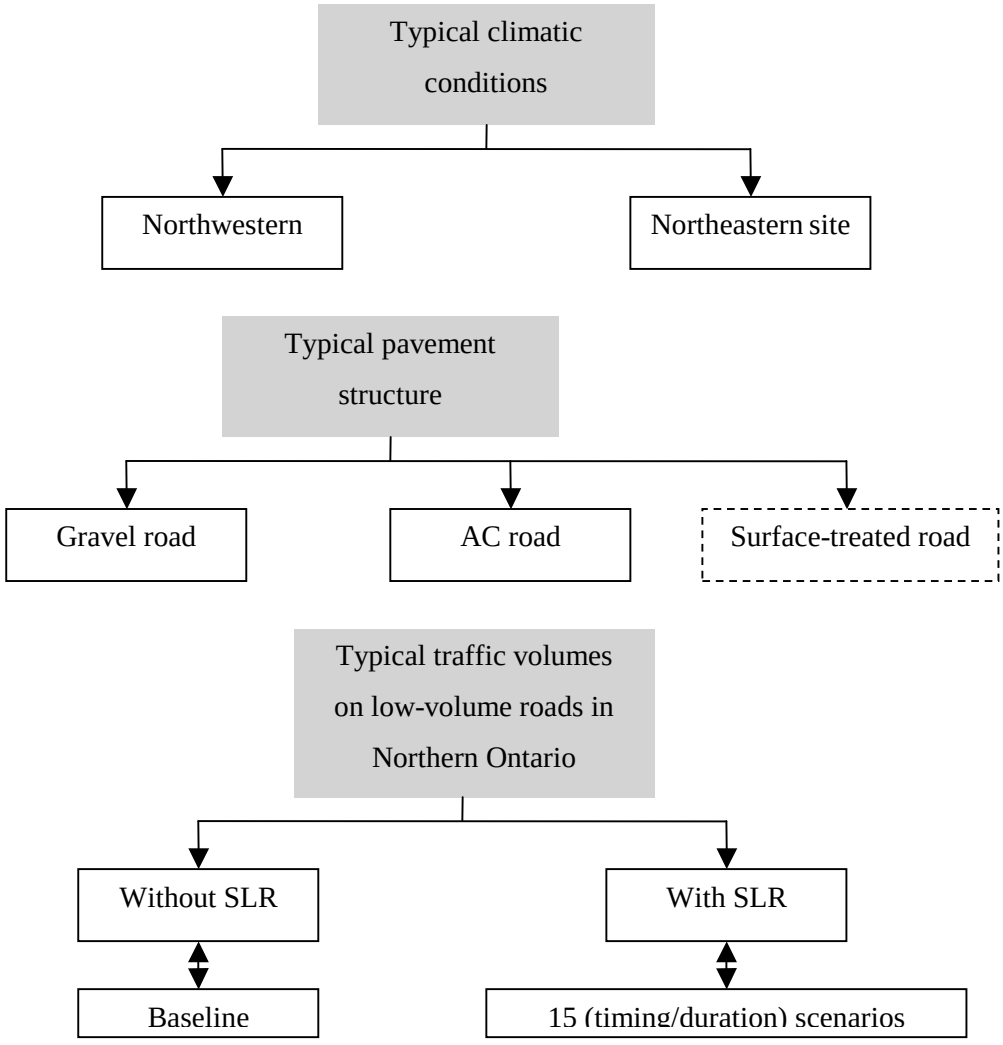

FIGURE 3-17 Summary of MEPDG Inputs

3.3.3 Analysis of the MEPDG Outputs

Once the pavement and climatic inputs were determined and several traffic scenarios generated, the MEPDG simulations were launched and the outputs retrieved. The pavement performance indicators of International Roughness Index (IRI), cracking (longitudinal and transverse) and rutting were compared for various SLR scenarios, with the no-restrictions case as the baseline. Special attention was given to the conversion of all the MEPDG software outputs from Imperial to Metric units.

3.3.3.1 Surface Roughness (IRI)

Surface roughness can be described as the human-vehicle-pavement interaction. It is an important parameter for managing road networks and ensuring safety. An absolutely perfect pavement profile, one with no vertical displacements, has an IRI (International Roughness Index) value equal to 0 m/km. The smoothness of the road decreases as the index value increases. At an IRI value greater than 2.15 m/km (design threshold used in this study), the pavement is in poor condition and riding over it becomes uncomfortable at speeds greater than 80 km/h [Tighe 2007].

3.3.3.2 Pavement Cracking

Pavement cracking is an important parameter for indicating wear. For the purpose of this analysis, it can be divided into fatigue cracking and thermal cracking, depending on how the crack was initiated (load associated versus environment associated). For example, excessive fatigue cracking can be related to overloading while thermal cracking is environment related. Once a crack is initiated, its depth will start growing depending on traffic volume, environment, etc., and its width will increase as water infiltrates the pavement and induces contraction/expansion movements [TAC 1997].

Fatigue cracking occurs when the maximum number of loads repetitions that the pavement can resist is reached. Reducing the stiffness of the asphalt can help the pavement structure be more resistant to bending stresses and thus exhibit less fatigue cracking. Top-down and bottom-up cracking are the two mechanisms responsible for fatigue cracking.

Longitudinal cracking refers to cracks that are initiated from the top layer of the pavement structure, down. These cracks are parallel to the centerline of the roadway, but if they happen to be located in the wheel tracks, they can also lead to Alligator cracking.

Alligator cracks begin as individual longitudinal cracks, and if not treated, they become interconnected and form a pattern similar to the skin of an alligator. This is a very serious structural condition which can only be cured through rehabilitation. Reflective cracking refers to cracks that are initiated from the bottom of an asphalt layer, and reflect up to the surface. It usually occurs in pavement overlays that were placed over unprepared pavements in poor condition. It can also occur when and asphalt is placed on top of an existing concrete pavement which has working joints.

Transverse cracking refers to cracks that are perpendicular to the centerline of the roadway. The more these cracks are separated from one another, the more lateral movement the crack will exhibit. Transverse cracking is caused by temperature changes which induce tensile stresses within the pavement structure and leads to material shrinkage. Decreasing the stiffness of the Hot-Mix-Asphalt (HMA) binder or increasing its thickness can help prevent this type of cracking.

Rutting is a permanent depression in the surface of the asphalt pavement. When the rutting is severe, the edges of the rutted area may be elevated. In warm conditions, if the loading occurs at low frequencies and high amplitude (e.g. slow moving heavy traffic) and if the HMA binder is not stiff enough, its dynamic modulus will suffer from viscosity changes and permanent deformation of the HMA layer within the vehicle wheel path will happen. Rutting can be a safety concern particularly on truck routes and should be addressed. In addition, rutting can cause hydroplaning as the water remains in the depressions. Moreover, when the subgrade is frost susceptible (fine grained subgrades such as

clay or silt soils), a high number of freeze-thaw cycles can result in rutting as the subgrade deforms under the pavement.

Chapter 4

ANALYSIS AND RESULTS

4.1 Model Enhancements

4.1.1 Starting Point

4.1.1.1 Qualitative Observations

Plots of the Freezing and Thawing indices over time from November 10, 2005 to April 19, 2006 (see FIGURE 4-1 below) showed the following: before a significant rise starting around mid-March, the TI was mostly equal to 0°C-days, except from December and a few random days when it displayed relatively small values. The FI rose continuously, almost linearly until mid-March when it started to decrease following a similar trend.

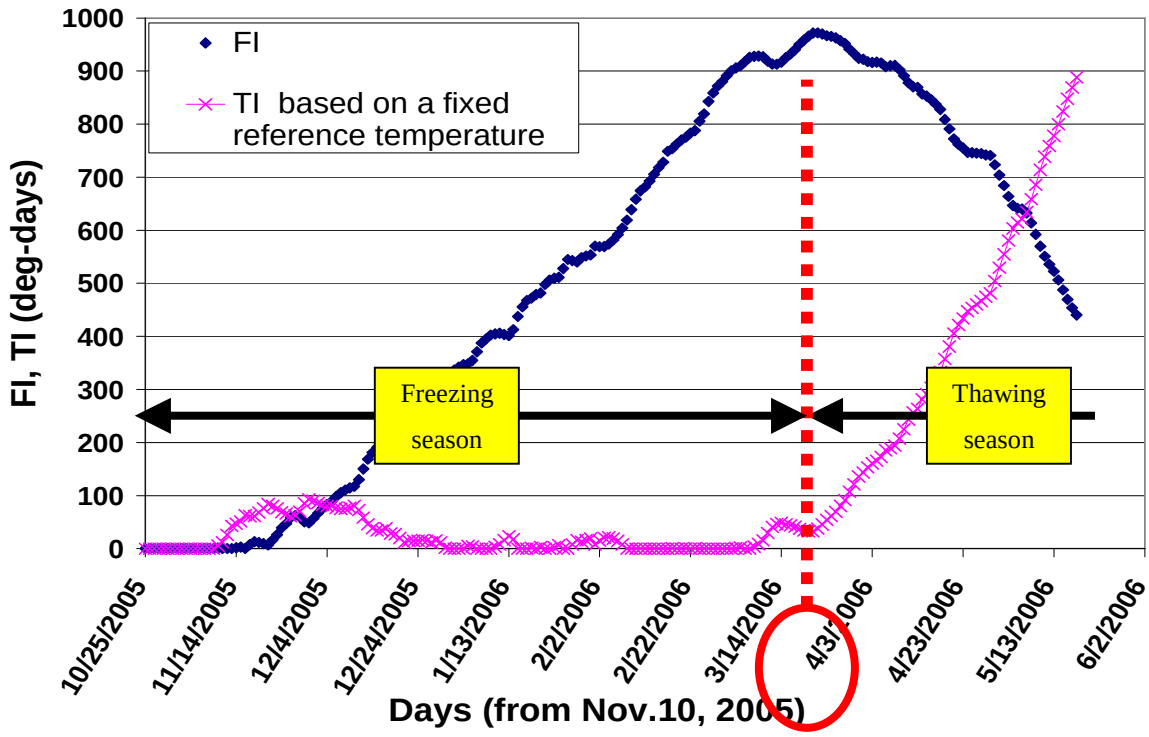

FIGURE 4-1 FI and TI Trends (Northeastern Experimental Site)

A possible explanation for these trend shifts was proposed: As the moisture located in the pavement freezes rapidly, the FI rises as a result and the TI stays equal to 0°C-days. Then spring-thaw season arrives by mid-March, frost in the pavement thaws progressively. As a result, the FI decreases while the TI increases. The positive TI values that were observed during the freezing season could be due to

the high number of freeze-thaw cycles experienced in that region, which would cause the upper part of the pavement to freeze but still partially thaw.

4.1.1.2 Initial Hypotheses

From these remarks, a new approach for the estimation of the depth of frost and the depth of thaw in the pavement was developed. As a starting point, a few initial hypotheses are listed below:

The amount of frost in the pavement results from both freezing and thawing. Therefore, it is likely to be related to both the FI and the TI.

As the preliminary analysis showed good correlation between the depth of frost and $\sqrt{FI}$ (relationship initially found by Chisholm and Phang 1977) the variables that are potentially involved in the estimation of the depths of frost and thaw would be $\sqrt{FI}$ and $\sqrt{TI}$.

As the TI calculation is based on a the reference temperature, which is constant related to the temperature gaps between the air and the pavement over a given period, a modification of the calculation of this constant could be investigated in order to smooth the " freeze-thaw" effects observed on the left portion of the TI plot on FIGURE 4-1. The purpose of this would be to use FI and TI plots to empirically identify the freezing season (rise in the FI while the TI equals 0°C-days) and the start of spring-thaw (rise in the TI as opposed to the FI).

FIGURE 4-2 below summarizes the calculation steps developed during this thesis in order to finalize the model.

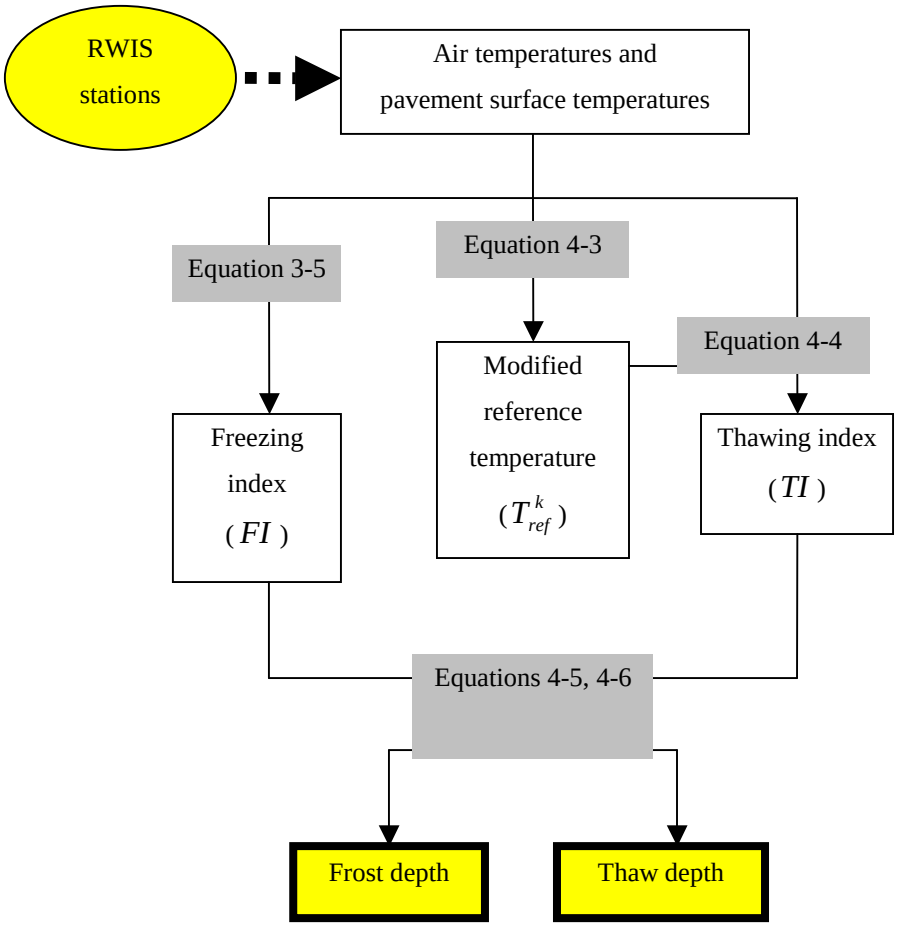

FIGURE 4-2 Steps for Frost and Thaw Depths Calculation using the Complete Model

4.1.2 Modification of the Reference Temperature Calculation

The reference temperature calculation presented in section 3.1.4.2 is based on approximately seven months of RWIS data. The approach proposed herein is to calculate the reference temperature based on one month of daily RWIS data in order to indicate more clearly the duration of warmer weather and its effect on the pavement surface. Equations 4-1 to 4-3 below are derived from this statement. In other words, the reference temperature is updated on a monthly basis.

$$\overline{T_{Air}^{k}} = \sum_{i=1}^{N_k} T_{Air_i} \qquad \textbf{4-1}$$

$$\overline{T_{Sfc}^{k}} = \sum_{i=1}^{N_k} T_{Sfc_i} \qquad \textbf{4-2}$$

$$T_{ref}^{k} = \overline{T_{Air}^{k}} - \overline{T_{Sfc}^{k}} * \frac{\sum (T_{Sfc_i} - \overline{T_{Sfc}^{k}}) * (T_{Air_i} - \overline{T_{Air}^{k}})}{\sum (T_{Sfc_i} - \overline{T_{Sfc}^{k}})^2} \qquad \textbf{4-3}$$

Where T_{ref}^{k} Reference temperature (in °C) for month k

N_k Number of days in month k

T_{Air_i} Air temperature value on the site on day i

T_{Sfc_i} Surface temperature value on the site on day i

Again, the reference temperature can be obtained by determining the y-axis intercept based on a best-fit regression line plotted through a set of x-values (the N_k values of surface temperature found in month k) and y-values (the N_k values of air temperature found it month k). The function "intercept" available on Excel is able to calculate such a constant. The reference temperature values associated with different months in 2005/2006 are plotted on FIGURE 4-3 below.

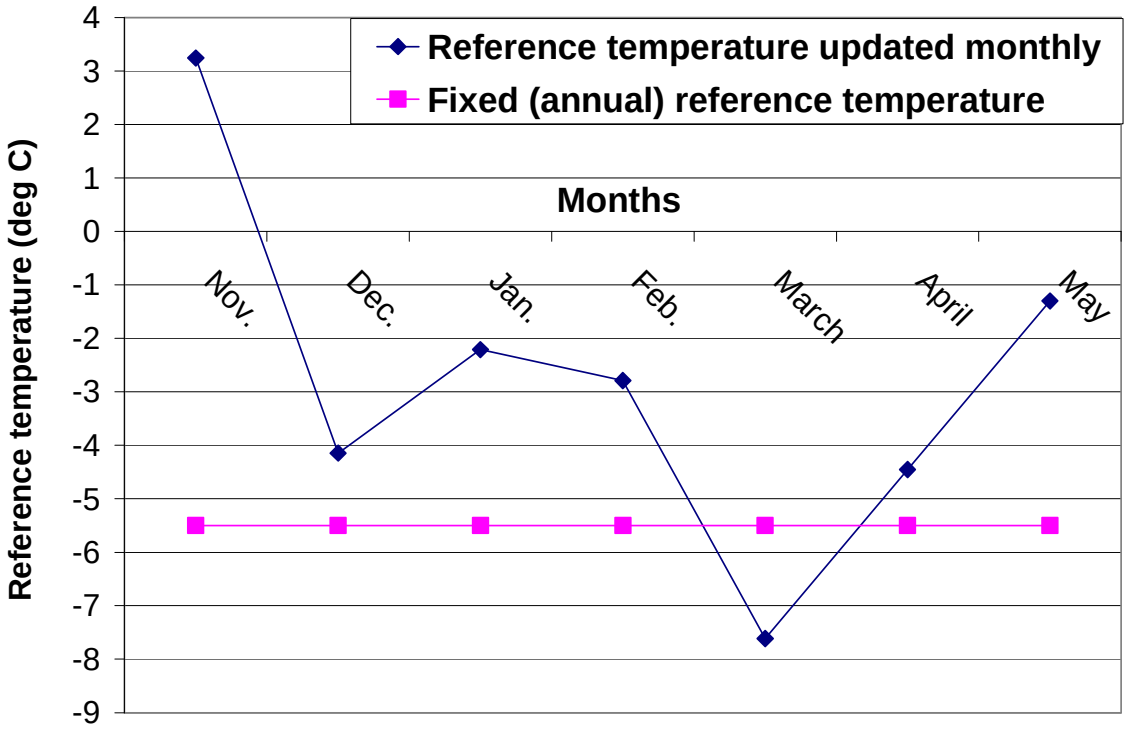

FIGURE 4-3 Fixed versus Monthly-updated Reference Temperature

The Thawing Index is calculated using Equation 4-4 using a "monthly-updated" reference temperature.

$$\begin{cases} TI_0 = -T_{ref}^{k} \\ TI_{i+1}^{k} = T_{i+1} - TI_i^{k} \\ TI_i^{k} < 0 \Rightarrow TI_i^{k} \equiv 0 \end{cases} \qquad \textbf{4-4}$$

Where i Number of days after the day indexed as day $i = 0$

$i = 0$ Day on which T_{Air_i} first falls below 0^0C

TI_0 Thawing Index value on day $i = 0$ (in ^{0}C -days)

T_{ref}^k Reference temperature calculated for month k

TI_i^k Thawing Index value on day i (in ^{0}C -days) during month k

The TI plot associated with a fixed reference temperature and the TI plot associated with a monthly-updated reference temperature are represented on FIGURE 4-4 below.

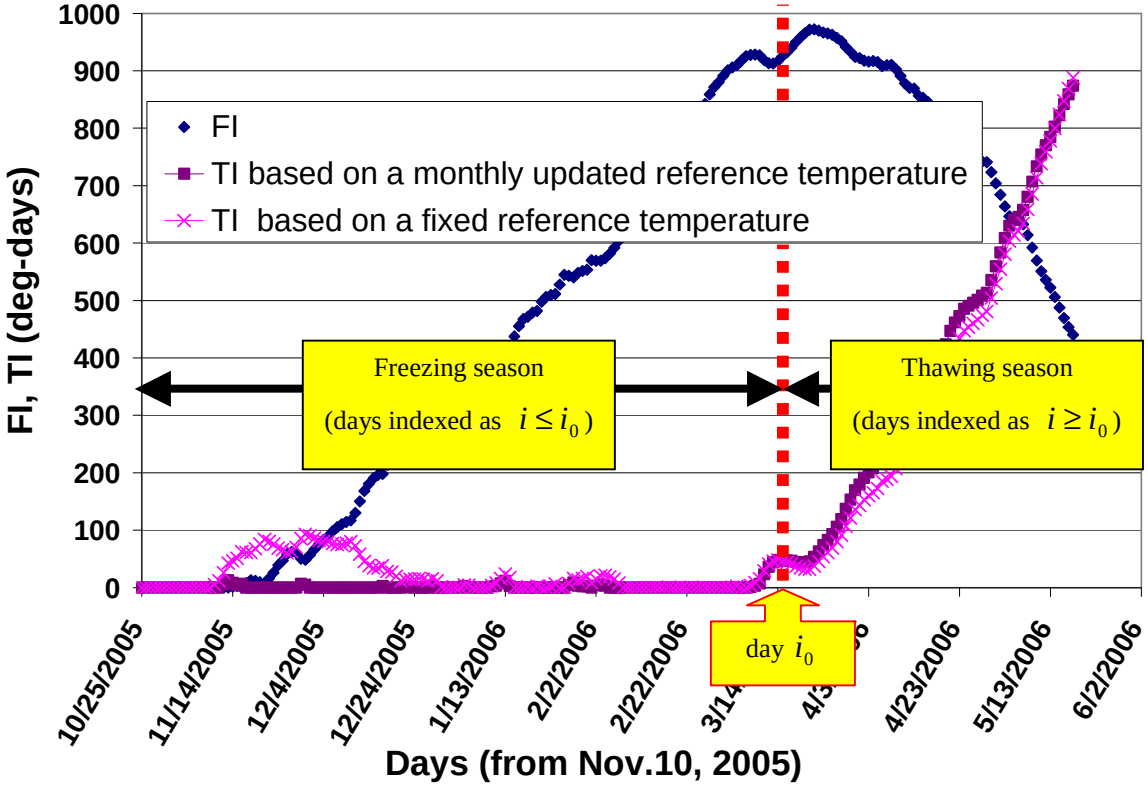

FIGURE 4-4 FI, TI and modified TI Trends (Northeastern Experimental Site)

FIGURE 4-4 shows than the trend of the TI that is based on a monthly-updated reference temperature is smoother that the trend of the TI that is based on a fixed reference temperature. The later TI displayed positive values during the freezing season. With the new reference temperature calculation, this phenomenon seems to be attenuated and the TI plot linear during a “freezing season” period and a “thawing period”, the transition from one to another occurring on a day indexed as day i_0 and used in the algorithms of frost and thaw depths prediction.

4.1.3 Predictors for the Depths of Frost and Thaw in the Pavement

The depth of the frost is very close to the total frost thickness during the first winter months since the ice develops from the top down. But at the onset of spring on, the frozen layers in the pavement begin to melt and also from top downwards. Models predicting the depth of frost as well as the depth of thaw were thus needed. As explained in section 4.1.1.2, a linear model that combines $\sqrt{FI}$ and $\sqrt{TI}$ can be proposed, as per Equations 4-5 and 4-6.

$$0 \le i \le i_0 \Rightarrow \begin{cases} FD_i = a + b\sqrt{FI_i} + c\sqrt{TI_i}) \\ TD_i = d + e\sqrt{FI_i} + f\sqrt{TI_i}) \end{cases} \quad \textbf{4-5}$$

$$i \ge i_0 \Rightarrow \begin{cases} FD_i = g + h\sqrt{FI_i} + i\sqrt{TI_i}) \\ TD_i = j + k\sqrt{FI_i} + l\sqrt{TI_i}) \end{cases} \quad \textbf{4-6}$$

Where i Number of days after the day indexed as day $i = 0$

$i = 0$ Day on which T_{Air_i} first falls below 0^0C

i_0 Day after which the TI consistently rises above 0^0C-days
(day of transition from Freezing season to Thawing season)

FD_i Depth of frost on day i (from the pavement surface, negative, in cm)

TD_i Depth of thaw on day i (from the pavement surface, negative, in cm)

FI_i Freezing Index value on day i (in ^{0}C -days)

TI_i Thawing Index value on day i (in ^{0}C -days)

a, b, c, d, e, f Calibration coefficients used during the Freezing season

g, h, i, j, k, l Calibration coefficients used during the Thawing season

The unique, site-specific coefficients used in this model account for the fact that the depth and duration of the frost penetration in the soil depend largely on the amount of precipitation on the site and on the moisture sensitivity of the materials that constitute the pavement structure. On each site, twelve coefficients can be calculated using statistical linear regression methods and best-fit algorithms such as the least squares estimation method. The transition from the use of the firsts set of coefficients (a, b, c, d, e, f) to the other (g, h, i, j, k, l) allows a natural transition from a period of predominant freezing to a period during which the thawing phenomenon gradually overcomes the freezing process, until all the frost present in the pavement has thawed.

4.1.4 Results of the Best-fit Statistical Analysis

Using the least squares estimation method to fit the model to the field data led to the values that have been incorporated in Equations 4-7 and 4-8 below. With only one season worth of field frost data to calibrate the model on the Northeastern experimental site, there is limited confidence that the coefficients generated can be used to predict future frost depth and thaw depth values on the site.

$$0 \le i \le i_0 \Rightarrow \begin{cases} FD_i = -22.1 - 4.2\sqrt{FI_i} - 2.6\sqrt{TI_i}) \\ TD_i = -0.495 + 0.038\sqrt{FI_i} - 0.675\sqrt{TI_i}) \end{cases} \quad \textbf{4-7}$$

$$i \ge i_0 \Rightarrow \begin{cases} FD_i = -145 - 0.85\sqrt{FI_i} - 0.01\sqrt{TI_i}) \\ TD_i = 848 - 24\sqrt{FI_i} - 13\sqrt{TI_i}) \end{cases} \quad \textbf{4-8}$$

Where i Number of days after the day indexed as day $i = 0$

$i = 0$ Day on which T_{Air_i} first falls below 0^0C

i_0 Day of transition from Freezing season to Thawing season

(around March 27, 2006 as per FIGURE 4-4)

FD_i Depth of frost on day i (from the pavement surface, negative, in cm)

TD_i Depth of thaw on day i (from the pavement surface, negative, in cm)

FI_i Freezing Index value on day i (in ^{0}C -days)

TI_i Thawing Index value on day i (in ^{0}C -days)

FIGURE 4-5 below illustrates the frost and thaw trends observed on the Northeastern experimental site as well as the fitted frost model.

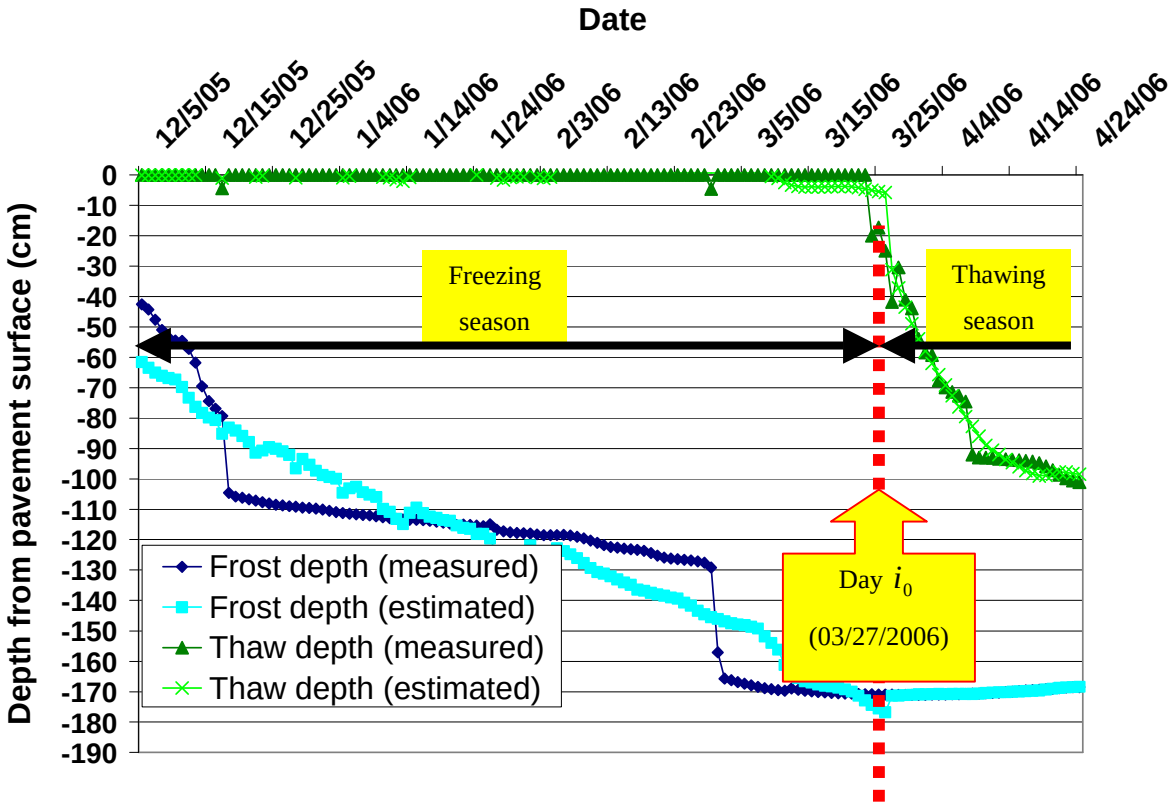

FIGURE 4-5 Measured vs. Estimated Frost Trends (Northeastern Experimental Site)

The plots above support the overall choice of the variables included in the model. The coefficients of determination for the depth of frost model and the depth of thaw model and were found to be 91% and 99.2% respectively. F-tests testing the overall significance of the models were positive with a 95% confidence level.

4.2 Utilization of the PFWD Data

As outlined in section 3.2.3, four series (four sample dates in a 7-week sampling period) of deflection data was collected on the Northeastern experimental site using the portable Falling Weight Deflectometer, and the modulus replicates were averaged to represent each of the six test point locations defined in FIGURE 3-13. A plot of these moduli against time is shown FIGURE 4-6.

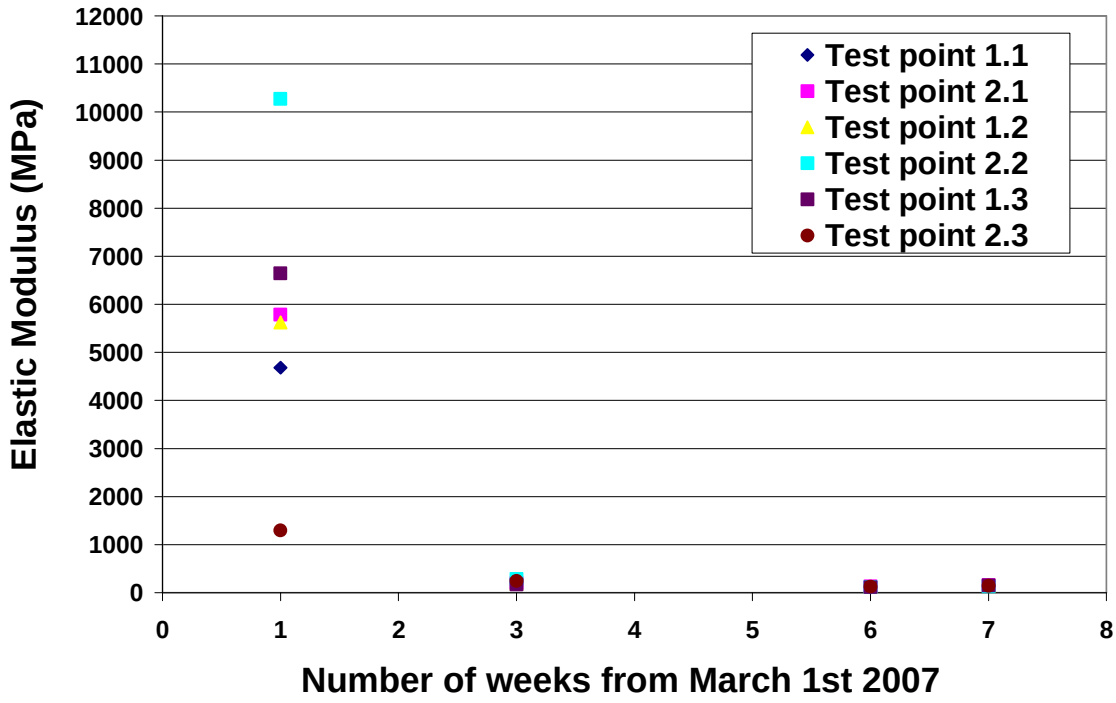

FIGURE 4-6 Elastic Modulus Trends throughout the Thawing Season (NE Experimental Site)

Also, the depths of frost and thaw associated with the four days of PFWD testing were calculated using the models presented in section 4.1.4. Frost thickness was obtained by calculating the difference between the depth of frost and the depth of thaw. This data was gathered in TABLE 4-1, alongside elastic modulus values that were calculated by summing each average with two times its associated standard deviation.

TABLE 4-1 Deflection and Frost Data over Time during Spring-Thaw Season

Weeks from 3/1/2007	Date	E (Mpa)	Depth of frost (cm)	Depth of thaw (cm)	Frost thickness (cm)
1	3/8/2007	7298	-150.3	-58.9	91.4
3	3/23/2007	302	-118.4	-66.4	52.0
6	4/11/2007	140	-99.5	-88.5	11.0
7	4/18/2007	168	-96.0	-96.0	0.0

Despite the insufficient amount of deflection data collected, a few observations can be drawn from FIGURE 4-6 and TABLE 4-1. Firstly, a dramatic drop in pavement strength occurred on most of the test points between week 1 (March 8, 2007) and week 3 (March 23, 2007). In the meantime, frost thickness decreased of 39 cm, mainly as a result of a bottom-up thawing (32 cm decrease in the depth of frost). From week 3 on, pavement strength did not vary much, while frost in the pavement progressively dissipated. These results seem to indicate that spring-thaw weakening started between

week 1 and week 3 on this site, which is consistent with changes in the trends of FI and TI starting from March 20, 2006. Deflection testing was not pursued long enough to observe any recovery trend.

4.3 Results of the MEPDG Simulations

The objective of this task was to use the Mechanistic Empirical Pavement Design Guide (MEPDG) software to assess the impact of the timing and duration of SLR on pavement distress for typical Ontario low-volume roads.

4.3.1 Analysis Parameters

The MEPDG outputs of interest and their associated design thresholds [ARA 2004] are summarized in TABLE 4-2. These thresholds are commonly used as triggers for pavement repair, rehabilitation, and reconstruction decisions [ARA 2004]. To account for the various uncertainties in predicting future pavement deterioration, each performance criteria is evaluated based on a user-inputted reliability level, which is defined as the probability that the criteria stays smaller than its associated design threshold over the design period. In accordance with the Design Guide recommendations for low volume pavements [ARA 2004], a reliability level of 75% was selected for all the performance criteria.

TABLE 4-2 Analysis Parameters used in the MEPDG Application (20-year Design Life)

Performance criteria	Design threshold
Terminal IRI (m/km) given initial IRI of 1.578	2.15
AC Longitudinal Cracking (m/km):	189.4
AC Reflective Cracking (%):	45
AC Thermal Cracking (m/km):	18.94
Permanent Deformation (Total Rutting) (mm):	8.90

4.3.2 Baseline Results

Firstly, the four baseline cases were simulated using the MEPDG software and the inputs that were presented in sections 3.3.2. The MEPDG outputs were regrouped to plot FIGURE 4-7 and 4-8 below to visualize pavement performance associated with each of the four typical sections.

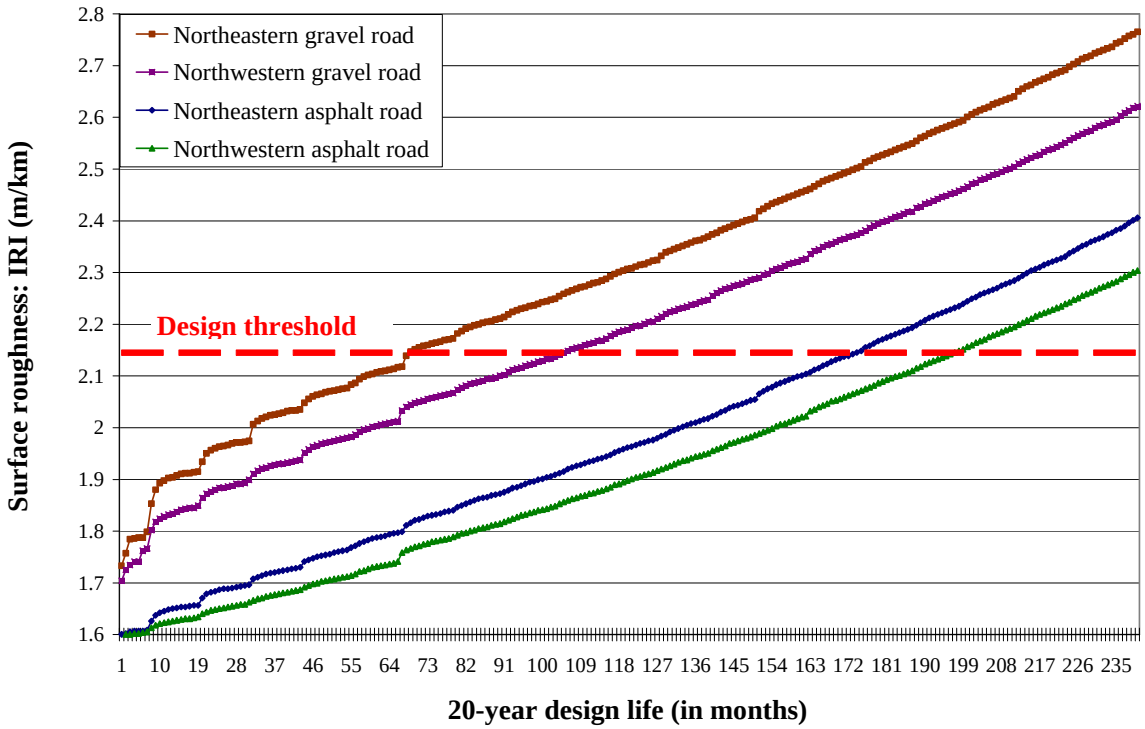

FIGURE 4-7 IRI Changes over a 20-year Design Life ("No SLR" Scenario)

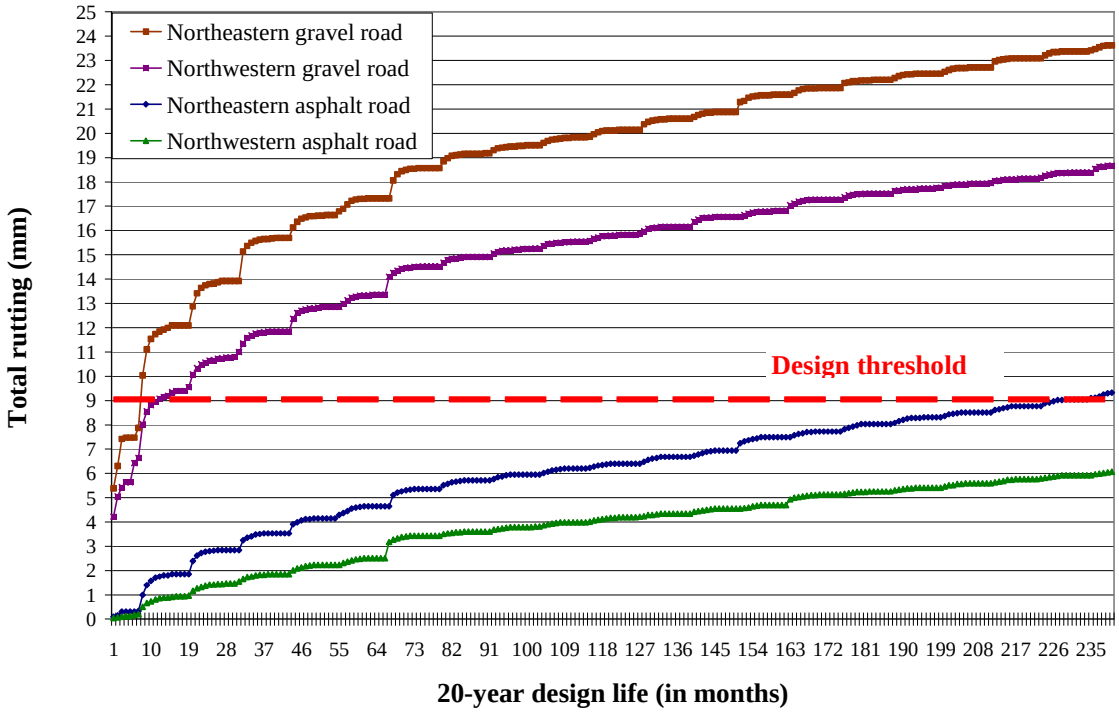

FIGURE 4-8 Rutting Changes over a 20-year Design Life ("No SLR" Scenario)

In the various MEPDG simulations, no thermal cracking was exhibited. This is largely related to the Superpave PG 58-34 binder of the HMA overlay. In short, the pavement performed very well under the environmental conditions used in the analysis. To check this assumption, this binder was replaced

by the traditional Superpave PG 64-22 and significant thermal cracking occurred on the very first year. Another explanation could be that the climatic files used as input were generated by interpolations from surrounding stations, but these stations were located at more than a hundred kilometers, and thus may not reflect the site-specific environmental conditions which are responsible for the thermal cracking observed in Northern Ontario. Hence, thermal cracking will not be considered in the rest of the analysis.

4.3.3 Results of the Various SLR Scenarios

The sixty-four MEPDG simulations were performed according to the load restriction scenarios defined in TABLE 4-3 below.

TABLE 4-3 Spring Load Restriction (SLR) Scenarios

Scenario	SLR in Feb.	SLR in March	SLR in April	SLR in May	SLR in June
1	NO	NO	NO	NO	NO
2	YES	NO	NO	NO	NO
3	NO	YES	NO	NO	NO
4	NO	NO	YES	NO	NO
5	NO	NO	NO	YES	NO
6	NO	NO	NO	NO	YES
7	YES	YES	NO	NO	NO
8	YES	YES	YES	NO	NO
9	YES	YES	YES	YES	NO
10	YES	YES	YES	YES	YES
11	NO	YES	YES	NO	NO
12	NO	YES	YES	YES	NO
13	NO	YES	YES	YES	YES
14	NO	NO	YES	YES	NO
15	NO	NO	YES	YES	YES
16	NO	NO	NO	YES	YES

The main purpose of the MEPDG simulations presented herein is to assess qualitatively the benefit of reducing loads during certain periods of the year in comparison to other periods of year, with the “no restrictions” case as the base line. The MEPDG outputs of interest are gathered and analyzed for each of the performance criterion used in the analysis (IRI, Longitudinal cracking, Reflective cracking and Total rutting) and for each of the four typical sites (Northeastern AC road, Northeastern Gravel road, Northwestern AC road and Northwestern Gravel road).

4.3.3.1 Time to Failure

FIGURE 4-9 below summarizes the results in terms of service life associated with the IRI criterion. Values greater than twenty years indicate that the design thresholds were not reached during the twenty-year design life.

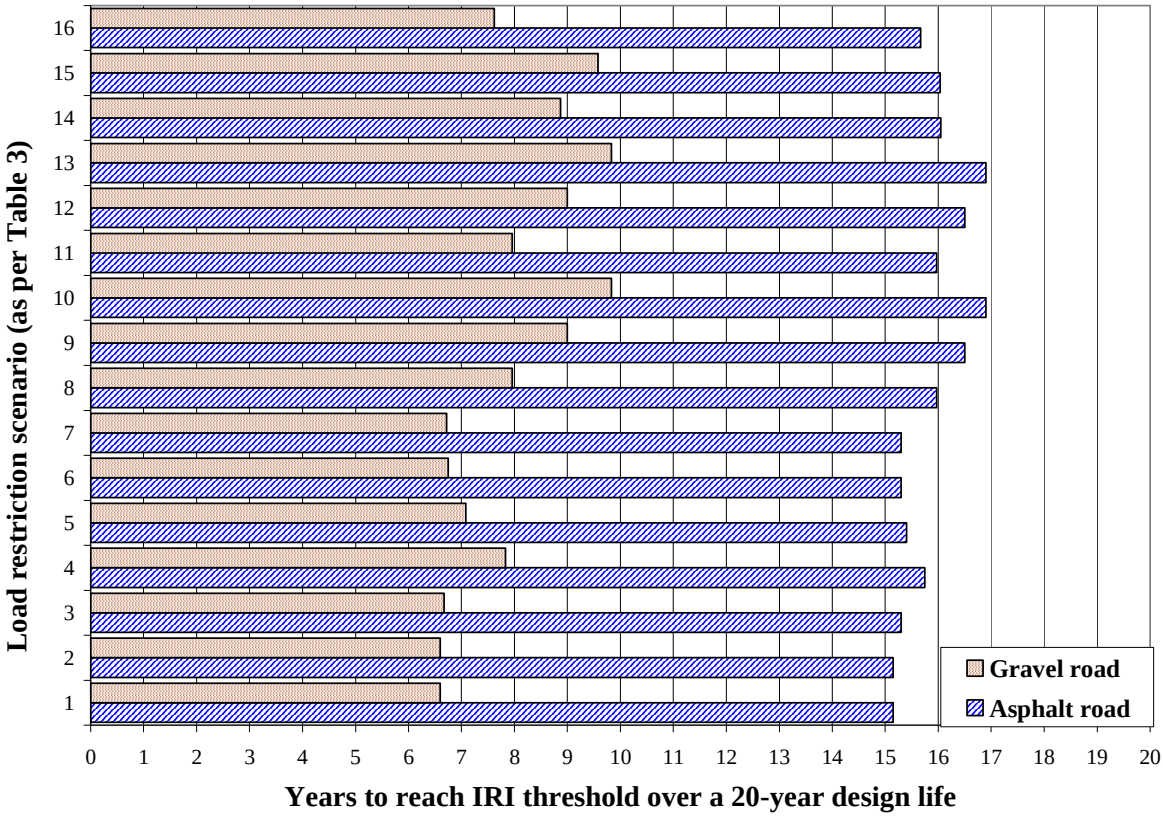

FIGURE 4-9 Number of Years to IRI Failure for the 16 SLR Scenarios (Northwest Region)

4.3.3.2 Terminal Values

In FIGURES 4-10 and 4-11 below, the terminal values of some performance criterion (values at year twenty) for each of the load restriction scenarios (scenarios #2 to #16 as defined in TABLE 4-3) are compared to the baseline cases (scenario#1: “No SLR” scenario).

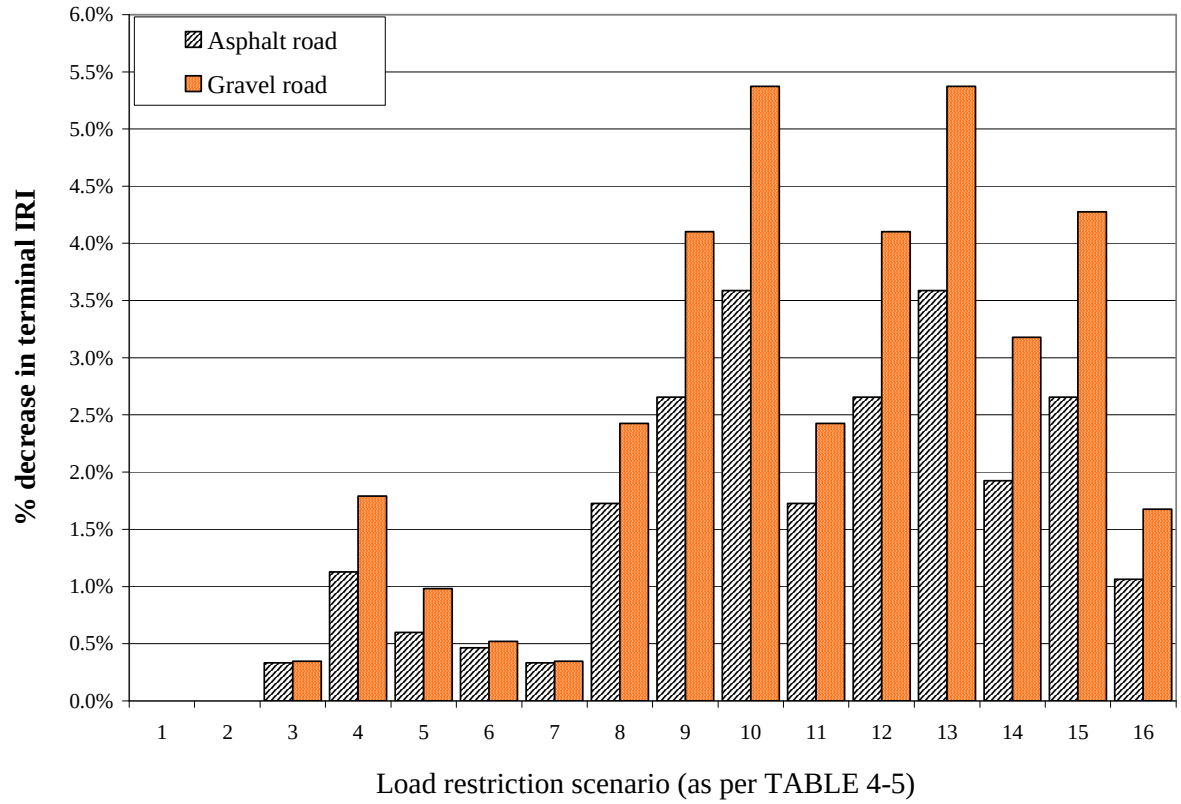

FIGURE 4-10 IRI Changes over the 16 SLR Scenarios (Northeast Region)

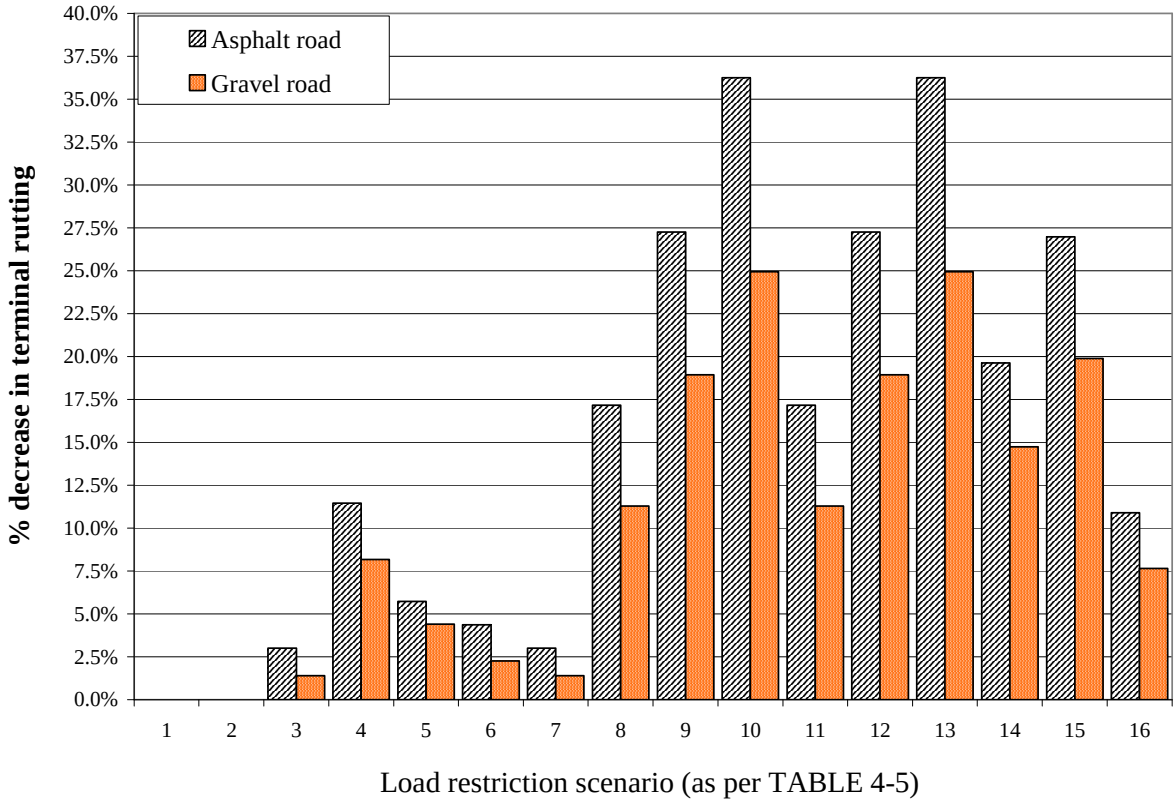

FIGURE 4-11 Total Rutting Changes over the16 SLR Scenarios (Northeast Region)

TABLE 4-4 below was calculated to summarize the service life values associated with the various criteria.

TABLE 4-4 Number of Years to reach the Design Thresholds on each Typical Section

Years to reach the performance limit	AC road		Gravel road	
	Northeast	Northwest	Northeast	Northwest
As per IRI criterion	15.2	17.1	6.6	9.6
As per longitudinal cracking criterion	13.8	>20	0	0
As per reflective cracking criterion	1.7	1.7	*	*
As per transverse cracking criterion	>20	>20	>20	>20
As per total rutting criterion	18.65	>20	0.62	0.83

* Reflective cracking is defined as cracking occurring in the HMA layer located below the AC overlay. Therefore, it is not defined on gravel roads with an overlay.

4.3.4 Conclusions based on the MEPDG Results

Firstly, it was found that the performance criterion providing us with the most information about the impact of load restrictions duration and scheduling on the pavement service life for both AC and gravel roads in Northern Ontario was the International Roughness Index, which reached its associated critical threshold with up to two years variation depending on the scenario. Longitudinal cracking changed consistently on Northeastern AC roads (up to six years of service life gained with scenarios #10, #13 and #15). Minimal differences were noted on gravel roads. This is not surprising though as gravel road performance is difficult to model. Reflective cracking did not change regardless of the amount of load restrictions, or schedule. Varying the duration of load restrictions between one and five months in the analysis revealed the following:

The greatest gain in pavement service life (based on IRI, longitudinal cracking or total rutting) is obtained with four or five month load restrictions. Since four and five month restrictions appear to equally mitigate pavement damage, and since shorter periods of restrictions translate into reduced disruption of hauling, four-month SLR should be favoured upon the five-month duration.

With a four-month load restriction duration (scenarios # 9 and #13 as per TABLE 4-3), the March-to-June schedule is slightly more efficient than the February-to-May schedule.

The three-month duration (scenarios #8, #12 and #15 as per TABLE 4-3) is roughly 1% less efficient than the four-month duration, and the March-to-May and April-to-June are equivalent.

The two-month duration (scenarios #7, #11, #14 and #16 as per TABLE 4-3) can be up to 3% less effective than the three-month duration in increasing the pavement service life, and the March-to-April and April-to-May schedule are the most significant contributors.

Any one-month SLR approach would provide limited benefit. The analysis showed however that load restrictions should imperatively be in place during April, as it appears to be the major contributor to pavement preservation.

It should be noted that differences of only up to 3% between service lives associated with each load restriction scenario seem to indicate that varying the schedule and duration of SLR will not have a significant impact on pavement preservation. However, even if these magnitudes are not what would have been expected (partly because of software calibration issues, see section 6.1), the results provide some insight into the impact of traffic and environment on the pavement structure during weakened conditions, and are consistent with real-world practices: three-month SLR (March 1st to May 31st) and four-month SLR (March 1st to June 31st) were implemented in 2007 on Ontario's secondary and tertiary roads respectively [MTO 2007].

Chapter 5
CONCLUSIONS AND RECOMMENDATIONS

5.1 Main Results

Ontario, as many of the other Canadian provinces is attempting to implement the MEPDG. This software was thus selected to simulate typical SLR scenarios as well as provide a long-term context for the findings. Analysis of relative pavement performance indicated that in general, longer periods of load restrictions could protect the pavement infrastructure and that better scheduling could result in up to six years additional service life for the pavement. The greatest gain (based on IRI, longitudinal cracking or total rutting) was obtained with either a four or five-month SLR period. As longer SLR periods might not have an overall economic benefit, shorter periods costs should be balanced against road user benefits. Moreover, the historical analysis showed that load restrictions should imperatively be in place during April, as it appears to be the major contributor to pavement preservation.

Building on the main findings of the preliminary analysis (first phase of the UW-MTO project), calculation of the reference temperature was modified in order to provide a smoother trend to the Thawing Index, which could now be potentially used to track the transition from the freezing season to spring-thaw. Based on the general form of the correlation found between the Freezing Index and the depth of frost in the roadway (as part of the preliminary analysis), models based on a linear combination of the Freezing index and the Thawing index were proposed. Based on the best fit regression statistical technique and using the Northeastern experimental site's field data (response variable) and RWIS temperatures (parameters), temporary calibration of these models was performed and provided reasonable estimates of the depths of frost and thaw in the pavement.

The development of a model that can be used for prediction and advance planning with sufficient confidence is critical because transportation agencies need to give the trucking companies at least a few days of advance notice when disseminating SLR and WWP schedules. The fitted model presented in section 4.1.4 provided a good estimation of the measured depths. However, some field depth values were inconsistent with the bulk of the data (outliers, spikes) and suspected to be due to equipment malfunction. As a result, little confidence can be placed in the calibration coefficients that were generated by the least square regression analysis. Smoothing techniques should have been used, but given the insufficient amount of data that was collected, this issue wasn't addressed.

In the long-term, provided sufficient historical records of frost depth are gathered and that knowledge is developed on how frost depth and thickness in the pavement relates to pavement strength (through

the monitoring of deflection for e.g.), frost and thaw depth indicators could be used not only to monitor the current pavement worst case condition using RWIS real-time data, but also and more importantly, to predict sub-network frost trends and future values five-days forecasts of air temperature. Safety margins can be determined based on an analysis of variance of the predicted data with actual conditions. Moreover, since values of the Freezing and Thawing indices can be predicted using five-days RWIS forecasts, trend shifts could thus be used to track the start and duration of spring-thaw.

Creation of an SLR application based on a model that relates to actual temperatures and moisture within the pavement structure and that can be defended with sound pavement engineering principles requires that the empirical model proposed on this report be used in conjunction with deflection testing to track changes in relative pavement strength. Advance warnings and cost-effective guidelines could then be derived and translated into a decision-support tool that assists MTO engineering professionals in the implementation of load restrictions. This approach is summarized in FIGURE 5-1 below.

The MEPDG software relies on mechanistic principles and over 525 empirical observations from the Long Term Pavement Performance (LTPP) database. As a result, it covers a wide range of both material and climatic conditions [ARA 2004]. Although the MEPDG results presented in this report seemed reasonable and provided some insight into the environmental and loading impacts on the pavement structure, it should be remembered that the MEPDG software has not been calibrated with material, traffic and environmental conditions typical for Canada. In particular, as seasonal variations in climate can have a huge impact on the results [Tighe 2005], the Transportation Association of Canada (TAC) is investigating this issue. Besides, a study conducted by the University of Waterloo in collaboration with Applied Research Associates (ARA) used the CPATT's portable FWD device to examine the relationship between major material characteristics of unbound subgrade materials and the stress state and in-situ moisture seasonal variations [Tighe 2005].

5.2 Next Steps toward a Practical Decision-Support Tool for the MTO

5.2.1 Conceptual Guidelines for the Imposition of SLR and WWP

FIGURE 5-1 below is a conceptual illustration that was developed as part of this study to schematize how SLR and WWP timing would be triggered or lifted when typical trends in frost depth and thickness in the pavement (obtained either by historical records or real-time monitoring of field data, or estimated by inputting RWIS forecasts into a properly calibrated model) reach pre-specified critical thresholds, with forecasts indicating a continued trend. Plain lines stand for field measurements and dotted lines stand for historical or predicted (estimated) values.

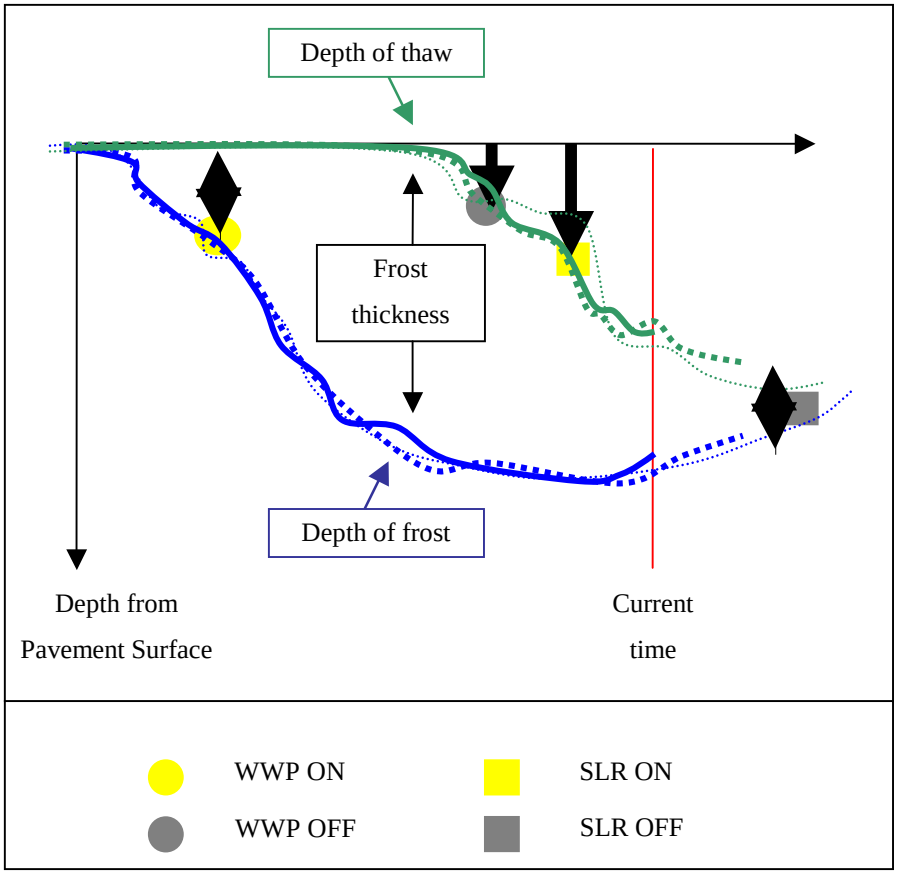

FIGURE 5-1 Conceptual Guidelines for the Determination of Start/ Stop SLR/WWP Dates.

The length of the load restriction period should approximate the time required to achieve complete thawing in the pavement structure. This duration could therefore be determined in real-time from deflection measurement or estimated using frost measurements provided significant correlation is established between the amount of frost in the pavement and its structural strength.

In the long term, this methodology can be derived into automatic algorithms and coupled with life cycle-cost analysis to find a good balance between the economic needs of the transportation industries and the level of serviceability of each roadway. The ability to use weather forecasts in the prediction is necessary to accommodate the advance notice required between the announcement of the limits and their application. Also, provided the frequency of magnitude changes does not exceed a workable rate for the truckers and that continuous movement is allowed on common freight routes, restrictions could be removed on certain roads of the network each time conditions would warrant. This strategy would provide Northern Ontario with means of estimating optimal schedules for the enforcement and removal of load restrictions or overloads on the low-volume road network.

5.2.2 Correlation of Deflection Data with Key Pavement and Environmental Variables

Decision to impose the restrictions mainly depends on whether or not frost and then thaw has penetrated into the subgrade [Haas 1985]. Determination of the structural strength associated with the amount of frost present in the pavement is necessary to assess the magnitude of traffic loading that can be allowed on this pavement. Therefore, rational determination of seasonal load limits should use thaw and frost depth criteria to set the timing of SLR and WWP application, while the limit magnitude required to keep the damage to that normally experienced by the pavement should be derived from a structural analysis carried out on representative test sections. Moreover, such limits could be adjusted periodically on each road if pavement strength is measured on-site and over time, by means of portable FWD equipment for example.

The objective of collecting pavement deflection data throughout the 2007 spring thaw was to examine if PFWD measurements could be used to identify critical shifts in the pavement bearing capacity and ultimately correlate to the depth of frost in the soil. However, the lack of frost and deflection data limited the analysis. As art of some future work, deflection and frost data collected should be tentatively correlated in order to predict the critical onset of the weakening period without having to perform extensive physical testing.

5.2.3 Potential Model Calibration Methodology

As summarized on FIGURE 5-2 below, equipment of the future RWIS stations with ground temperature probes and moisture sensors will be required to calibrate and validate the model. Tracking the changes in the calibration coefficients values over the years, or plotting the residuals of the best-fit regression analysis (estimated versus measured frost and thaw depths) against on-site moisture trends records for example, could lead to a better understanding of how unique environmental and soil type characteristics influence frost depth formation and dissipation in the roadbed, and ultimately to the incorporation of moisture as a parameter in the model or within the calibration steps. It is also important to note that, due to variations in climate throughout Ontario, values of the reference temperature will vary from site to site, and probably from one year to the other. A challenge for implementation will be determining how to calibrate the model for locations without ground temperature probes. Again, a strategy focused on estimating conditions for worst case sections in a sub-network may suffice.

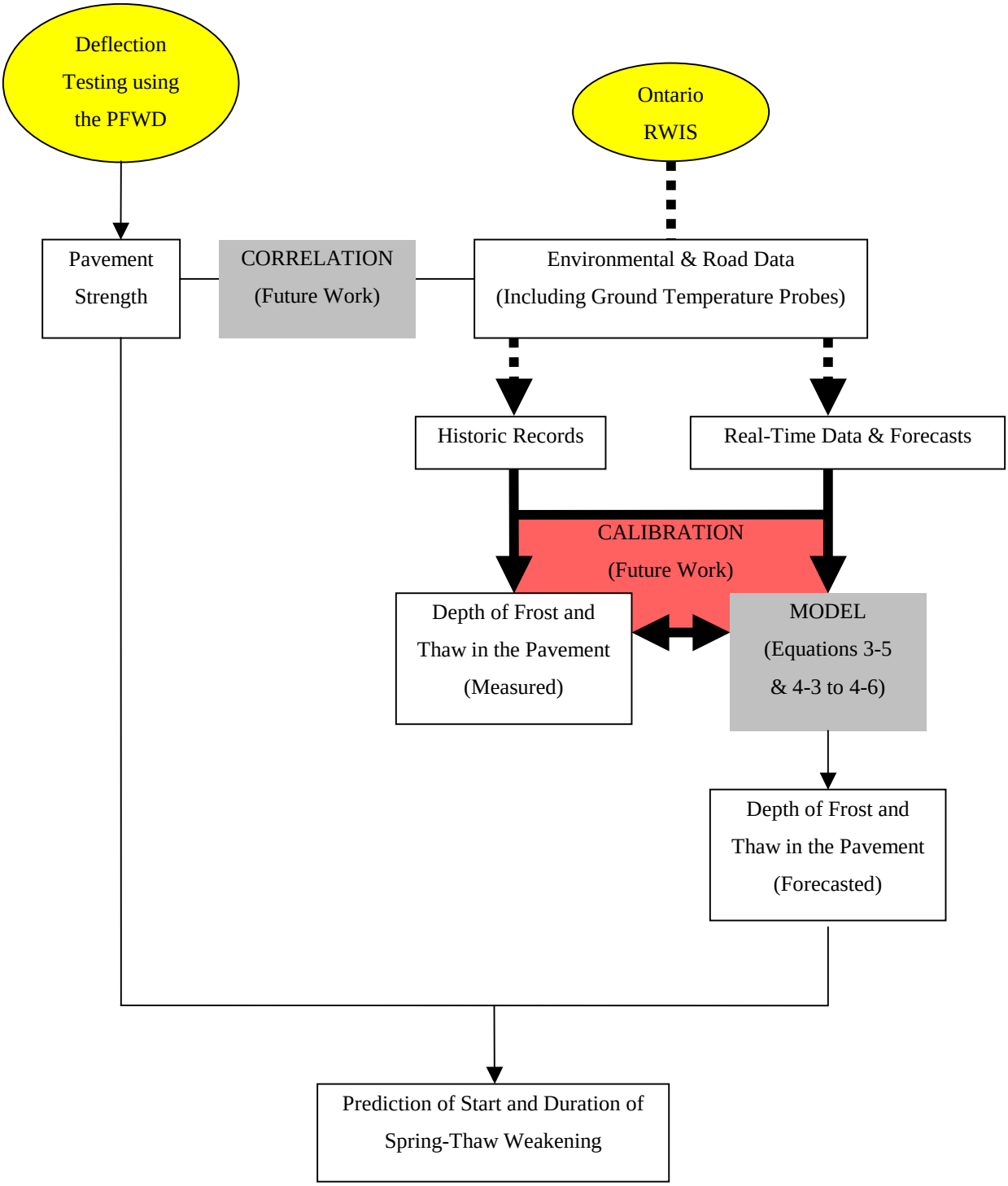

FIGURE 5-2 Summary of the Proposed Model Calibration Methodology and Future Work

5.2.4 Data Collection Needs and Prospects

This study proposed a site-specific empirical model that can potentially relate a few and readily available climatic variables to the frost depth and thickness in the pavement. The results are encouraging but no definitive conclusion can be drawn. There is a dire need to increase the database and accumulate several years of frost data used and model calibration in order to fully justify the safe use of this model for prediction. Some data fusion and estimation of local conditions is required as

well. More generally, data collection on strategic sections of low-volume roads should be encouraged in order to better identify where the heaviest loads travel, how the roads are built and how they perform.

Creating additional RWIS sites that would be also equipped with frost depth probes, investigating the incorporation of other critical and site-specific parameters such as deflection or moisture in the analysis, carefully selecting solid and reliable sensing equipment, further automating data retrieval, as well as integrating the models and calibration algorithms in centralized ITS systems, are all additional examples of steps towards the creation of a practical, flexible and reliable tool. In particular, linking the data to GPS coordinates and creating GIS mapping could be extremely beneficial. As Central Tire Inflation (CTI) Systems are becoming more widely used across Canada [Bullock 2006], load restrictions could be dynamically determined based on in-situ measurements and SLR schedules broadcasted in real time to trucking companies.

The fundamental basis to create such an SLR application and stay coherent with the Canadian ITS (Intelligent Transportation Systems) architecture have already been laid in a recent and comprehensive study [Bullock 2006], in which the various data requirements (pavement structure and performance, climate, traffic) were extensively investigated. In particular, there is a critical need to properly estimate the number of loads and respective weight of each load. Coordination of traffic data with the pavement structural data could ensure that the roads are not being overloaded during the weakest periods of the year. Besides, such data could also be used to improve low volume road design practices across Ontario. But most importantly, it is critical that all agencies and institutes develop ways to share information relating to SLR and WWP to help to advance research in this area.

REFERENCES

Ahmed, Z.; Maher, M. and Marshall, P.C. (2006). "Context Sensitive Pavement Design for Low-Volume Roads Applications". 2006 Annual Conference of the Transportation Association of Canada, Charlottetown, Prince Edward Island.

AMEC RWIS (2007) "Road Weather Information System portal, Ontario RWIS". http://rwis.na.amec.com/rwisweb/ (accessed 04/21/2007)

Applied Research Associates (ARA) and Inc., ERES Consultants Division (2004). "Guide for Mechanistic Empirical Design of New and Rehabilitated Pavement Structures (NCRHP Project 1-37A)". National Cooperative Highway Research Program, Washington, DC.

AURORA (2007). "Aurora Program Website". http://www.aurora-program.org/ (accessed 08/01/2007)

Boselly, S.E.; Doore, G.S. and Ernst, D.D. (1993). "Road Weather Information Systems Volume 2: Implementation Guide". University of Washington Seattle, Strategic Highway Research Program SHRP-H-351, National Research Council, Washington, DC.

Buchanan, F. and Gwartz, S.E. (2005). "Road Weather Information Systems at the Ministry of Transportation, Ontario". Annual Conference of the Transportation Association of Canada, Calgary, Alberta.

Bullock, M.; Tighe, S. and Bolduc P. (2006). "The Opportunities for Intelligent Transportation Systems to assist with Spring Load Restrictions and Winter Weight Premiums". Annual Conference of the Transportation Association of Canada, Charlottetown, Prince Edward Island.

Canadian Good Roads Association, CGRA (1962). "Pavement Evaluation Studies in Canada". International Conference on the Structural Design of Asphalt Pavements, University of Michigan, Ann Arbour, Michigan, p. 137-218.

Chisholm, R.A. and W.A. Phang (1977). "Measurement and Prediction of Frost Penetration in Highway". Transportation Research Board Record 918, Washington, DC.

Coghlan, G.T. (2000). “Opportunities for Low-Volume Roads”, Transportation Research Board CD-Rom A3B05, Transportation in the New Millennium: State of the Art and Future Directions, Perspectives from Transportation Research Board Standing Committees.

Dore, G. (1998). “Developpement d’un modele de prediction des conditions de degel de la route”, Ministere des Transports du Quebec.

Dore, G. and C. Imbs (2002). “Development of a New Mechanistic Index to Predict Pavement Performance During Spring Thaw”. 11th Cold Regions Specialty Conference.

Dore, G.; Tighe, S. and Hein, D. (2005). “Roadmap for the calibration and Implementation of the Mechanistic-Empirical Design of New and Rehabilitated Pavement Structures”. Transportation Association of Canada (TAC), Ottawa, Ontario.

Dynatest International A/S. (2004). “Keros Prima 100 Portable FWD User Manual”. Issue: 010704.

ECIM (2006). “ICM File Formats”. http://www.trb.org/mepdg/ICM_Formats.htm (accessed 10/09/2006)

FHWA-LTPP (2000). “LTPP Manual for Falling Weight Deflectometer Measurements Operational Field Guidelines”. Prepared for the U.S.DOT Federal Highway Administration LTPP Team.

Goodings, D.J.; Van Deusen, D.; Kestler, M. and O’Connor, B. (2000). “Frost Action”. Transportation Research Board Conference Proceedings 00784362.

Haas, R. and Gough, G.W. (1985). “Development of a Rational System for Seasonal Load Restrictions”. Roads and Transportation Association of Canada (RTAC) Forum.

Haas, R.; Falls, L.C.; MacLeod, D. and Tighe, S. (2004). “Climate Change Impacts and Adaptions on Roads in Northern Canada”. Cold Regions Engineering and Construction Conference and Expo, Edmonton, Alberta.

Highway Traffic Act (1990). “Reduced Load Periods: chapter H.8, section 122”. http://www.e-laws.gov.on.ca/html/statutes/english/elaws_statutes_90h08_e.htm#BK183 (accessed 07/20/2007)

Hoffmann, O.; Guzina, B. and Drescher, A. (2003). "Enhancements and Verification Tests for Portable Deflectometers". Minnesota Department of Transportation, Mn/DOT Report 2003-10.

Isotalo, J. (1995). "Seasonal Truck Load Restrictions: Mitigating Effects on Seasonal Strength Variations". Transportation Research Board Conference Proceedings 00680732.

Janoo, V. and Cortez, E. (2002). "Pavement Evaluation in Cold Regions". 11th Cold Regions Engineering International Conference, Anchorage, Alaska.

Kestler, M.A.; Knight, T. and Krat, A.S. (1998). "Thaw Weakening on Low Volume Roads and Load Restriction Practices". Transportation Research Board Conference Proceedings.

Kestler, M.A. (2005). "Portable Falling Weight Deflectometers for Tracking Seasonal Stiffness Variations in Asphalt Surfaced Roads". Department of Civil and Environmental Engineering, University of Maine, USDA Forest Service, New England Transportation Consortium.

Leong, P.; S. Tighe and Dore, G. (2005). "Using LTPP Data to Develop Spring Load Restrictions: A Pilot Study". Transportation Research Board Conference Proceedings 05-1284.

Levinson, D.; Marasteanu, M.; Voller, V.; Margineau, I.; Smalkoski, B.; Hashami, M.; Li, N.; Corbett, M. and Lukanen, E. (2005). "Cost/Benefit Study of: Spring Load Restrictions". Minnesota Department of Transportation, Report No. MN/RC.

Ministry of Transportation of Ontario, MTO (2004). "Provincial Highways Traffic Volumes, 1988-2004". http://www.raqsa.mto.gov.on.ca/techpubs/TrafficVolumes.nsf/tvweb (accessed 02/10/2007)

Ministry of Transportation of Ontario, MTO (2007). "Notice to Truckers, Spring Load Restrictions 2007". http://www.mto.gov.on.ca/english/trucks/loadnotice.pdf (accessed 03/12/2007)

Mokwa, R. (2004). "Transportation Engineering in Cold Regions: State of the Practice Review". Cold Regions Engineering and Construction Conference and Expo, Edmonton, Alberta.

Nazzal, M.D.; Abu Farsakh, M.Y.; Alshibli, K.A. and Louay, M.N. (2007). "Evaluating the Light FWD Device for In-situ Measurement of Elastic Modulus of Pavement Layers". Transportation Research Board 2007 Annual Meeting CD-ROM 07-0035.

NCHRP Research Result Digest 308 (2006). “Changes to the Mechanistic-Empirical Pavement Design Guide Software through Version 0.900 July 2006”. National Cooperative Highway Research Program.

NCHRP (2007). “1-37A Design Guide”. http://www.trb.org/mepdg/guide.htm (accessed 04/05/2007)

Ningyuan, L.; Kasmierowski, T. and Lane, B. (2006). "Long-Term Monitoring of Low-Volume Road Performance in Ontario". 2006 Annual Conference of the Transportation Association of Canada, Charlottetown, Prince Edward Island.

Popik, M.; Tighe, S. and Olidis, C. (2005). “The Effect of Seasonal Variations on the Resilient Modulus of Unbound Materials”. 2005 Annual Conference of the Transportation Association of Canada, Calgary, Alberta.

Transportation Association of Canada, TAC (1997). “Pavement Design and Management Guide”. Ottawa, Ontario.

Tighe, S. (2005). “Evaluation of the MEPDG for Canadian Conditions”. Transportation Association of Canada, University of Waterloo, Progress Report.

Tighe, S.; Huen, K. and Perchanok, M. (2006). “Development of Tools for Improved Spring Load Restriction Policies in Ontario”. University of Waterloo, Civil Engineering. 2006 Annual Conference of the Transportation Association of Canada, Charlottetown, Prince Edward Island.

Tighe, S.T.; Smith, J.; Mills, B. and Andrey, J. (2007). “Mechanistic-Empirical Pavement Design Guide: A Canadian Climatic Sensitivity Analysis”. 86th Annual Meeting of the Transportation Research Board, Washington, DC.

University of Washington (2005). “Interactive Training Guides”. http://training.ce.washington.edu/ (accessed 03/08/2007)

Wagner, C. (2005). “FHWA DGIT Activities”. 85th Annual Meeting of the Transportation Research Board, Washington, DC.

Appendix A

Primary frost heaving theories

Adapted from Tighe 2006.

1. Capillary Rise Theory

Capillary rise theory was introduced by Martin in 1959. The theory is that negative pressure, as a result of the ice formation, induces suction at the ice-water interface. Capillary rise is driven by surface tension at the interface between ice and pore water.

2. Secondary Heave Theory

The body of soil is divided into three regions based on a theory developed by Miller in the 1970s: already frozen, frozen fringe and unfrozen. A frost fringe is an area whereby ice and water coexist in the pores of the soil. In the event these three layers exist, this comprises the Secondary Heave theory. The premise of this theory is that water travels through a frost fringe which is an area that is partially frozen. Modeling the rate of water migration is a limitation of this theory as it is difficult to predict pressures, material properties such as hydraulic conductivity, within this fringe area. Secondary frost heave is characterized by the existence of a partially frozen zone, underlying the frozen soil, in which ice and water coexist in the pore space.

3. Segregation Potential Theory

Uneven heat flow at the frost fringe as a result of various temperature changes is the basis of this theory. The segregation potential theory attempts to simulate the heat and mass transfer in frozen soil based on laboratory tests. This theory is defined as the ratio of moisture migration to the temperature gradient in a frozen soil near the 0°C. Water flow is the result of suction at the growth surface of the ice lens and the hydraulic conductivity, based on the amount of liquid water, near the surface (in the frozen fringe).

Appendix B

Excerpts from the preliminary analysis progress report

As outlined in section 1.4, this research is the second phase of a two-year MTO project that was carried out by the University of Waterloo, under the supervision of Dr. Susan Tighe. Below are selected excerpts from the progress report prepared for the MTO.

Excerpt 1

There are many jurisdictions, both in Canada and the U.S., that have attempted to model the effects of freeze and thaw. Canadian jurisdictions such as Quebec and Manitoba and Minnesota in the United States have developed models. In the majority of cases, field testing to determine an empirical model was performed at several satellite test sites. The following is a brief summary of the relationships developed.

1. The Freezing and Thaw Indices

The freezing index (FI) is the accumulation of the daily mean temperatures. However, the trigger is when the mean daily temperature first falls below 0^oC. At this point, the equation below is employed daily with a constraint that the freezing index must be greater or equal to 0^oC.

$$FI = \sum \left(0^o C - T_{MEAN_i}\right)$$

During the thawing period, a thaw index (TI) can be used to understand the approximate level of thaw based on air temperature and a reference temperature. The state of Minnesota uses the following equation to determine the thaw index.

$$TI = \sum \left(T_{MEAN_i} - T_{REF}\right)$$

Although the models listed below are currently in use in their respective jurisdictions, the direct transfer of a model to another jurisdiction is not recommended. As described earlier, the models are empirically based. Therefore, calibration for each model is specific to the originating area. Climate and soil conditions differ among all regions and therefore, are accounted for in the coefficients within the model. For example, Quebec has a unique suite of climatic trends as well as soil characteristics, both moisture and type. Compared to Minnesota, where the climate is significantly different in terms of precipitation and temperature, the coefficients in Minnesota model are different to the Quebec model.

2. Quebec

Within the province of Quebec, a study conducted by [Dore 1998] to investigate ground frost. A field experiment was developed and completed to predict the frost depth in relation to ambient air

temperatures. The instrumentation used in this experiment included a thermister assembly that is placed into the roadbed to measure the vertical temperature profile. In developing the empirical model, the following relationships were also employed into the model created by Dore 1998. The mean air temperatures, in centigrade, are calculated.

$$T_{MEAN} = \frac{T_{MAX} + T_{MIN}}{2}$$

Where T_{MEAN} - Mean daily air temperature (ºC)

T_{MAX} - Maximum daily air temperature (ºC)

T_{MIN} - Minimum daily air temperature (ºC)

In the event the mean air temperature is not zero, the corrected surface temperature must be calculated:

$$T_{CORR} = 0 \qquad \text{if } T_{MEAN} = 0$$

$$T_{CORR} = T_{MEAN} + \left[\left(T_{MAX} - T_{MIN}\right) \cdot F\right] + CONST \qquad \text{if } T_{MEAN} \neq 0$$

Where T_{CORR} - Corrected pavement surface temperature (ºC)

T_{MEAN} - Mean daily air temperature (ºC)

T_{MAX} - Maximum daily air temperature (ºC)

T_{MIN} - Minimum daily air temperature (ºC)

F Regression constant

CONST Regression constant

To determine the freezing index, the following incorporates the corrected temperature for a given day and the freezing index of the previous day. Conditional inequalities apply to this relationship.

$$FI_i = T_{CORR_i} + FI_{i-1} \qquad \text{if } T_{CORR_i} + FI_{i-1} > 0$$

$$FI_i = T_{CORR_i} \qquad \text{if } T_{CORR_i} + FI_{i-1} \leq 0 \text{ and } T_{CORR_i} > 0$$

$$FI_i = 0 \qquad \text{if } T_{CORR_i} + FI_{i-1} \leq 0 \text{ and } T_{CORR_i} \leq 0$$

Where T_{CORR} - Corrected pavement surface temperature (ºC)

FI_i - Freezing Index for a day i (ºC-days)

FI_{i-1} - Freezing Index for previous day (i-1) (ºC-days)

The depth of frost is related to this empirical equation involving a constant F and the freezing index.

$$P = F \cdot FI^{0.5}$$

Where P - Projected frost depth (cm)

F - Regression constant

FI_i - Freezing Index for day I (ºC-days)

The final corrected frost depth model for Quebec is determined through the following relationship. The related factors include constants, sum of square errors, freezing index, and thaw depth, and was developed through statistical regression. In this case, a confidence of level of 60% was selected.

$$P_i^* > 0 \qquad \text{if } P_i = P_{i-1}$$

$$P_i^* = P_i \qquad \text{if } P_i \neq P_{i-1}$$

$$P_{CORR} = P^* + \left[c \cdot S_e \cdot \left(1 + \frac{1}{398}\right) + \left(\frac{\left(FI^{0.5} - X_{MEAN}\right)^2}{\sum \left(X_i - X_{MEAN}\right)^2} \right)^{0.5} \right]$$

Where P_{CORR} - Corrected frost depth – includes regression constants and statistical variables

P* - Projected frost depth (cm) (must be greater than zero)

c - Confidence interval for a population mean

A function of Significance Level (alpha = 0.4), one standard deviation and a sample size of one.

S_e - Sum of squared errors

FI - Freezing Index (ºC-days)

X_i - Observed frost depth (cm)

X_{MEAN} - Average Observed frost depth (cm)

3. Manitoba

Within Manitoba, a specific method in determining the thaw index is employed. This method utilizes a modified mean air temperature value as well as a reference temperature based on March 1 at a value of 1.7ºC. A trigger value of TI = 15 will result in the enforcement of reduced loads on specified roadways.

$$T_{MOD} = \frac{T_{MEAN}}{2} \qquad \text{if} \quad T_{MEAN} < 0$$

$$T_{MOD} = T_{MEAN} \qquad \text{if} \quad T_{MEAN} \geq 0$$

$$TI_i = TI_{i-1} + T_{MOD} + T_{REF}$$

$$T_{REF} = 1.7 + 0.06i$$

Where T_{MOD} - Modified Temperature (ºC)

T_{MEAN} - Mean air temperature (ºC)

T_{REF} - Reference air temperature (ºC) – 1.7ºC

TI_i - Thaw index for day i (ºC-day)

TI_{i-1} - Thaw index for day i-1 (ºC-day)

i - Number of days since March 1

4. Minnesota

The state of Minnesota has investigated the impacts of SLR thoroughly. A variety of models are discussed in [Levinson 2005]. This includes air and subgrade temperature models. In general, an empirical model requires data to be fit onto a curve, through parametric coefficients. Surface temperature is estimated through the minimum daily air and the daily mean air temperatures as represented by the following models.

$$T_{Surf} = 0.859 T_{Min,Air} + 1.7$$

$$T_{Mean} = 0.859 T_{Air} + 7.7$$

Where $T_{Min,Air}$ - One Day Minimum Air Temperature (ºC)

T_{Air} - Mean Daily Air Temperature (ºC)

T_{Mean} - Mean Pavement Surface Temperature (ºC)

T_{Surf} - Pavement Surface Temperature (ºC)

The following is a model that estimates the temperature within the soil as a function of depth and time is also described [Levinson et al. 2005]. It is important to note that with the level and type of input required for this relationship, the use of such would be on a micro-level or area specific basis. It is not suitable for network level management. Thermal diffusivity is a measure of the ability of the soil to transmit a thermal disturbance. In other words, a high thermal diffusivity results in a rapid transmission of either high or low temperatures through the soil medium.

$$T(x,t) = T_{Mean} + A \exp\left(-x\sqrt{\frac{2\pi}{P\alpha}}\right)\sin\left(\frac{2\pi}{P}t - x\sqrt{\frac{2\pi}{P\alpha}}\right)$$

Where $T(x,t)$ - Soil temperature as a function of depth and time

x - Depth below surface (m)

t - Time when the measured air temperature is greater than the mean surface temperature (days)

T_{Mean} - Mean surface temperature (ºC)

A - Maximum temperature amplitude ($T_{Max} - T_{Mean}$) (ºC)

α - Thermal diffusivity of the soil (m^2/days)

P - Period of cycle (days)

Temperature profile in pavement layers can be computed using the following developed by [Witczak 1972]:

$$T_P = T_A\left(1+\frac{1}{z+4}\right)-\left(\frac{34}{z+4}\right)+6$$

Where T_p - Average seasonal pavement temperature (ºF)

T_A - Average seasonal air temperature (ºF)

z - Depth of predicted temperature (in) – typically z = 1/3 of HMA thickness

[Leong 2005] utilized Canadian long term pavement performance (C-LTPP) data to establish a reference temperature of 3.4ºC and a threshold thaw index of 13ºC-Days through regression. [Levinson 2005] refers to a model developed by [Chisholm and Phang 1977]. This model relates freezing index to frost depth (P).

$$P = -0.328 + 0.0578\sqrt{FI}$$

Where P - Frost depth (m)

P* - Projected frost depth (cm) (must be greater than zero)

c - Confidence interval for a population mean

A function of Significance Level (alpha = 0.4), one standard deviation and a sample size of one.

S_e - Sum of squared errors

FI - Freezing Index (ºC-days)

Excerpt 2

The RWIS temperature data was inputted into the relationships and the frost data output was generated. The first is a modified Quebec model, second is a modified Manitoba model and the final is a modified Minnesota model. The first utilizes a model that uses freeze index along with a corrected temperature to estimate the frost depth. The second uses a modified temperature and a reference temperature that generates a thaw index. The final model, based on Minnesota, utilizes a frost index to develop a maximum frost depth. The duration of the thaw is developed in the Minnesota

model based on the thaw and freeze indices. Utilizing the original coefficients of these models, recent ARWIS data are inputted into this model and its result is compared with field thermister data.

Excerpt 3

Although the modified models provide a means of predicting the frost depth, the curve created does not fit the field data perfectly. This will be corrected as a higher number of data points are gathered from both ARWIS sites and from the field study sites. Calibration of these models, which are not based in Ontario, will be performed with the data that will be acquired. Further description to the intended calibration procedure can be found in the subsequent section. The following is a representation of the modification of Model 1 with respect to the thermister data acquired.

Corrected Temperature:

Original Model: $T_{CORR} = T_{MEAN} + [(T_{MAX} - T_{MIN}) \cdot 0.178] + 1.628$

Modified Model: $T_{CORR} = T_{MEAN} + [(T_{MAX} - T_{MIN}) \cdot 0.1] + 10$

Frost depth:

Original Model: $P = -8.254 \cdot FI^{0.5}$

Modified Model: $P = -8 \cdot FI^{0.5}$

Model 2 does not directly affect the frost depth. However, the thaw duration will be affected as the output of this model is thaw index. Further investigation on thaw duration is to be completed in the following stage of the project. The third model estimates the frost depth by incorporating the frost index.

Frost depth:

Original Model: $P = -0.328 + 0.0578\sqrt{FI}$

Modified Model: $P = -0.1 + 0.0578\sqrt{FI}$

The final model to be developed will be calibrated to Ontario data and may require a different model structure to conform to the trends seen in the data.

Appendix C

Leading edge in empirical modeling of spring-thaw weakening

Below is an excerpt from [Bullock 2006], in which one of the latest quantitative approaches used to model spring-thaw weakening for load restriction purposes is presented.

Excerpt

A recent study by Dore and Imbs [Dore 2005] suggests that the three most important factors affecting the behaviour of pavements during spring thaw include:

1. The amount of frost heave that occurs per unit thickness in the considered layer.
2. The rate at which the layer is thawing.
3. The rate at which the layer consolidates.

The work by Dore further suggests that a thaw weakening index should be developed to assist in predicting weakening in the pavement structure. It is proposed as:

$$TWin = (h / D) * (X / S)$$

Where	TWin	Thaw weakening index
h	Total heave resulting from frost action in subgrade soil (min)	
D	Thickness of subgrade soil affected by frost action (min)	
X	Thawing rate (mm/day)	
S	Settlement rate (mm/day)	

This dimensionless index incorporates several factors that have been identified as being important with respect to the weakening behaviour of a given material. The rate of thawing is identified as a function of the climatic conditions during spring, and the resulting thermal response of the material. In addition, the consolidations and volume change is incorporated into the prediction [Dore 2005].

The TWin then needs to involve a field validation which includes collection of the more specific site data [Dore 2005]:

- Thickness of the frozen soil layer (frost depth);
- Total frost heave (assuming no significant frost heave occurs in the pavement granular layers);
- Thaw progression as a function of time during the spring;
- Relative elevation of the pavement structure as a function of time during spring thaw and the associated recovery period; and

• A measurement of the evolution of the pavement bearing capacity with time.

Appendix D

Additional Instrumentation Memorandum

This Appendix provides a document that was prepared as part of this research in order to outline the equipment needs on the experimental sites.

NORTHWESTERN PILOT SITE
Requirements of the current instrumentation
Location of the site

Lat 49°20’ N / Long 89° W / Elevation 459.3 ft
On Highway 527, 0.5km north of Hwy 811
East and South exposure

The panel will have to be oriented to capture maximum energy during the winter solstice (vegetation will not be an issue).

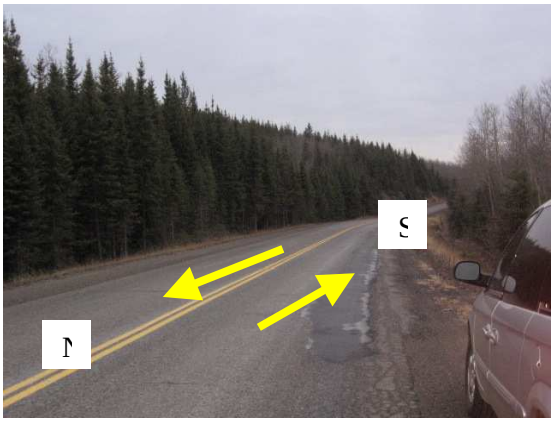

FIGURE D-1 The Northwestern Pilot Site

Specifications of the equipment

13 Temperature Probes
Thermistors (output: Resistance measurement)
Able to withstand external forces such as damage due to backfilling, slight volumetric changes in the surrounding oils, weather extremes and corrosion.
Thermistor assembly:
Typical overall life expectancy: 5 years

Total depth of monitoring = 2.5m

T1 at -5cm under pavement surface

T2 at -15cm; T3 at -30cm; T4 at -45cm; T5 at -60cm; T6 at -75cm; T7 at -90cm and T8 at -105cm.

T9 at -135cm; T10 at -165cm; T11 at -195cm; T12 at -225cm and T13 at -255cm.

Data Acquisition System

General requirements

Robust, accurate and reliable capturing of data at regular intervals

Sufficient channel capacity

A redundant power supply

Sufficient data storage

Nearly stand alone system

Handle extreme temperatures

Environment Canada recorded:

NE region: -34°C/+32°C in 2003; -37°C/+29°C in 2004

NW region: -37°C/+33°C in 2003 and 2004

In a weather resistant cabinet

Hot-pressed glass fiber reinforced polyester

Summary of specifications of the DT800 datalogger (DALIMAR INSTRUMENTS) used on both study sites

Physical

-45°C to +70°C

85% RH

Power Inputs

110/220V AC

11-28V DC

1A

Power Consumption

5W Normal mode

5mW Sleep mode

Channels

12 Analogue (4 terminals per channel)

16 Digital

Data Storage

2MB internal

ATA Flash PC Card Expansion

Communication

Ethernet, USB

RS232 – 57,600 Baud rate with Modem Support

Accuracy

Resistance

0.04% @ 25°C

0.20% @ -45 to 70°C

DC Voltage

0.02% @ 25°C

0.10% @ -45 to 70°C

Industrial Phone Modem (+AC/DC adapter)

NE Study site:

DALIMAR INSTRUMENTS - Model VT-MODEM 1 WW

Manufactured by Sixnet

Ability to withstand the extreme temperatures from -30ºC to +70ºC

Match the environmental specifications of the data logger (DT800).

TABLE D-1 Specifications of VT-MODEM 1 as provided by Sixnet.

Telephone Line	Max Data Rate	33.6 kbps (V.34)
	Compatibility	V.34, V.32 bis, V.32, V.22, V.22A/B, V.23, V.21, Bell 212A
	Data Compression	V.44 / V.42 bis MNP 5
	Error Correction	V.42 MNP 2-4
	Max Fax Modem Rate	14.4 kbps
	Fax Modem Capabilities	Group 3 (V.33, V.17, V.29, V.27 ter, V.21 channel 2)
	Ringer Equivalent	0.3
	Line Jack	RJ11
	Phone Jack	RJ11
RS-232 Port	Max RS-232 Rate	115.2 kbps
	RS-232 Signal Support	TXD, RXD, CTS, RTS, DCD, DTR, DSR, RI, GND
	RS232 Connector	DB9 female

	Command Set	All standard AT and S register commands, including Class 1 and Class 2 Fax Commands
General Characteristics	Dimensions	8.2W x 12.1L x 3.4H cm
	Input Power	10-30 VDC
	Input Current (Normal mode)	50 mA @ 24 VDC (typical)
	Input Current (Low power mode)	30 mA @ 24 VDC (typical)
	Operating Temperature	-30° to 70° C
	Storage Temperature	-40° to 85° C
	Humidity	5% to 95% RH (non-condensing)
Other Items	Flammability (module plastic) UL 94V-0 materials	
	Telecom FCC part 68 (Reg. #5KNUSA-32535-MM-E), Industry Canada (Cert. #29918926A), Contact SIXNET for other countries	
	Electrical Safety UL 508, CSA C22.2/14; EN61010-1 (IEC1010),CE	
	EMI Emissions FCC part 15, ICES-003, Class A; EN55022, CE	
	EMC immunity EN50082-1 (IEC801-2, 3, 4), CE	
	Vibration IEC68-2-6	
	Hazardous locations UL 1604, CSA C22.2/213-M1987, (Class I, Div 2, Groups A, B, C, D), EN50021 (zone 2)	
	Marine/offshore locations Det Norske Veritas (DNV) No. 2.4 (Class A and B)	

Additional instrumentation at NW Pilot site if funding is available

Supplier: SPS SOLTEK POWER SOURCE LTD

Systems ideally designed for remote data collection sites and used in RWIS stations.

Nearest local dealer: Barrie, ON / 888-300-3037

Contact: **Richard Thorne**, Sales Representative / 613-2774-881

Suggested product: MAP-2BP365-2SC92-12

MAPPS (Modular Autonomous Photovoltaic Power Supply): Complete prepackaged stand-alone power system in waterproof enclosure.

Composed of:

2 BP SOLAR modules (BP-365)

Mounted in parallel

Total power: 2*65 W

Peak current: 2*3.69 A

Peak Voltage: 17.6 V

Dimensions of each panel: 111.1cm * 60.2cm * 5cm / 7.2kg

Pole Mounting Structure

Either “pole mounted” APM2-BP365 (45° to 90°)

Or “top of pole” TPM2-BP365 (10° to 70°)

Charge Controller ASC-12/12

Battery

Either Solar Cell series 2SC92 (196 Ah)

Or EXTREME-1000 Solar Battery (100 Ah)

1 “charging day” per week

7 days autonomy at least

Waterproof enclosure

Compact model (30 l)

Powder coated Aluminum or Steel (NEMA 3R or 4)

Able to contain the data acquisition equipment

May not be necessary as the MTO NW Field team is considering to construct 3m*3m housing cabinet along with a concrete base and a pole on the NW site (Contact: Doug Flegel).

Wiring, Manuals, …

Warranty of each of the above components: 5 to 20 years.

TWO ADDITIONAL SITES

The following assumes that both a thermistor string similar to the current NW/NE pilot sites and as well RWIS capabilities are appropriate. Note below given discussion with Mickey Major, Site A would be equipped with an RWIS and Site B would not. No other stations locations were supplied for NW Region.

Location of the sites

The two locations that have been selected by the MTO (Contact: Mickey Major) are the following

Site A: On King’s Hwy 66

Future RWIS station → Data collected will be centralized by the AMEC RWIS server.

Not subject to seasonal load restrictions

Hydro and phone service are available.

Site B: On Provincial road SH-624

“Weak link” / Connection to Hwy 66 at Larder Lake (West of Virginiatown)

Not eligible to be part of the RWIS network → Data collected will be separately downloaded via modem

Subject to seasonal load restrictions

Hydro and Phone service are available but not installed yet.

Parts list proposal for Site A

Site A will be equipped as any other RWIS stations would, but, as detailed below, the instrumentation will be supplemented by thermistor strings in order to monitor ground temperatures.

Sensors

Pavement sensors

Surface Temperature (3.2mm below roadway surface)

Subsurface Temperature (43.2cm below roadway surface)

Ground Temperatures: 13 probes (UW team proposal) – 16 probes (Alaska RWIS stations)

Moisture

Atmospheric sensors

Air Temperature (2.44m above ground)

Relative Humidity

Wind Speed and Direction (9.15m above ground)

Precipitation

Camera

Remote Processing Unit (RPU)

Data acquisition unit: 6 single channels (+ 10 to 18 differential channels for the data probes) would be needed.

→ It should be noted that the DALIMAR INSTRUMENTS datatakers provide more channel capacity than the CAMPBELL SCIENTIFIC units. Originally, DALIMAR was selected for this reason (NW/NE pilot sites). Robustness under harsh climatic conditions, high memory storage, stand-alone ability and minimal power consumption are important criteria. Note that some of the existing RWIS stations use the CAMPBELL SCIENTIFIC CR10X-Series unit, which has 12 single channels but can be expendable to 28 channels.

Data transmission: Via modem

Power : From the grid (wall outlet + AC/DC adapter)

Waterproof and locked enclosure

Wiring

Parts list proposal for Site B

As Site B is not a future RWIS station, the instrumentation will be minimal.

Sensors

Pavement sensors

Surface Temperature (3.2mm below roadway surface)

Ground Temperatures: 13 probes (UW team proposal) – 16 probes Alaska RWIS stations)

Moisture (?)

Atmospheric sensor : Air Temperature (2.44m above ground)

Camera (?)

Remote Processing Unit (RPU)

Data acquisition unit : 2 to 4 single channels (+ 10 to 18 differential channels for the data probes) would be needed

Data transmission: Via modem

Power : From the grid (wall outlet + AC/DC adapter)

Waterproof and locked enclosure

Wiring

Note that the five RWIS equipment suppliers of preference are:

SURFACE SYSTEMS INC (SSI)

LUFFT

BOSCHUNG

VAISALA

CAMPBELL SCIENTIFIC

They were initially selected through a biding process among vendors whose products had technical specifications in accordance with the national standards.

ZYDAX can provide:

Freeze point detection sensors

Surface/Subsurface Temperature + Ground Moisture dual sensors

Air Temperature + Relative Humidity sensors.

Appendix E

VBA code developed to convert thermistor data into frost and thaw depths

This appendix provides the Visual Basic code of the Excel macro that was writen to process the field data into a frost depths and thaw depths and provide for long term data collection and storage.

TABLE E-1 Thermistor Depths and Temperature Codes.

Thermistor depth (cm)	Associated temperature (^{0}C)
- 5	T01
-15	T02
- 30	T03
- 45	T04
- 60	T05
- 75	T06
- 90	T07
-105	T08
- 135	T09
- 165	T10
- 195	T11
- 225	T12
-255	T13

Function **Frost_Depth**(ThresholdTemp, T01, T02, T03, T04, T05, T06, T07, T08, T09, T10, T11, T12, T13)

D01 = 5

D02 = 15

D03 = 30

D04 = 45

D05 = 60

D06 = 75

D07 = 90

D08 = 105

D09 = 135

```
D10 = 165
D11 = 195
D12 = 125
D13 = 255

If T13 < ThresholdTemp Then
   Depth = D13
ElseIf T12 < ThresholdTemp And T13 > ThresholdTemp Then
   Depth = ((D13 - D12) / (T13 - T12)) * (ThresholdTemp - T12) + D12
ElseIf T11 < ThresholdTemp And T12 > ThresholdTemp Then
   Depth = ((D12 - D11) / (T12 - T11)) * (ThresholdTemp - T11) + D11
ElseIf T10 < ThresholdTemp And T11 > ThresholdTemp Then
   Depth = ((D11 - D10) / (T11 - T10)) * (ThresholdTemp - T10) + D10
ElseIf T09 < ThresholdTemp And T10 > ThresholdTemp Then
   Depth = ((D10 - D09) / (T10 - T09)) * (ThresholdTemp - T09) + D09
ElseIf T08 < ThresholdTemp And T09 > ThresholdTemp Then
   Depth = ((D09 - D08) / (T09 - T08)) * (ThresholdTemp - T08) + D08
ElseIf T07 < ThresholdTemp And T08 > ThresholdTemp Then
   Depth = ((D08 - D07) / (T08 - T07)) * (ThresholdTemp - T07) + D07
ElseIf T06 < ThresholdTemp And T07 > ThresholdTemp Then
   Depth = ((D07 - D06) / (T07 - T06)) * (ThresholdTemp - T06) + D06
ElseIf T05 < ThresholdTemp And T06 > ThresholdTemp Then
   Depth = ((D06 - D05) / (T06 - T05)) * (ThresholdTemp - T05) + D05
ElseIf T04 < ThresholdTemp And T05 > ThresholdTemp Then
   Depth = ((D05 - D04) / (T05 - T04)) * (ThresholdTemp - T04) + D04
ElseIf T03 < ThresholdTemp And T04 > ThresholdTemp Then
   Depth = ((D04 - D03) / (T04 - T03)) * (ThresholdTemp - T03) + D03
ElseIf T02 < ThresholdTemp And T03 > ThresholdTemp Then
   Depth = ((D03 - D02) / (T03 - T02)) * (ThresholdTemp - T02) + D02
ElseIf T01 < ThresholdTemp And T02 > ThresholdTemp Then
   Depth = ((D02 - D01) / (T02 - T01)) * (ThresholdTemp - T01) + D01
End If

Frost Depth = -Depth
End Function
```

```
Function Thaw_Depth(ThresholdTemp, T01, T02, T03, T04, T05, T06, T07, T08, T09, T10, T11,
T12, T13)

D01 = 5
D02 = 15
D03 = 30
D04 = 45
D05 = 60
D06 = 75
D07 = 90
D08 = 105
D09 = 135
D10 = 165
D11 = 195
D12 = 125
D13 = 255

If T01 < ThresholdTemp Then Depth = 0
ElseIf T02 < ThresholdTemp And T01 > ThresholdTemp Then
   Depth = ((D02 - D01) / (T02 - T01)) * (ThresholdTemp - T01) + D01
ElseIf T03 < ThresholdTemp And T02 > ThresholdTemp Then
   Depth = ((D03 - D02) / (T03 - T02)) * (ThresholdTemp - T02) + D02
ElseIf T04 < ThresholdTemp And T03 > ThresholdTemp Then
   Depth = ((D04 - D03) / (T04 - T03)) * (ThresholdTemp - T03) + D03
ElseIf T05 < ThresholdTemp And T04 > ThresholdTemp Then
   Depth = ((D05 - D04) / (T05 - T04)) * (ThresholdTemp - T04) + D04
ElseIf T06 < ThresholdTemp And T05 > ThresholdTemp Then
   Depth = ((D06 - D05) / (T06 - T05)) * (ThresholdTemp - T05) + D05
ElseIf T07 < ThresholdTemp And T06 > ThresholdTemp Then
   Depth = ((D07 - D06) / (T07 - T06)) * (ThresholdTemp - T06) + D06
ElseIf T08 < ThresholdTemp And T07 > ThresholdTemp Then
   Depth = ((D08 - D07) / (T08 - T07)) * (ThresholdTemp - T07) + D07
ElseIf T09 < ThresholdTemp And T08 > ThresholdTemp Then
   Depth = ((D09 - D08) / (T09 - T08)) * (ThresholdTemp - T08) + D08
ElseIf T10 < ThresholdTemp And T09 > ThresholdTemp Then
   Depth = ((D10 - D09) / (T10 - T09)) * (ThresholdTemp - T09) + D09
ElseIf T11 < ThresholdTemp And T10 > ThresholdTemp Then
```

```
    Depth = ((D11 - D10) / (T11 - T10)) * (ThresholdTemp - T10) + D10
ElseIf T12 < ThresholdTemp And T11 > ThresholdTemp Then
    Depth = ((D12 - D11) / (T12 - T11)) * (ThresholdTemp - T11) + D11
ElseIf T13 < ThresholdTemp And T12 > ThresholdTemp Then
    Depth = ((D13 - D12) / (T13 - T12)) * (ThresholdTemp - T12) + D12
Else
    Depth = 0
End If
Thaw_Depth = -Depth
End Function
```

Appendix F

Portable Falling Weight Deflectometer Testing Procedure

Provided in this Appendix is the procedure that was developed as part of this research in order to guide the MTO personnel who were in charge of carrying out the PFWD testing on the Northeastern experimental site from March to April 2007, using the Prima 100 device (Dynatest International 2004, Denmark).

Synthesis of Field Work Activity at a typical test section

The following list of field activities provide the PFWD operator with an overall perspective of a typical work to be performed at a test section.

Step 1: Arrive on the test section (2 sections per site; 2 sites: Hwy 569 and Hwy 624).

Step 2: Coordinate personnel
Traffic control crew
One person required for testing

Step 3: Inspect and clean the 3 test locations. They should be dry.

Step 4: Prepare PFWD equipment and PDA using the PFWD Procedure document prepared by CPATT. At this point, the PDA file should be created, the batteries checked and the connection between PDA and PFWD established. If the connection is lost, batteries have to be disconnected and reconnected so that a green light can be temporarily activated and the connection reestablished.

Step 5: Perform 6 drops per test location. After each drop, the shape of the load and deflection curves should be similar to Figure 1.b). If not, an additional drop should be carried out (but no file should be deleted so that they can all be examined afterwards).

Step 4: When moving the PFWD from one test location to the other (on the same section).
Close the current PDA file.
The PFWD mass should be in bottom position.
Place the PFWD very carefully on the hand truck and ensure that it is correctly fixed.
Drive the hand truck to the desired test location and place it on the specified marking.
Check that the connection between PDA and PFWD is established (Tool menu).

Step 5: Wrap up

Step 6: Download the test files from the PDA to the laptop using the guidelines of the PFWD Procedure document prepared by CPATT (see after)

Step 7: Send the files to the University of Waterloo HIIFP 2006 Project Research Team

Research Assistant: Baizsarah@aol.com
Supervisor: sltighe@civmail.uwaterloo.ca

Step 8: Make sure to keep the PDA batteries and the PFWD batteries charged.

Important safety remarks

At any time during which onsite activities are performed on highway pavements, the safety of the operating crew as well as the traveling public is of the utmost importance. As the tests will be carried out in the mid-lane, traffic control should be implemented during testing. Also, one should keep in mind that the weight may drop unexpectedly.

Additional remarks on deflection variability in the pavement structure

It should be noted that deflection variation can occur:

Between tests points within a section (15% to 60%): This variation reflects the changes in layer thickness, material properties, moisture and temperature conditions, subgrade support and contact pressure between the load plate and the pavement surface [FHWA-LTPP. 2000]. Therefore, PFWD operators should not be overly concerned with point to point variations in the deflection response.

At a given load for a fixed test point (less than above): This variation can be due to precision limitations of the sensors or to changes in the material properties due to repeated loading. The variations that occur from equipment and operational aspects can be reduced by ensuring that the PFWD operator is properly trained.

Appendix G

Procedure for Operating Dynatest Prima 100 Portable FWD

FIGURE G-1 Load Cell

1. Attach load plate to main unit using screws and Allen key. The largest load plate (300mm diameter)* should be used.

FIGURE G-2 Load Plate attached to Load Cell

2. Screw in 4 rubber buffers.

FIGURE G-3 Four Rubber Buffers

3. Screw in bottom shaft to main unit between the rubber buffers. Note that the 2 shafts are NOT interchangeable, so be sure to use the right one.

4. Screw the two extra 5 kg weights onto the main weight using Allen key.

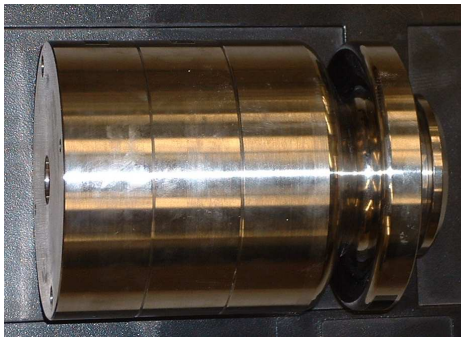

FIGURE G-4 20 kg weight

5. Carefully slide the 20 kg weight down the shaft until it rests on the buffers. Note that there is a small grey plastic tube that acts as a guide just inside the weight. This tube should not slide out.

6. Screw top shaft onto bottom shaft.

7. Slide trigger handle onto the top shaft.

FIGURE G-5 Trigger Handle

8. Move trigger handle to desired (up to 85cm measured from the top of the buffers to the bottom of the drop mass) drop height (instructions on this matter will be provided on the training day by UW). Do not over tighten the trigger handle. The angle of the handle can be changed by pulling out and rotating to an angle which does not catch the weight.

FIGURE G-6 Assembled PFWD Device

9. Unscrew knob on Bluetooth battery case.

FIGURE G-7 Bluetooth Signal Provider and Battery Pack

10. Plug in batteries (4*A4) and rescrew battery case. Make sure green light is on; this means that a signal is being sent out to connect with the pocket computer.

11. Turn on PDA.

12. Run KP100, located in the start menu.

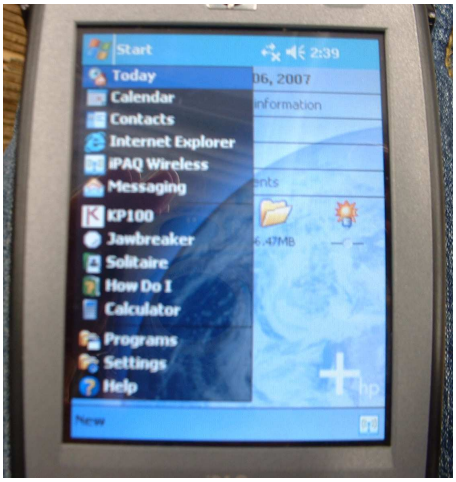

FIGURE G-8 Start Menu

13. Check the settings.

TABLE G-1 Prima 100 PFWD Input Parameters used for this study

Setup Menu Item	Input Parameter	Value
Trigger	Pretrig time (ms)	10*
	Pulsebase (%)	24*
	Trig Level (kN)	0.90*
View	Sample Time (ms)	60*
Mechanical	Load Plate Radius (mm)	150
	Number of sensors	3
	$D_{(1)}$ offset (cm)	0
	$D_{(2)}$ offset (cm)	20.7
	$D_{(3)}$ offset (cm)	40.7
Formula	Poisson's Ratio	0.35**
	Stress Distribution, *f*	2.0

** - default values recommended by manufacturer.*
*** - Huang (2004).*

14. Enter file name and set file path.

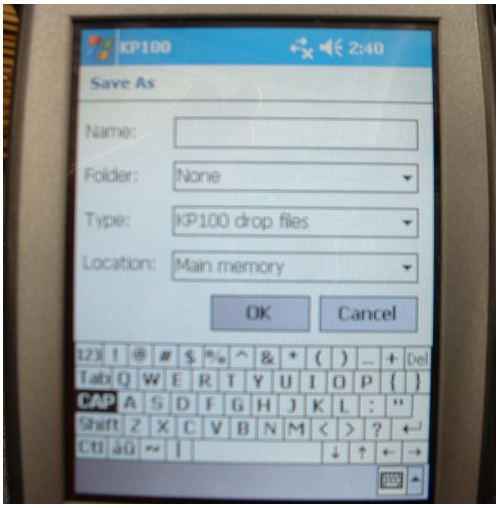

FIGURE G-9 Save File

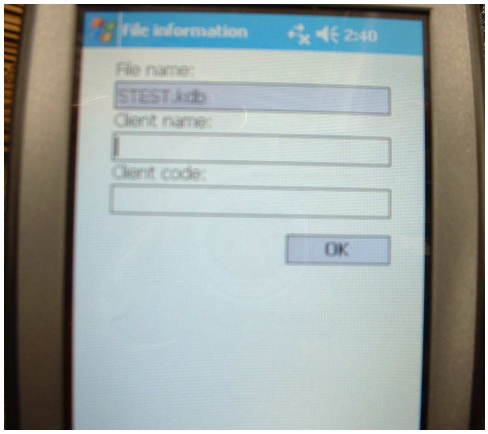

FIGURE G-10 File Information

15. Record location point ID, description, ambient temperature and any additional comments.

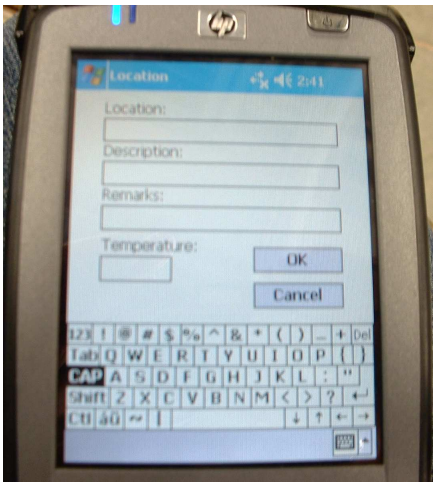

FIGURE G-11 Location Information

16. In the tools menu click *Connect to Prima.*

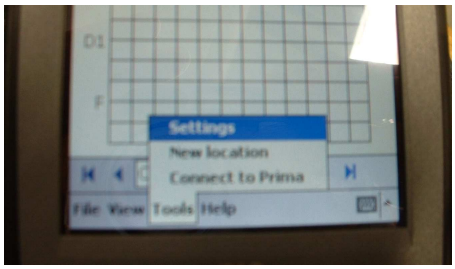

FIGURE G-12 Tools Menu

17. Click on the Prima icon.

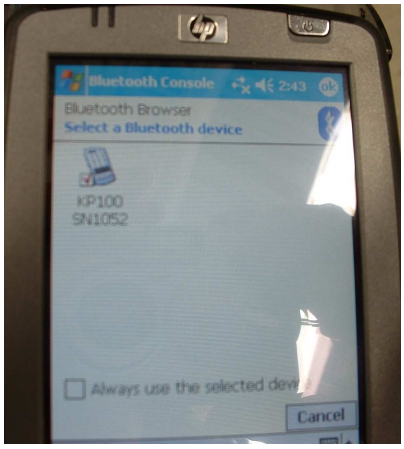

FIGURE G-13 Bluetooth Connection

18. After the connection is complete, the pocket computer will sound to indicate that it is ready for a drop.

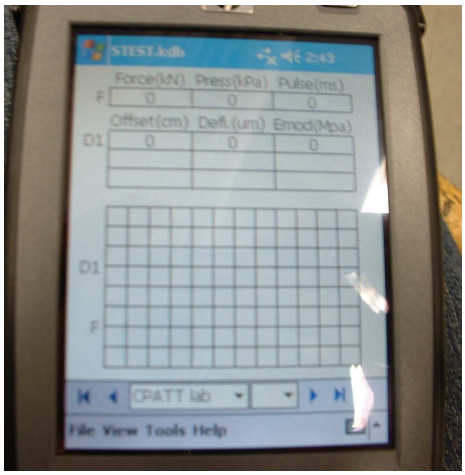

FIGURE G-14 Test Screen

19. Carefully raise the weight and set it below the trigger. Note that when the button on the trigger is up the trigger is locked and the weight will not fall. To release the lock, press the button.

20. Pull the handle and let the weight fall.

21. Repeat steps 19 and 20 for desired number of falls. Six falls at a fixed drop height are recommended at one location [Kestler 2005].

22. Once all data has been recorded, connect pocket computer to laptop using cables provided.

23. Connect the two devices (the required PDA software CDRom will be provided by UW along with the PDA and should first be installed on the laptop used for the next steps).

24. Left-click the icon on the lower right hand corner of the screen and click explore.

FIGURE G-15 Explore Icon

25. Transfer files from pocket computer to laptop using cut and paste.

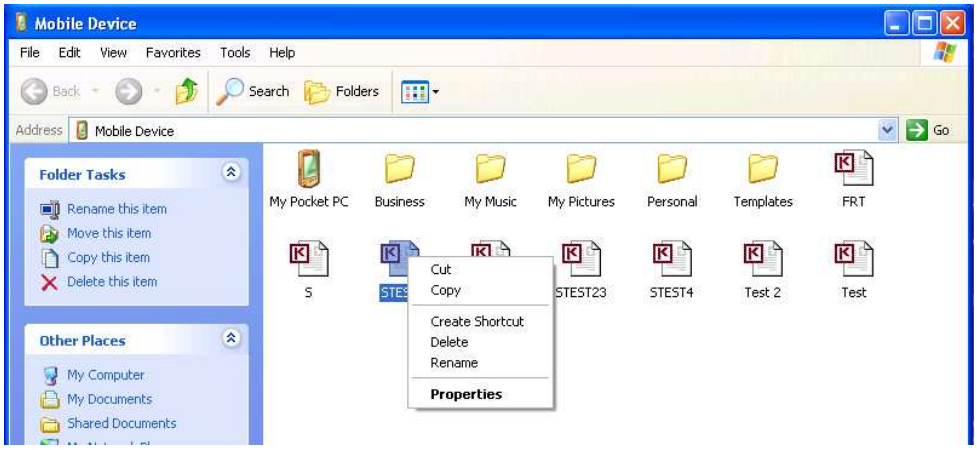

FIGURE G-16 File Transfer

26. You can open the files on the laptop using Excel if that program is installed on the laptop computer.

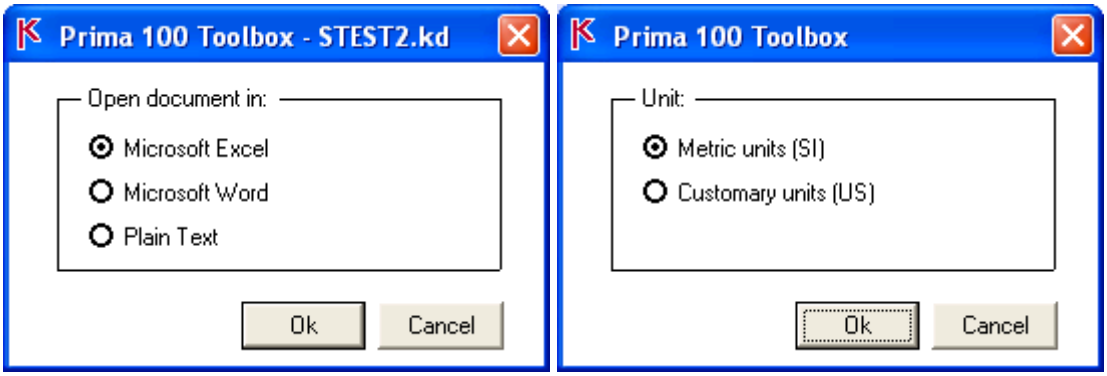

FIGURE G-17 File Opening

27. In order to log the file information, repeat steps 24 and 25 but select “open the document with Microsoft Word”.

Appendix H

List of weather stations entered into the MEPDG

In Canada

- Alberta: Edmonton City Center Airport; Edmonton International Airport; New Brunswick; Fredericton International Airport;
- Nova Scotia: Halifax International Airport; Halifax Shearwater Airport;
- Quebec: Montreal Pierre Trudeau International Airport
- Ontario: North Bay International Airport; Ottawa International Airport; Toronto Buttonville International Airport; Toronto Lester B. Pearson International Airport
- Saskatchewan: Regina International Airport
- Newfoundland: St John's International Airport
- British Columbia: Vancouver International Airport
- Manitoba: Winnipeg International Airport

In Northern USA

- North Dakota: Bismarck Municipal Airport; Dickinson Municipal Airport; Hector International Airport; Grand Forks International Airport; Hettinger Municipal Airport; Jamestown Regional Airport; Minot International Airport; Sloulin Field International Airport
- Minnesota: Chandler Field Airport; Baudette International Airport; Brainerd Lakes Regional Airport; Duluth International Airport; Chisholm-Hibbing Airport; Falls International Airport; Minplis-St-Paul International Airport; Crystal Airport Flying Cloud Airport; Rapids Muni-Kinshok Federal Airport; Redwood Falls Municipal Airport; Rochester International Airport
- Wisconsin: John F. Kennedy Memorial Airport; Chippewa Valley Regional Airport; Austin Straubel International Airport; Sawyer County Airport; Kenosha Regional Airport; La Crosse Municipal Airport; Tri-County Regional Airport; Dane Co Regional-Truax Federal Airport; General Mitchell International Airport; Whittman Regional Airport; John H Batten Airport; Rhinelander-Oneida Co Airport; Sheboygan Co Memorial Aiport; Alexander Federal S Wood Co Airport;
- Michigan: Adrian Lenawee County Aiport; Ann Arbor Municipal Airport; W K. Kellogg Airport; SW Michigan Regional Airport; Detroit City Airport; Willow Run Airport; Detroit Metro Wayne Co Airport; Bishop International Airport; Otsego County Airport; Gerald R. Ford International Airport; Houghton County Memorial Airport; Roscommon County Airport; Ford Airport; Kalamazoo Creek International Airport; Capital City Airport; Muskegon County Airport; Pellston Regional Airport; Oakland International Airport; Cherry Capital Airport;

- New York: Albany International Airport; Buffalo Niagara International Airport; Dansville Municipal Airport; Dunkirk Airport; Elmira/Corning Regional Airport; Republic Airport; Floyd Bennett Memorial Airport; Long Island Mac Arthur Airport; Massena International Airport; Orange County Airport; La Guardia Airport; Central Park Airport; JFK International Airport; Niagara Falls International Airport; Clinton County International Airport; Dutchess County Airport; GTR Rochester International Airport; Brookhaven Airport; Syracuse Hancock International Airport; Oneida County Airport; Watertown International Airport; Tarentine Federal Airport; Westchester County Airport
- Vermont: Edward F Knapp State Airport; W.H. Morse State Airport; Burlington International Airport;
- Maine: Augusta State Airport; Bangor International Airport; Eastern Slopes Regional Airport; Millinocket Municipal Airport; Portland International Jetport Airport; Wiscasset Airport;